Asymptotic Transient Solutions of Stochastic Fluid Queues Fed By A Single ON-OFF Source

by

Yu Shao

A thesis submitted to The Johns Hopkins University
in conformity with the requirements for the degree of
Master of Science

Baltimore, Maryland
May, 2019

Abstract

Stochastic Fluid Queues (SFQs) have served many applications in different research fields including understanding the performance measurements of network switches in High-Performance Computing (HPC) environment and understanding the surplus processes in the context of ruin theory. Although many advancements have been made to understand the stationary behavior of SFQs, the transient analysis is an open research area, where Laplace-Stieltjes Transforms (LST) are used to understand time-dependent behavior. However, performing the inversion is impractical in many cases.

Chapter 2 and 3 of this work revisits the work of fluid-queues driven by a single "ON-OFF" source in the context of resource allocation in HPC environments. The asymptotic analysis is performed to produce equivalent representations that depict short and long-time behavior. Next, an expansion is proposed that holistically considers these behaviors while also providing a direct correlation between the packets injection rates and state transition rates. The numerical experiments validate our proposed schema, where the results can be adapted to provide better resource estimation of fast-packet switching within HPC environment.

Chapter 4 and 5 of this work explores theorizing the collective risk of a single insurance firm during periods of distress, where its current revenues are less than its initial surplus. This behavior can be modeled as a fluid queue fed by a single ON-OFF source, where our contributions are two-fold. First, we found explicit solutions consisting of combinations of modified Bessel functions of the first kind. Next, we obtain asymptotic expansions of our resulting solutions for short and long-time behavior to propose a comprehensive solution that fuses these results. Numerical experiments further demonstrate the viability of our proposed method where only a few terms are needed to effectively approximate the temporal behavior of the surplus probability density function during periods of financial distress. Furthermore, we also show that our asymptotic expansions provide a direct correlation between the firm's revenue gains, its claim sizes, and the current surplus behavior. The results of this work can be directly applied and extended to audit the solvency of firms operating in adverse financial conditions as well as help effectively identify potential troubled corporations at various stages.

Thesis Committee

Primary Readers

Antwan D. Clark (Primary Advisor)
Associate Research Scientist
Department of Applied Mathematics and Statistics
Johns Hopkins Whiting School of Engineering

Daniel Q. Naiman (Reader)
Professor
Department of Applied Mathematics and Statistics
Johns Hopkins Whiting School of Engineering

Acknowledgments

I sincerely acknowledge my research advisor, Dr. Antwan Clark for instructing me in the world of mathematical research and guiding me to write the thesis. He skillfully delivers me the knowledge needed and patiently shows me the way to become an eligible independent researcher. In addition to research, he is also an excellent counselor for my life, study and career. I can never forget the evening conversations when his opinions illuminate my enthusiasm towards diving into the deeper ocean of mathematical study and research. His encouragement helps me finish my Master's degree and continue my further travels of pursuing Ph.D.

Moreover, I would like to express heartfelt thanks to Professor Daniel Naiman and Dr. John Miller, for their instruction and advice during my Master's life at the Johns Hopkins University. They helped me overcome most obstacles in my study and indicated directions for me when I was perplexed.

Furthermore, I would like to appreciate my colleague Jiawen Bai, who has worked with me for a long time and contributed lots of enlightening ideas towards this work. Lastly, I also want to thank my friends, my families and

all the people who have supported me. Their company and love provide me hope and courage to continue my study and research.

This work is based upon work supported by the U.S. Department of Defense (DoD) under award numbers FA8075-14-D-0002-0007. The views and conclusions contained in this work are those of the author and should not be interpreted as necessarily representing the official policies, either expressed or implied, of the DoD.

Table of Contents

List of Tables

List of Figures

Chapter 1

Introduction

1.1 Motivation

1.1.1 HPC Resource Allocation

High-Performance Computing (HPC) systems aim to support parallel execution of high performance critical and large-scale applications with minimum initial investment, operating costs and energy consumption costs [1]. The execution of job flows in HPC systems requires multiple kinds of resources including the execution time of Central Processing Unit (CPU), the Input/Output (I/O) channel, the bandwidth of network and so on. The goal of HPC resource allocation is to manage the batch schedulers in the parallel computing environment to maximize the utilization of the synchronous networks [2].

Recently, researchers have widely applied HPC systems in fields of high-energy physics, geophysics and bioinformatics for complex large-scale experiments. To meet the increasing demand for computational science, high-frequency processors are employed to improve computational capability [3]. This change in hardware and architecture presents new challenges when making scheduling and resource allocating decisions. Firstly, with the scale of HPC systems growing, the complexity and variety of the jobs to be executed are increasing exponentially, making it harder to allocate the required resource immediately after the job burst flow occurs. Furthermore, the gap between the speed of I/O operation and that of CPU makes accessing data resources a bottleneck for the utility of HPC [4]. Therefore, there is a pressing need to estimate the distribution of the amount of required resource beforehand in a large HPC system. Predicting resource consumption in the system can help

the schedulers to make the proper resource allocation strategy in advance to prevent the deadlock and frequent suspend state of jobs in an HPC system.

1.1.2 Ruin Theory

Insurance companies play an essential role in the modern financial system, providing a way for corporations to transfer their risks. The nature of this business means that insurers will face more uncertainties than other enterprises. On the other hand, the insolvency of insurers may pose a risk to society as a whole. Evidence from the past several decades suggests that the bankruptcy of insurance company is approximately three-to-five times more expensive than that of other financial institutions [5].

After the financial crisis in 2008, the insurance industry has faced more challenges, which calls for more effective ways of managing the risk exposure faced by insurances companies [6]. In this environment, ruin theory becomes a core consideration for assessing insurance risk. Ruin theory assesses an insurer's vulnerability to insolvency. The primary goal for analyzing transient behavior in ruin theory is to determine the likelihood of ruin within a particular time interval, which can be either finite or infinite. Therefore, finding the exact solution of ruin probability can make it easier for us to predict the surplus for a given insurance company [7]. Moreover, managers of insurance companies can benefit from this analysis, because they can use the information to make risk management plans to protect their companies from bankruptcy.

1.2 Related Work

1.2.1 Related Work for HPC Resource Allocation

Recent research focusing on the operation of resource management systems is based on the queuing approaches in the environment of HPC systems [8]. For instance, Milidrag et al. model the packets transmitted in the network as fluid traffic and provide an event-driven simulation of the fluid network as well as hybrids of packet/fluid and event/time-driven simulation strategies [9]. Anick et al. consider a physical model in which a buffer receives packets from a finite number of statistically independent and identical information sources that asynchronously alternate between exponentially distributed periods in the ON and OFF states. They analyze the equilibrium buffer distribution by a set of differential equations. The numerical results show that model is useful for a data-handling switch in a computer network [10]. Liu et al. study the problem of resource allocation in the context of stringent quality of service constraints considering the joint impact of spectral bandwidth, power, and code rate. Their work obtains an analytical expressions for the probability distribution function of buffer content in the fluid queue model, as well as its associated exponential decay rate and the effective capacity [11].

Although many advancements have been made to understand stationary behavior of the stochastic fluid queues applied in the computing world, understanding transient behavior is still an open area of research [12]. Recent techniques involve the use of either Fourier-Stieltjes Transforms (FST) and Laplace-Stieltjes Transforms (LST), where matrix analytic methods (MAMs)

have been used to understand transient behavior [13] [14]. For example, Tanaka et al. analyze a multi-source on-off fluid queue model with input generated by a Markov modulated rate. They give an analytical solution of buffer content in a form of Laplace Transform [15]. Parthasarathy and Vijayashree's obtain the transient solution of a fluid queue driven by a single ON-OFF source in terms of modified Bessel's function of the first kind using double Laplace transform [16]. However, the transient solutions are based on either recurrence relations or numerically inverse Laplace transform, without an explicit expression provided [17]. Hence, it is still hard to obtain the explicit form of solutions due to the complexity of the problem, whereas such form of solutions is useful for gaining insight and comparing the relative advantages of different numerical techniques.

1.2.2 Related Work for Ruin Theory

For the risk management of insurance industries, the solvency of a company is often regarded as a matter for the relevant supervisory authorities. However, solvency is a variable affected by many uncertainties like the perspective of claims, the impact of investment returns, interest rates and inflations [18]. In the theory of insurance risk management, because people haven't recognized or grasped the deterministic law of solvency accurately, in order to facilitate evaluation, the solvency of capability is usually regarded as a stochastic process [19]. The classical model in the field of ruin theory is the Cramér–Lundberg model, also known as the compound-Poisson model,

which regards the surplus of insurance companies as a stochastic process with constant premium rate and Poisson distributed claim arrivals [20]. One of the famous generalizations of the Cramér–Lundberg model is given by Gerber and Shiu, in which the ruin probability is regarded as a function with respect to the initial surplus and time[21]; sequentially, the expected discounted penalty function is considered in the analysis of the insurer's surplus behavior [22]. Explicit forms of the probability of ruin are given under some specific assumptions like all claims are of constant size or exponentially distributed. Dufresne and Gerber further expand the model to a joint density of initial surplus, surplus before the ruin and the deficit at the ruin [23]. Laplace transformation is applied for solving the distribution density functions of ruin.

Recent works have modeled the behavior of insurance surplus process using the Stochastic Fluid Queues (SFQs). The transient analysis of the ruin probability bases on Laplace Transforms with Matrix Analytic Methods (MAMs) in the Laplace domain; however, inversions are mainly numerical [24]. Ramaswami proposes a quadratically convergent algorithm to invert the resulting matrices from the Laplace domain and provides an expression of the distribution of the first passage time for the SFQs model, which has become a basis for analyzing the transient behavior [25]. Zhou et al. apply a neural network method using the trigonometric function as the activation function and design an improved Extreme Learning Machine algorithm which is suitable for the risk model and which can calculate the probability of ruin accurately and quickly at an arbitrary time point [26]. Previous approaches have their limitations. First,

they only provide numerical solutions from which we can not get the correlation between the outputs and the parameters like the claim sizes. Second, the machine learning method also requires data for training the model, which is not always available.

Additionally, because of the significance of insurance companies, many countries have established a comprehensive insurance regulation system to prevent insurance companies from bankruptcy. For example, according to the Risk-Based Capital (RBC) for Insurers Model Act, when state regulators identify a distressed insurance company, they may take control of the company's assets, change the company's management or change the company's operations to help the insurer return to the marketplace. The National Association of Insurance Commissioners (NAIC) may also prohibit the insurer from writing new business and suspend current claims payments until the rehabilitation of the company [27]. Nonetheless, among previous research, how to evaluate the market value and potential risk of ruin have not been considered for distressed companies whose current surpluses are below the initial capital. Analyzing the situation can give a guideline to investors who intend to invest for the raising of new capital of such companies as it provides the level of risk of such investment. Meanwhile, this analysis can help the regulator to determine the likelihood of successful rehabilitation and the severity of the problem faced by the distressed insurer, so that proper action can be undertaken to minimize the risk of loss to policyholders. Together with the previous works, we provide the complete situation analysis to both the investors and regulators.

1.3 Approach

We analyze the transient behavior of a stochastic fluid queue fed by a single ON-OFF source considering both ON and OFF state as the initial state and get analytic solutions containing convolutions of modified Bessel functions of the first kind. Then, we perform the asymptotic analysis of the solution for both short and long time behaviors, as well as providing a comprehensive expansion for all time. Numerical experiments and Monte Carlo simulations are conducted to illustrate the fidelity of our method, where absolute differences of distribution functions are computed as the criteria for evaluation. Numerical results show that a few terms included in our expansion can achieve a high accuracy of the approximation. The result from Monte Carlo simulations also verifies the robustness of our proposed method. This result also reveals the direct connection between the buffer content, the injection rate of the states and the transfer rates between states. The high accuracy of our approximation with few terms implies that our approach can be more efficient than the traditional numerical methods for solving the probability distribution function of the buffer content.

We apply our result to modeling the behavior of the job burst processes in the context of HPC resource allocation and the insurance surplus process in the ruin theory. Our contributions are two-fold. First, we innovatively perform the asymptotic analysis of the solution behaviors in HPC resource allocation and ruin theory considering both short and long-time cases. Moreover, we propose an expansion form for these behaviors which construct a compositive

approximation of the solutions for all time. Our result provides an explicit solution for the buffer content probability distribution. The conclusion from our work can not only be applied for further understanding the HPC resource allocation and the bankruptcy determining mechanism but also be incorporated into evaluating the expectation of future equity prices and the Value at Risk (VaR) for distressed companies.

The rest of this paper is organized in the following manner. **Chapter** 2 establish the stochastic fluid queue model in the HPC environments, where an in-depth analytical assessment and the asymptotic analysis of the transient behavior of the fluid queue are presented for short and long-time. **Chapter** 3 provides the numerical experiments highlighting the robustness of asymptotic analysis for the HPC resource allocation problem. **Chapter** 4 applies the stochastic fluid queue model in the context of insurance ruin theory, as well as the analytical assessment and the asymptotic analysis. **Chapter** 5 provides the numerical results for the ruin theory. **Chapter** 6 concludes and presents some avenues of future exploration.

Chapter 2

Stochastic Fluid Queue Model for HPC Resource Allocation

2.1 Overview

In this chapter, we derive the Stochastic Fluid Queue (SFQ) model in the context of the job burst behavior analysis in the HPC environment. The relationship between job sources and job waiting buffer in an HPC environment can be illustrated by the stochastic fluid model. Different types of jobs share a common processor to execute jobs, where the limited maximum capacity of the processor is given as C packets per second (PPS). Each ball symbolizes a possible state of users with an specific job submission rate. In this scenario, each state S_i in the model representing for one kind of users who submit jobs at a particular rate r_i. If the total job submitting rate of all users is greater than the processing capacity C of the traffic, the excess jobs will be temporarily suspended in a buffer, namely the job waiting buffer $Q(t)$. The content of $Q(t)$ will be accumulated until the processor is not occupied.

Users distributed in the HPC environment may have finite virtual and physical properties. These attributes construct a space of the system environment S with finite states $S = \{S_1, \cdots, S_M\}$. Because of the change of virtual or physical environment, the system may transition from one state S_i to another state S_j with a rate λ_{ij}, which is a constant determined by the relationship of two states. With the assumption that the duration within each state follows exponential distribution, we can define each of the states as an either ON or OFF state according to the total uploading rate of the whole network. Within an ON state S_i, work flows into the targeted processor at a relatively steady rate of r_i PPS, which is determined by the properties of current state. We can

analyze the behavior of the buffer content $Q(t)$ in as **Table 2.1**.

	Condition	Description of Buffer Content Behavior
I	$r_i > C$	The buffer content $Q(t)$ *increases* at rate $r_i - C$. The processor is completely occupied by the running jobs. Thus, the new uploaded jobs will be suspended and wait temporarily in the buffer Q until the processor is spare.
II	$r_i \leq C, Q(t) > 0$	The buffer content $Q(t)$ *decreases* at rate $C - r_i$. The processor is still completely occupied by the jobs. However, the job submitting rate is less than the processing capacity. Although the new jobs will still be suspended in the buffer, buffer content $Q(t)$ will be released until it is empty.
III	$r_i \leq C, Q(t) = 0$	The buffer content $Q(t) = 0$ has *no change*. This condition implies that jobs can be executed without waiting and the HPC system is efficient.

Table 2.1: The Changing Behavior of Buffer Content $Q(t)$ in HPC Context

In HPC environments, if we want to analyze statistical properties of the buffer for an ensure the stability of the system, an effective measure is the Cumulative Distribution Function (CDF) of buffer content $Q(t)$ at time t, namely,

$$W^i(t,x) = P\left\{Q(t) \leq x, S(t) = S_i\right\}. \tag{2.1.1}$$

Consequently, the unconditional cumulative distribution function of the buffer content $Q(t)$ at time t can be given by

$$F(t,x) = P\left(Q(t) \leq x\right) = \sum_{i=1}^{M} W^i(t,x). \tag{2.1.2}$$

To model the job burst behavior in the HPC environment, we consider an ON-OFF system with all possible states, expressed as

$$S = \{S_1, \ldots, S_M\}, \tag{2.1.3}$$

where M is the total number of states. Suppose that there exists a public traffic with constant capacity C and buffer Q that are shared by all states. On each state $S_i \in S$, a fluid with given rate r_i will flow into the traffic. We define an ON state S_m to be a state in which the fluid rate $r_m > C$. Within an ON state, the public traffic is fully occupied by the injecting fluid, and the overload part of the fluid will be held in the buffer. Thus, buffer content $Q(t)$ will increase with rate $r_m - C$. On the other hand, an OFF state S_n is defined as the state in which the fluid rate $r_n \leq C$. Within an OFF state, the traffic is unoccupied, and if the buffer is not empty, the buffer content $Q(t)$ will decrease at rate $C - r_n$ until either it is empty or the state changes to an ON state again. Thus, the relationship between the changing of buffer content Q with respect to time t and current state $S(t)$, can be described as

$$\frac{dQ(t)}{dt} = \begin{cases} r_i - C & \text{when } Q(t) > 0, \text{ for state } S_i \\ 0 & \text{otherwise} \end{cases}. \tag{2.1.4}$$

Table 2.2 summarizes such conditions and **Figure** 2.1 visually illustrates the relationship between the buffer and the states.

	Condition	Buffer Content Behavior	Changing Rate
I	$S(t) = S_i$ *and* $r_i > C$	Increase	$r_i - C$
II	$S(t) = S_i, r_i \leq C$ *and* $Q(t) > 0$	Decrease	$C - r_i$
III	$S(t) = S_i, r_i \leq C$ *and* $Q(t) = 0$	No change	0

Table 2.2: The Changing Behavior of Buffer Content $Q(t)$

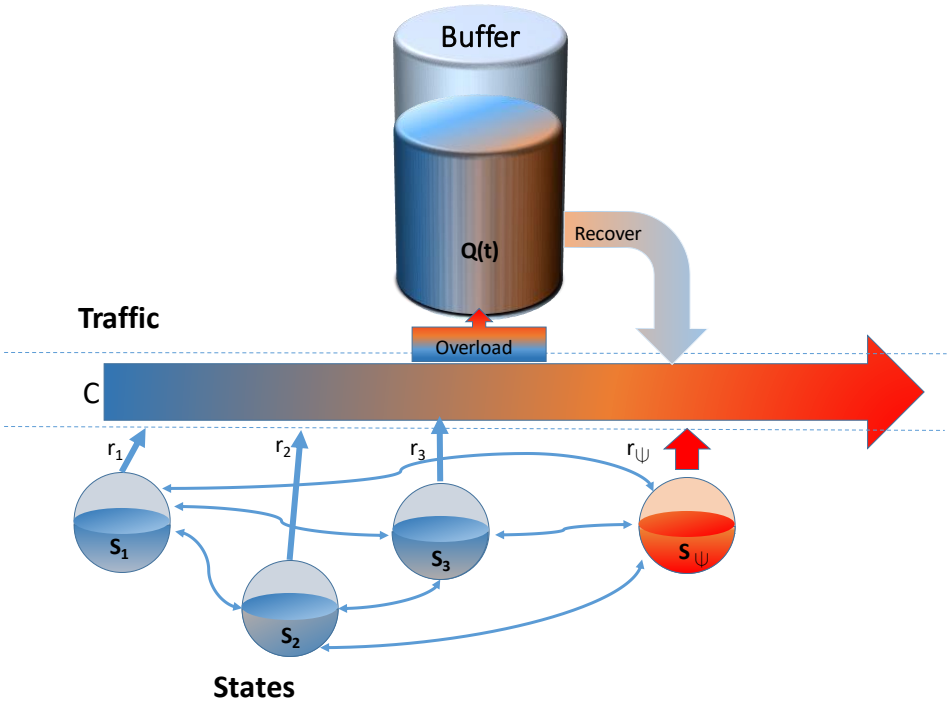

Figure 2.1: The Relationship between Buffer, Traffic and States

Additionally, we assume that the system changes from state S_i to S_j following a continuous time Markov chain, which means the transition rate is a constant λ_{ij} and the duration within each state is exponential distributed. Then the

transition matrix of states is

$$P = \begin{pmatrix} \lambda_{11} & \lambda_{12} & \dots & \lambda_{1M} \\ \lambda_{21} & \lambda_{22} & \dots & \lambda_{2M} \\ & \dots & & \\ \lambda_{M1} & \lambda_{M2} & \dots & \lambda_{MM} \end{pmatrix}, \tag{2.1.5}$$

where λ_{ij} means the rate of the system to change from state S_i to S_j defined as

$$\lambda_{ij} = \lim_{\Delta t \to 0} \frac{1}{\Delta t} P\left\{S(t+\Delta t) = j | S(t) = S_i\right\}, \tag{2.1.6}$$

and $S(t)$ denotes the state of the system at time t. With the property of the transition matrix that

$$\sum_{j=1}^{M} \lambda_{ij}\Delta t = \lambda_{ii}\Delta t + \sum_{j \neq i}^{M} \lambda_{ij}\Delta t = 1, \tag{2.1.7}$$

we have

$$\lambda_{ii}\Delta t = 1 - \sum_{j \neq i}^{M} \lambda_{ij}\Delta t. \tag{2.1.8}$$

Suppose the system stays in state S_i for time T_i, and has rate λ_i of probability to remain in S_i. By Markov property, for small $\Delta t > 0$, the probability of the remaining time T_i to be greater than Δt can be described as

$$\begin{aligned} P(T_i > \Delta t) &= P\left(S\left(t+\Delta t\right) = i | S(t) = S_i\right) \\ &= \lambda_i \Delta t + O(\Delta t) \end{aligned} \quad . \tag{2.1.9}$$

Consequently, we have

$$P(T_i \leq \Delta t) = (1 - \lambda_i \Delta t) + O(\Delta t). \tag{2.1.10}$$

If multi-transitions occur within a small time period Δt, we have the following remark.

Remark 1.

$$P\left(\textit{Two or more transitions within } \Delta t | S(t) = S_i\right) = O\left((\Delta t)^2\right). \tag{2.1.11}$$

Proof. Suppose that the state for the system is S_i at time t. If two or more transitions occur within Δt, then the system goes to state S_j ($j \neq i$) and leaves S_j before $t + \Delta t$. The memoryless property of such transitions yields the following relationship:

$$\begin{aligned}
P\left(T_i + T_j \leq \Delta t\right) &\leq P\left(T_i \leq \Delta t, T_j \leq \Delta t\right) \\
&= P\left(T_i \leq \Delta t\right) P\left(T_j \leq \Delta t\right) \\
&= \left(1 - \lambda_i \Delta t + O(\Delta t)\right)\left(1 - \lambda_j \Delta t + O(\Delta t)\right) \\
&= \left(\sum_{k \neq i}^{M} \lambda_{ik} \Delta t + O\left(\Delta t\right)\right)\left(\sum_{l \neq j}^{M} \lambda_{jl} \Delta t + O(\Delta t)\right) \\
&\sim O\left((\Delta t)^2\right).
\end{aligned} \tag{2.1.12}$$

Let S_j go through any state except S_i. Equation (2.1.12) shows that the probability of two or more transitions occurring in a time interval Δt is

$$\begin{aligned} & P(\text{Two or more transitions by } \Delta t | S(t) = S_i) \\ & = \sum_{j \neq i}^{M} P\left(T_i + T_j \leq \Delta t\right) \\ & \sim O\left((\Delta t)^2\right). \end{aligned} \tag{2.1.13}$$

□

What we are interested in is the behavior of the buffer content, specifically, its probability distribution. In this case, it is reasonable for us to assume that the buffer never becomes empty, namely, $Q(t) > 0$, for $\forall t > 0$. Otherwise, we can split the analyzing process into several different time period, during each of which the buffer is non-empty, and in the time intervals between the periods, the buffer content is zero and unchanged. Then, we can analyze the buffer content for each non-empty period.

For each state S_i, let

$$W^i(t, x) = P\left\{Q(t) \leq x, S(t) = S_i\right\}, i = 1, \ldots, M, \tag{2.1.14}$$

which denotes the probability of the buffer content $Q(t)$ less or equal to a given level x while the system is in state S_i. Consequently, because states are disjointed, the probability distribution function of buffet content at time t, $F(t, x)$, can be described as the summation of $W^i(t + \Delta t, x)$ of all possible

states S_i in the state space S, namely,

$$F(t,x) = P\{Q(t) \le x\} = \sum_{i=1}^{M} W^i(t+\Delta t, x). \tag{2.1.15}$$

By equation (2.1.9) and equation (2.1.11), we have:

$$\begin{aligned} W^i(t+\Delta t,x) &= (\lambda_{ii}\Delta t)W^i\left(t, x-(r_i-C)\Delta t\right) && \text{(no transition)} \\ &+ \sum_{j\neq i}^{M} \lambda_{ji}\Delta t W^j\left(t, x-(r_j-C)\Delta t\right) && \text{(one transition)} \\ &+ O\left(\Delta t^2\right) && \text{(two or more transitions).} \end{aligned} \tag{2.1.16}$$

Correlate equation (2.1.16) with the relationship between λ_{ii} and λ_{ij} which described in equation (2.1.8), we have

$$\begin{aligned} W^i(t+\Delta t,x) = &\left(1-\sum_{j\neq i}^{M}\lambda_{ij}\Delta t\right) W^i\left(t, x-(r_i-C)\Delta t\right) \\ &+ \sum_{j\neq i}^{M} \lambda_{ji}\Delta t W^j\left(t, x-(r_j-C)\Delta t\right) + O\left(\Delta t^2\right). \end{aligned} \tag{2.1.17}$$

Reorder terms in equation (2.1.17), we have

$$\begin{aligned} &\frac{W^i(t+\Delta t,x)-W^i(t,x)}{\Delta t} + (r_i-C)\frac{W^i(t,x)-W^i\left(t,x-(r_i-C)\Delta t\right)}{(r_i-C)\Delta t} \\ &= \sum_{j\neq i}^{M}\left(-\lambda_{ij}W^i\left(t,x-(r_i-C)\Delta t\right) + \lambda_{ji}W^j\left(t,x-(r_j-C)\Delta t\right)\right) + \frac{O\left(\Delta t^2\right)}{\Delta t}. \end{aligned} \tag{2.1.18}$$

As $\Delta t \to 0$, the stochastic fluid queue is expressed as:

$$\frac{\partial W^i(t,x)}{\partial t} + (r_i-C)\frac{\partial W^i(t,x)}{\partial x} = \sum_{j\neq i}^{M}\left(\lambda_{ji}W^j(t,x) - \lambda_{ij}W^i(t,x)\right), \tag{2.1.19}$$

where $W^i(t,x)$ is the probability of buffer content bounded by a given level x, which defined in equation (2.1.14), r_i is the injection rate of state S_i, C is the link capacity and λ_{ij} is the transition rate between state S_i and S_j.

Suppose only one of the states in the state space S is an OFF state, denoted as S_1, and we assume that the system stays at S_1 *almost surely* at the initial point $t = 0$. By definition,

$$W^1(0,x) = P\{Q(0) \leq x, S(0) = S_1\} = P\{Q(0) \leq x\} \tag{2.1.20}$$

is the probability distribution function of initial buffer content $Q(0)$, given by external conditions of the system. Meanwhile, the probability $W^i(0,x)$ should be 0 for any other state S_i, where $i \neq 1$. Thus, initial conditions of the system can be described as the following equation,

$$W^i(0,x) = \begin{cases} f(x) & \text{when } i = 1 \\ 0 & \text{otherwise} \end{cases}, \tag{2.1.21}$$

where $f(x)$ is a general cumulative distribution function with respect to x, which can be derived given the distribution of initial buffer content $Q(0)$. Additionally, if we assume that the initial buffer is empty, namely $Q(0) = 0$, and the buffer content $Q(t)$ is *almost surely* nonnegative afterwards, then $f(x) = 1$.

Boundary condition $W^i(t,0)$ depicts the probability of the buffer content $Q(t)$ being empty at state S_i. For all ON states, the buffer is *almost surely* nonempty.

Hence, the boundary conditions are described as

$$W^i(t,0) = \begin{cases} q_0(t) & \text{when } i = 1 \\ 0 & \text{otherwise} \end{cases}. \tag{2.1.22}$$

where $q_0(t)$ is a function with respect to time t, the value of which is the probability of $Q(t) = 0$. If we assume that the buffer content will never be empty then $q_0(t) = 0$.

Furthermore, assuming that $Q(t) < \infty$ for any $t < \infty$, by the definition of $W^i(t,x)$,

$$\lim_{x\to+\infty} \sum_{i=1}^{M} W^i(t,x) = \lim_{x\to\infty} \sum_{i=1}^{M} P\{Q(t) < x, S(t) = S_i\} = \lim_{x\to\infty} P\{Q(t) < x\} = 1, \tag{2.1.23}$$

which gives us a boundary condition for the system as $x \to \infty$. Condition (2.1.23) implies for all i, the solution $W^i(t,x)$ should be bounded as $x \to \infty$.

Therefore, the cumulative distribution functions of the Stochastic Fluid Queue are governed by

$$\boxed{\frac{\partial W^i(t,x)}{\partial t} + (r_i - C)\frac{\partial W^i(t,x)}{\partial x} = \sum_{j\neq i}^{M}\left(\lambda_{ji}W^j(t,x) - \lambda_{ij}W^i(t,x)\right), i = 1, \cdots, M} \tag{2.1.19}$$

with the initial condition

$$\boxed{W^i(0,x) = \begin{cases} f(x) & \text{when } i = 1 \\ 0 & \text{otherwise} \end{cases}} \tag{2.1.21}$$

and boundary conditions

$$\boxed{W^i(t,0) = \begin{cases} q_0(t) & \text{when } i = 1 \\ 0 & \text{otherwise,} \end{cases}} \tag{2.1.22}$$

and

$$\boxed{\lim_{x\to+\infty}\sum_{i=1}^{M} W^i(t,x) = 1}. \tag{2.1.23}$$

2.2 Transient Analysis

In this section, we analyze the transient behavior of the system elaborated in **Section 2.1**. For simplicity, a special case of SFQ fed by a single ON-OFF source is discussed. By taking Laplace transformation and inverse Laplace transformation, a theoretical solution of the SFQ is provided with given initial and boundary conditions.

Let $\mathcal{L}_t$ denotes the Laplace Transform with respect to t, and $f(t,x)$ is a continuous function with respect to t and x. Then, we have the following properties:

Property 1.

$$\mathcal{L}_t\left\{\frac{\partial f(t,x)}{\partial t}\right\} = s\hat{f}(s,x) - f(0,x). \tag{2.2.1}$$

Property 2.

$$\mathcal{L}_t\left\{\frac{\partial f(t,x)}{\partial x}\right\} = \frac{d}{dx}\hat{f}(s,x). \tag{2.2.2}$$

We apply these properties to perform transient analysis of the solutions for the SFQ.

For the special case of a single ON-OFF source, the state space are constructed as $S = \{S_1, S_2\}$, where S_1 is the initial OFF state, and S_2 is the incremental ON state. Let $\phi_i = r_i - C, i = 1,2$ denote the net injection rate of state i. Then the SFQ will be simplified to a couple system of the form:

$$\begin{aligned} \frac{\partial W^1(t,x)}{\partial t} + \phi_1\frac{\partial W^1(t,x)}{\partial x} &= -\lambda_{12}W^1(t,x) + \lambda_{21}W^2(t,x) \\ \frac{\partial W^2(t,x)}{\partial t} + \phi_2\frac{\partial W^2(t,x)}{\partial x} &= \lambda_{12}W^1(t,x) - \lambda_{21}W^2(t,x) \end{aligned}, \tag{2.2.3}$$

subject to the initial conditions

$$W^1(0,x) = 1 \qquad W^2(0,x) = 0. \tag{2.2.4}$$

and boundary conditions

$$W^1(t,0) = q_0(t) \qquad W^2(t,0) = 0. \tag{2.2.5}$$

and

$$\lim_{x\to+\infty} \quad W^1(t,x) + W^2(t,x) = 1 \tag{2.2.6}$$

where $q_0(t)$ is the probability of the buffer to be empty with respect to time t.

Take Laplace transform for equations (2.2.3) with respect to time t, yielding

$$\begin{aligned} s\hat{W}^1(s,x) - W^1(0,x) + \phi_1 \frac{d\hat{W}^1(s,x)}{dx} &= -\lambda_{12}\hat{W}^1(s,x) + \lambda_{21}\hat{W}^2(s,x) \\ s\hat{W}^2(s,x) - W^2(0,x) + \phi_2 \frac{d\hat{W}^2(s,x)}{dx} &= \lambda_{12}\hat{W}^1(s,x) - \lambda_{21}\hat{W}^2(s,x) \end{aligned} \tag{2.2.7}$$

Plug the initial condition in, new equations after reconstruction are given as

$$\begin{aligned} \frac{d\hat{W}^1(s,x)}{dx} &= -\frac{\lambda_{12}+s}{\phi_1}\hat{W}^1(s,x) + \frac{\lambda_{21}}{\phi_1}\hat{W}^2(s,x) + \frac{1}{\phi_1} \\ \frac{d\hat{W}^2(s,x)}{dx} &= \frac{\lambda_{12}}{\phi_2}\hat{W}^1(s,x) - \frac{\lambda_{21}+s}{\phi_2}\hat{W}^2(s,x), \end{aligned} \tag{2.2.8}$$

subject to the initial conditions,

$$\begin{aligned} \hat{W}^1(s,0) &= \mathcal{L}_t\{q_0(t)\} := \hat{q}_0(s), \\ \hat{W}^2(s,0) &= \mathcal{L}_t\{0\} = 0. \end{aligned} \tag{2.2.9}$$

Let

$$\hat{\mathbf{W}} = \hat{\mathbf{W}}(s,x) = \begin{pmatrix} \hat{W}^1(s,x) \\ \hat{W}^2(s,x) \end{pmatrix}, \tag{2.2.10}$$

denote the vector function with respect to a single variable x. then general form for equations (2.2.8) can be written as

$$\frac{d\hat{\mathbf{W}}(x)}{dx} = \mathbf{A} \cdot \hat{\mathbf{W}} + \mathbf{H}, \tag{2.2.11}$$

where

$$\mathbf{A} = \begin{pmatrix} -\dfrac{\lambda_{12}+s}{\phi_1} & \dfrac{\lambda_{21}}{\phi_1} \\ \dfrac{\lambda_{12}}{\phi_2} & -\dfrac{\lambda_{21}+s}{\phi_2} \end{pmatrix} \tag{2.2.12}$$

and

$$\mathbf{H} = \begin{pmatrix} \dfrac{1}{\phi_1} \\ 0 \end{pmatrix}, \tag{2.2.13}$$

subject to the initial conditions

$$\hat{\mathbf{W}}(s,0) = \begin{pmatrix} \hat{q}_0(s) \\ 0 \end{pmatrix}, \tag{2.2.14}$$

where

$$\hat{q}_0(s) = \mathcal{L}_t \left\{ q_0(t) \right\}. \tag{2.2.15}$$

First, we should find the solution for the homogeneous differential equations:

$$\frac{d\hat{\mathbf{W}}}{dx} = \mathbf{A} \cdot \hat{\mathbf{W}}. \tag{2.2.16}$$

To solve the equation system, first we calculate the eigenvalues of $\mathbf{A}$. Let

$\omega_0(s), \omega_1(s)$ be the eigenvalues of $\mathbf{A}$. $\omega_0(s), \omega_1(s)$ are the roots of function:

$$\begin{vmatrix} -\frac{1}{\phi_1}(\lambda_{12}+s)-\omega & \frac{1}{\phi_1}\lambda_{21} \\ \frac{1}{\phi_2}\lambda_{12} & -\frac{1}{\phi_2}(\lambda_{21}+s)-\omega \end{vmatrix} = 0, \tag{2.2.17}$$

which can also be written as

$$\phi_1\phi_2\omega^2 + [(\phi_1+\phi_2)s + \lambda_{12}\phi_2 + \lambda_{21}\phi_1]\omega + s(s+\lambda_{12}+\lambda_{21}) = 0. \tag{2.2.18}$$

Solving the equation above yields

$$\begin{aligned} \omega_0(s) &= -\frac{(\phi_1+\phi_2)s + \lambda_{12}\phi_2 + \lambda_{21}\phi_1}{2\phi_1\phi_2} + \frac{\sqrt{T(s)}}{2\phi_1\phi_2} \\ \omega_1(s) &= -\frac{(\phi_1+\phi_2)s + \lambda_{12}\phi_2 + \lambda_{21}\phi_1}{2\phi_1\phi_2} - \frac{\sqrt{T(s)}}{2\phi_1\phi_2}, \end{aligned} \tag{2.2.19}$$

where

$$T(s) = [(\phi_1+\phi_2)s + \lambda_{12}\phi_2 + \lambda_{21}(\phi_1)]^2 - 4\phi_1\phi_2 s(s+\lambda_{12}+\lambda_{21}), \tag{2.2.20}$$

with the assumption that $T(s) > 0$.

Thus, the eigenvectors of $\mathbf{A}$ are

$$\mathbf{V}_0 = \begin{pmatrix} \frac{(\lambda_{21}+s)+\phi_2\omega_0(s)}{\phi_2} \\ \frac{\lambda_{12}}{\phi_2} \end{pmatrix}, \tag{2.2.21}$$

$$\mathbf{V}_1 = \begin{pmatrix} \frac{(\lambda_{21}+s)+\phi_2\omega_1(s)}{\phi_2} \\ \frac{\lambda_{12}}{\phi_2} \end{pmatrix}. \tag{2.2.22}$$

Consequently, we have

$$\hat{\mathbf{W}} = K_0 \mathbf{V}_0 e^{\omega_0 x} + K_1 \mathbf{V}_1 e^{\omega_1 x}, \tag{2.2.23}$$

where K_0 and K_1 are constants to be determined by the boundary conditions. Let

$$\mathbf{\Phi} = \mathbf{\Phi}(s, x) =$$

$$\begin{pmatrix} \dfrac{(\lambda_{21} + s) + \phi_2 \omega_0(s)}{\phi_2} e^{\omega_0 x} & \dfrac{(\lambda_{21} + s) + \phi_2 \omega_1(s)}{\phi_2} e^{\omega_1 x} \\ \dfrac{\lambda_{12}}{\phi_2} e^{\omega_0 x} & \dfrac{\lambda_{12}}{\phi_2} e^{\omega_1 x} \end{pmatrix}, \tag{2.2.24}$$

then equation (2.2.23) can be reconstructed as

$$\hat{\mathbf{W}} = \mathbf{\Phi} \cdot \mathbf{K}, \tag{2.2.25}$$

where

$$\mathbf{K} = (K_0, K_1)^T \tag{2.2.26}$$

is an arbitrary constant vector with respect to x.

Now we try to solve the non-homogeneous equation system (2.2.11). Apply the method of variation of constants, equation (2.2.11) has solution with the form of

$$\hat{\mathbf{W}} = \mathbf{\Phi} \left(\mathbf{K} + \int_0^x \mathbf{\Phi}^{-1}(s, y) \cdot \mathbf{H} dy \right), \tag{2.2.27}$$

where $\mathbf{K}$ is determined by the initial conditions and

$$\mathbf{\Phi}^{-1}(s,x) = \frac{\phi_1\phi_2^2}{\lambda\sqrt{T(s)}}\cdot$$

$$\begin{pmatrix} \frac{\lambda_{12}}{\phi_2}e^{-\omega_0(s)x} & -\frac{\lambda_{21}+s+\phi_2\omega_1(s)}{\phi_2}e^{\omega_0(s)x} \\ -\frac{\lambda_{12}}{\phi_2}e^{-\omega_1(s)x} & \frac{\lambda_{21}+s+\phi_2\omega_0(s)}{\phi_2}e^{-\omega_1(s)x} \end{pmatrix}, \tag{2.2.28}$$

Plug in the initial condition, we have

$$\hat{\mathbf{W}}(s,0) = \mathbf{\Phi}(s,0)\left(\mathbf{K} + \int_0^0 \mathbf{\Phi}^{-1}(s,y)\cdot\mathbf{H}dy\right), \tag{2.2.29}$$

and consequently,

$$\mathbf{K} = \mathbf{\Phi}^{-1}(s,0)\,\hat{\mathbf{W}}(s,0). \tag{2.2.30}$$

Therefore we have the expression for $\hat{\mathbf{W}}(s,x)$ as follows

$$\hat{\mathbf{W}}(s,x) = \mathbf{\Phi}(s,x)\cdot\left(\Phi^{-1}(s,0)\cdot\hat{\mathbf{W}}(s,0) + \int_0^x \mathbf{\Phi}^{-1}(s,y)\cdot\mathbf{H}dy\right). \tag{2.2.31}$$

With the boundary condition

$$\hat{\mathbf{W}}(s,0) = \begin{pmatrix} \mathcal{L}_t\{q_0(t)\} \\ 0 \end{pmatrix} = \begin{pmatrix} \hat{q}_0(s) \\ 0 \end{pmatrix}, \tag{2.2.32}$$

substitute (2.2.28) and (2.2.32) into equation (2.2.31), we will get

$$\mathbf{\Phi}^{-1}(s,0)\cdot\hat{\mathbf{W}}(s,0) = \frac{\phi_1\phi_2}{\sqrt{T(s)}}\begin{pmatrix} \hat{q}_0(s) \\ -\hat{q}_0(s) \end{pmatrix} \tag{2.2.33}$$

and

$$\int_0^x \mathbf{\Phi}^{-1}(s,y)\cdot\mathbf{H}dy = \begin{pmatrix} -\frac{\phi_2}{\sqrt{T(s)}\omega_0(s)}\left(e^{-\omega_0(s)x}-1\right) \\ \frac{\phi_2}{\sqrt{T(s)}\omega_1(s)}\left(e^{-\omega_1(s)x}-1\right) \end{pmatrix}. \tag{2.2.34}$$

Thus,

$$\hat{\mathbf{W}}(s,x) = \begin{pmatrix} \frac{\lambda_{21}+s}{s(s+\lambda_{12}+\lambda_{21})} + \frac{1}{\sqrt{T(s)}}\left(\frac{\lambda_{21}+s+\phi_2\omega_0(s)}{\omega_0}e^{\omega_0(s)x} - \frac{\lambda_{21}+s+\phi_2\omega_1(s)}{\omega_1(s)}e^{\omega_1(s)x}\right) \\ +\phi_1\left(\frac{(\lambda_{21}+s+\phi_2\omega_0(s))}{\sqrt{T(s)}}e^{\omega_0(s)x} - \frac{(\lambda_{21}+s+\phi_2\omega_1(s))}{\sqrt{T(s)}}e^{\omega_1(s)x}\right)\hat{q}_0(s) \\ \\ \frac{\lambda_{12}}{s(s+\lambda_{12}+\lambda_{21})} + \frac{\lambda_{12}}{\sqrt{T(s)}}\left(\frac{e^{\omega_0(s)x}}{\omega_0(s)} - \frac{e^{\omega_1(s)x}}{\omega_1(s)}\right) \\ +\frac{\lambda_{12}\phi_1}{\sqrt{T(s)}}\left(e^{\omega_0(s)x} - e^{\omega_1(s)x}\right)\hat{q}_0(s) \end{pmatrix}. \tag{2.2.35}$$

The boundary condition (2.2.6) implies that $\hat{\mathbf{W}}(s,x)$ is bounded as $x\to\infty$. However, notice that $\omega_1(s) > 0$ for $s > 0$, and $e^{\omega_1(s)x}$ diverge to infinity as $x\to\infty$, in order to satisfy the boundary condition, $\hat{q}_0(s)$ has to be properly chosen so that the exponential terms with respect to x are canceled. Therefore, $\hat{q}_0(s)$ needs to satisfy

$$\hat{q}_0(s) = -\frac{1}{\phi_2\omega_1(s)} \quad , \tag{2.2.36}$$

which yields

$$\mathbf{K} = \begin{pmatrix} -\dfrac{\phi_2}{\sqrt{T(s)}\omega_1(s)} \\ \dfrac{\phi_2}{\sqrt{T(s)}\omega_1(s)} \end{pmatrix}. \tag{2.2.37}$$

Substituting into equation (2.2.29), $\hat{\mathbf{W}}(s,x)$ is simplified to

$$\begin{aligned} \hat{\mathbf{W}}(s,x) &= \mathbf{\Phi}(s,x) \cdot \begin{pmatrix} \dfrac{\phi_2}{\sqrt{T(s)}} \left(-\dfrac{e^{-\omega_0(s)x}}{\omega_0(s)} + \dfrac{1}{\omega_0(s)} - \dfrac{1}{\omega_1(s)} \right) \\ \dfrac{\phi_2}{\sqrt{T(s)}} \dfrac{e^{-\omega_1(s)x}}{\omega_1(s)} \end{pmatrix} \\ &= \begin{pmatrix} \dfrac{\lambda_{21}}{\lambda_{12}+\lambda_{21}} \cdot \dfrac{1}{s} + \dfrac{\lambda_{12}}{\lambda_{12}+\lambda_{21}} \cdot \dfrac{1}{s+\lambda_{12}+\lambda_{21}} - \dfrac{s+\lambda_{21}+\phi_2\omega_0(s)}{s(s+\lambda_{12}+\lambda_{21})} \cdot e^{\omega_0(s)x} \\ \dfrac{\lambda_{12}}{\lambda_{12}+\lambda_{21}} \cdot \left(\dfrac{1}{s} - \dfrac{1}{s+\lambda_{12}+\lambda_{21}} \right) \cdot \left(1 - e^{\omega_0(s)x} \right) \end{pmatrix}. \end{aligned} \tag{2.2.38}$$

Next, we take the inverse Laplace Transform of $\hat{\mathbf{W}}(s,x)$ where $\hat{W}^1(s,x)$ and $\hat{W}^2(s,x)$ are given by

$$\begin{aligned} \hat{W}^1(s,x) = &\left(\frac{\lambda_{21}}{\lambda_{12}+\lambda_{21}} \right) \left(\frac{1}{s} \right) + \left(\frac{\lambda_{12}}{\lambda_{12}+\lambda_{21}} \right) \left(\frac{1}{s+\lambda_{12}+\lambda_{21}} \right) \\ &- \left(\frac{s+\lambda_{21}+\phi_2\omega_0(s)}{s(s+\lambda_{12}+\lambda_{21})} \right) e^{\omega_0(s)x} \end{aligned} \tag{2.2.39}$$

and

$$\hat{W}^2(s,x) = \left(\frac{\lambda_{12}}{\lambda_{12}+\lambda_{21}} \right) \left(\frac{1}{s} - \frac{1}{s+\lambda_{12}+\lambda_{21}} \right) \left(1 - e^{\omega_0(s)x} \right). \tag{2.2.40}$$

Consider that

$$\begin{aligned} T(s) &= \left[(\phi_1+\phi_2)s+\lambda_{12}\phi_2+\lambda_{21}(\phi_1)\right]^2-4\phi_1\phi_2 s(s+\lambda_{12}+\lambda_{21}) \\ &= \left[(\phi_2-\phi_1)s+\lambda_{12}\phi_2-\lambda_{21}\phi_1\right]^2+4\lambda_{12}\lambda_{21}\phi_1\phi_2 \\ &= (\phi_2-\phi_1)^2\times\left(\left(s+\frac{\lambda_{12}\phi_2-\lambda_{21}\phi_1}{\phi_2-\phi_1}\right)^2+\frac{4\lambda_{12}\lambda_{21}\phi_1\phi_2}{(\phi_2-\phi_1)^2}\right). \end{aligned} \tag{2.2.41}$$

Recall the assumption that S_2 is the ON state and S_1 is the OFF state, we have $\phi_2 > 0 \geq \phi_1$, we have

$$\begin{aligned} \omega_0(s) &= -\frac{(\phi_1+\phi_2)s+\lambda_{12}\phi_2+\lambda_{21}\phi_1}{2\phi_1\phi_2}+\frac{\sqrt{T(s)}}{2\phi_1\phi_2} \\ &= -\frac{1}{2}\left(\left(\frac{1}{\phi_1}+\frac{1}{\phi_2}\right)s+\left(\frac{\lambda_{12}}{\phi_1}+\frac{\lambda_{21}}{\phi_2}\right)\right)+\frac{1}{2}\left(\frac{1}{\phi_1}-\frac{1}{\phi_2}\right)\sqrt{\frac{T(s)}{(r_2-r_1)^2}} \\ &= -\left(\frac{s}{\phi_2}+\frac{\lambda_{21}}{\phi_2}\right)-\frac{1}{2}\left(\frac{1}{\phi_1}-\frac{1}{\phi_2}\right)\left(s+\frac{\lambda_{12}\phi_2-\lambda_{21}\phi_1}{\phi_2-\phi_1}\right) \\ &\quad +\frac{1}{2}\left(\frac{1}{\phi_1}-\frac{1}{\phi_2}\right)\cdot\left[\left(s+\frac{\lambda_{12}\phi_2-\lambda_{21}\phi_1}{\phi_2-\phi_1}\right)^2+\frac{4\lambda_{12}\lambda_{21}\phi_1\phi_2}{(\phi_2-\phi_1)^2}\right]^{\frac{1}{2}}. \end{aligned} \tag{2.2.42}$$

Thus, $\omega_0(s)$ can be defined as

$$\omega_0(s) = \beta(s)+\eta(s), \tag{2.2.43}$$

where $\beta(s)$ and $\eta(s)$ are defined as

$$\beta(s) = -\left(\frac{1}{\phi_2}s+\frac{\lambda_{21}}{\phi_2}\right) \tag{2.2.44}$$

$$\eta(s) = b\left((s+a)-\left((s+a)^2-\alpha^2\right)^{\frac{1}{2}}\right), \tag{2.2.45}$$

and the constants a, b and α^2 are defined as

$$a = \frac{\lambda_{12}\phi_2 - \lambda_{21}\phi_1}{\phi_2 - \phi_1} \tag{2.2.46}$$

$$b = -\frac{1}{2}\left(\frac{1}{\phi_1} - \frac{1}{\phi_2}\right) \tag{2.2.47}$$

$$\alpha^2 = -\frac{4\lambda_{12}\lambda_{21}\phi_1\phi_2}{(\phi_2 - \phi_1)^2}. \tag{2.2.48}$$

Next, we take inverse Laplace Transform of $\hat{W}^1(s,x)$ with respect to s, which yields

$$W^1(t,x) = \begin{cases} \dfrac{\lambda_{21}}{\lambda_{12}+\lambda_{21}} + \dfrac{\lambda_{12}}{\lambda_{12}+\lambda_{21}} e^{-(\lambda_{12}+\lambda_{21})t}, & 0 < t < \dfrac{x}{\phi_2} \\ \dfrac{\lambda_{21}}{\lambda_{12}+\lambda_{21}} + \dfrac{\lambda_{12}}{\lambda_{12}+\lambda_{21}} e^{-(\lambda_{12}+\lambda_{21})t} \\ \qquad -e^{-\frac{\lambda_{21}}{\phi_2}x} \displaystyle\int_0^t f_1(t-v,x) \cdot h(v,x)\, dv, & t > \dfrac{x}{\phi_2}. \end{cases} \tag{2.2.49}$$

where

$$h(t,x) = \frac{b\alpha^2\phi_2}{2(\lambda_{12}+\lambda_{21})} e^{-at}\left(I_0[\rho(t,x)] - \frac{1}{\kappa^2(t,x)} I_2[\rho(t,x)]\right) \quad , \tag{2.2.50}$$

$$f_1(t,x) = 1 - e^{-(\lambda_{12}+\lambda_{21})\left(t-\frac{x}{\phi_2}\right)}, \tag{2.2.51}$$

$$\kappa(t,x) = \left(\frac{t+2bx}{t}\right)^{\frac{1}{2}} = \left(1 - \left(\frac{1}{\phi_1} - \frac{1}{\phi_2}\right)\frac{x}{t}\right)^{\frac{1}{2}}, \tag{2.2.52}$$

$$\rho(t,x) = \alpha\kappa(t,x)t, \tag{2.2.53}$$

and $I_n(x), n = 0, 1, 2$ are the modified Bessel functions of the first kind.

Similarly, we have

$$\begin{aligned} W^2(t,x) &= \mathcal{L}^{-1}\left\{\hat{W}^2(s,x)\right\} \\ &= \mathcal{L}^{-1}\left\{\left(\frac{\lambda_{12}}{\lambda_{12}+\lambda_{21}}\right)\left(\frac{1}{s}-\frac{1}{s+\lambda_{12}+\lambda_{21}}\right)\left(1-e^{\omega_0(s)x}\right)\right\} \\ &= \frac{\lambda_{12}}{\lambda_{12}+\lambda_{21}}\cdot\left(\mathcal{L}^{-1}\left\{\frac{1}{s}\right\}-\mathcal{L}^{-1}\left\{\frac{1}{s+\lambda_{12}+\lambda_{21}}\right\}\right. \\ &\qquad \left.-\mathcal{L}^{-1}\left\{\left(\frac{1}{s}-\frac{1}{s+\lambda_{12}+\lambda_{21}}\right)e^{\omega_0(s)x}\right\}\right), \end{aligned} \tag{2.2.54}$$

which yields

$$W^2(t,x) = \begin{cases} \dfrac{\lambda_{12}}{\lambda_{12}+\lambda_{21}}\left(1-e^{-(\lambda_{12}+\lambda_{21})t}\right), 0 < t < \dfrac{x}{\phi_2} \\ \dfrac{\lambda_{12}}{\lambda_{12}+\lambda_{21}}\left(1-e^{-(\lambda_{12}+\lambda_{21})t}\right. \\ \qquad \left.-e^{-\frac{\lambda_{21}}{\phi_2}x}\displaystyle\int_0^t f_1(t-v,x)\cdot g(v,x)\,dv\right), t > \dfrac{x}{\phi_2}, \end{cases} \tag{2.2.55}$$

where $f_1(t,x)$ is defined in (2.2.51) and $g(t,x)$ is defined as

$$g(t,x) = e^{-at}\left(\frac{\alpha}{2\kappa(t,x)}\left(\kappa(t,x)^2-1\right)I_1\left[\rho(t,x)\right]+\delta(t)\right) \tag{2.2.56}$$

where $\delta(t)$ is the Dirac function.

In summary, we get solutions of the Stochastic Fluid Queue which are shown as the following:

$$W^1(t,x) = \begin{cases} \dfrac{\lambda_{21}}{\lambda_{12}+\lambda_{21}} + \dfrac{\lambda_{12}}{\lambda_{12}+\lambda_{21}} e^{-(\lambda_{12}+\lambda_{21})t}, & 0 < t < \dfrac{x}{\phi_2} \\ \dfrac{\lambda_{21}}{\lambda_{12}+\lambda_{21}} + \dfrac{\lambda_{12}}{\lambda_{12}+\lambda_{21}} e^{-(\lambda_{12}+\lambda_{21})t} \\ \qquad -e^{-\frac{\lambda_{21}}{\phi_2}x} \displaystyle\int_0^t f_1(t-v,x) \cdot h(v,x)\, dv, & t > \dfrac{x}{\phi_2}. \end{cases} \tag{2.2.49}$$

and

$$W^2(t,x) = \begin{cases} \dfrac{\lambda_{12}}{\lambda_{12}+\lambda_{21}} \left(1 - e^{-(\lambda_{12}+\lambda_{21})t}\right), 0 < t < \dfrac{x}{\phi_2} \\ \dfrac{\lambda_{12}}{\lambda_{12}+\lambda_{21}} \left(1 - e^{-(\lambda_{12}+\lambda_{21})t} \right. \\ \qquad \left. -e^{-\frac{\lambda_{21}}{\phi_2}x} \displaystyle\int_0^t f_1(t-v,x) \cdot g(v,x)\, dv \right), t > \dfrac{x}{\phi_2}, \end{cases} \tag{2.2.55}$$

where

$$h(t,x) = \frac{b\alpha^2\phi_2}{2(\lambda_{12}+\lambda_{21})} e^{-at} \left(I_0[\rho(t,x)] - \frac{1}{\kappa^2(t,x)} I_2[\rho(t,x)] \right), \tag{2.2.50}$$

$$g(t,x) = e^{-at} \left(\frac{\alpha}{2\kappa(t,x)} \left(\kappa(t,x)^2 - 1\right) I_1[\rho(t,x)] + \delta(t) \right), \tag{2.2.56}$$

$$\kappa(t,x) = \left(1 - \left(\frac{1}{\phi_1} - \frac{1}{\phi_2}\right)\frac{x}{t}\right)^{\frac{1}{2}}, \tag{2.2.52}$$

$$\rho(t,x) = \alpha\kappa(t,x)t, \tag{2.2.53}$$

and

$$f_1(t,x) = 1 - e^{-(\lambda_{12}+\lambda_{21})\left(t - \frac{x}{\phi_2}\right)} \tag{2.2.51}$$

where the theoretical details of computing the inverse Laplace transform can be found in **Appendix C** (see **Section** 7.3).

2.3 Asymptotic Expansions of Solutions

It is noteworthy to mention that solutions given by (2.2.49) and (2.2.55) are not of concise form, especially the inclusion of modified Bessel functions in the integral expression. Therefore, understanding the transient behavior is limited. To overcome these restrictions, we here introduce a comprehensive expansion for a more straightforward analysis of the properties of $W^1(t,x)$ and $W^2(t,x)$. The vital approximation of the solutions can be provided with only the first few leading terms of them. To be specific, we can try to represent the convolution expressions from equation (2.2.49) and (2.2.55) in terms of asymptotic expansions, which the first few terms will show the dominating behavior. This expansion makes our analysis easier while also being accurate. Additionally, the solution can be easily achieved computationally. In this section, we will expand Bessel functions for short-time and long-time behavior as $t \to 0$ and $t \to \infty$, respectively.

Notice that the integrals in solutions (2.2.49) and (2.2.55) can be expressed as (2.3.1) and (2.3.2),

$$\begin{aligned} e^{\frac{-\lambda_{21}}{\phi_2}x}\int_0^t f_1(t-v,x)h\left(v,x\right)dv &= -e^{\frac{-\lambda_{21}}{\phi_2}x}\int_0^t h(v,x)dv \\ &+ e^{\left\{-(\lambda_{12}+\lambda_{21})t+\frac{\lambda_{12}}{\phi_2}x\right\}}\int_0^t e^{(\lambda_{12}+\lambda_{21})v}h(v,x)dv, \end{aligned} \tag{2.3.1}$$

$$e^{-\frac{\lambda_{21}}{\phi_2}x}\int_0^t f_1(t-v,x)g\left(v,x\right)dv = -e^{\frac{-\lambda_{21}}{\phi_2}x}\int_0^t g(v,x)dv + e^{\left\{-(\lambda_{12}+\lambda_{21})t+\frac{\lambda_{12}}{\phi_2}x\right\}}\int_0^t e^{(\lambda_{12}+\lambda_{21})v}g(v,x)dv. \tag{2.3.2}$$

Therefore, when $t > \frac{x}{\phi_2}$

$$W^1\left(t,x\right) = \frac{\lambda_{21}}{\lambda_{12}+\lambda_{21}} + \frac{\lambda_{12}}{\lambda_{12}+\lambda_{21}}e^{-(\lambda_{12}+\lambda_{21})t} + e^{\frac{-\lambda_{21}}{\phi_2}x}\int_0^t h(v,x)dv - e^{\left\{-(\lambda_{12}+\lambda_{21})t+\frac{\lambda_{12}}{\phi_2}x\right\}}\int_0^t e^{(\lambda_{12}+\lambda_{21})v}h(v,x)dv, \tag{2.3.3}$$

$$W^2\left(t,x\right) = \frac{\lambda_{12}}{\lambda_{12}+\lambda_{21}}\left(1 - e^{-(\lambda_{12}+\lambda_{21})t} + e^{\frac{-\lambda_{21}}{\phi_2}x}\int_0^t g(v,x)dv - e^{\left\{-(\lambda_{12}+\lambda_{21})t+\frac{\lambda_{12}}{\phi_2}x\right\}}\int_0^t e^{(\lambda_{12}+\lambda_{21})v}g(v,x)dv\right). \tag{2.3.4}$$

The key terms we should focus on to analyze $W^1(t,x)$ and $W^2(t,x)$ are $\int_0^t h(v,x)dv$, $\int_0^t e^{(\lambda_{12}+\lambda_{21})v}h(v,x)dv$, $\int_0^t g(v,x)dv$, and $\int_0^t e^{(\lambda_{12}+\lambda_{21})v}g(v,x)dv$.

2.3.1 Short-time Behavior Analysis — Power Series Expansion

For short-time behavior, from equation (2.2.53) we know that for any $x \in \mathbb{R}$, $\rho = \rho(t, x) \to 0$ as $t \to 0$. The modified Bessel function $I_n(\rho)$ can be expressed using power series expanding approach around $\rho = 0$ as,

$$I_n(\rho) = I_n^P(\rho) = \left(\frac{\rho}{2}\right)^n \sum_{k=0}^{\infty} \frac{1}{\Gamma(k+1)\,\Gamma(n+1+k)} \left(\frac{\rho}{2}\right)^{2k}. \tag{2.3.5}$$

Expression (2.3.53) is defined as the **power series** of $I_n(\rho)$, denoted by $I_n^P(\rho)$.

Let $I_n^{P,m}(\rho)$ denotes the sum of preceding m terms of $I_n^P(\rho)$, namely,

$$I_n^{P,m}(\rho) = \left(\frac{\rho}{2}\right)^n \sum_{k=0}^{m} \frac{1}{\Gamma(k+1)\,\Gamma(\gamma+1+k)} \left(\frac{\rho}{2}\right)^{2k}, \tag{2.3.6}$$

then

$$\begin{aligned} \left|I_n(\rho) - I_n^{P,m}(\rho)\right| &= \left|\left(\frac{\rho}{2}\right)^n \sum_{k=m+1}^{\infty} \frac{1}{\Gamma(k+1)\,\Gamma(\gamma+1+k)} \left(\frac{\rho}{2}\right)^{2k}\right| \\ &< \left|\left(\frac{\rho}{2}\right)^n \sum_{k=m+1}^{\infty} \left(\frac{\rho^k}{\Gamma(k+1)}\right)^2\right| \\ &< \left|\left(\frac{\rho}{2}\right)^n o(\rho^{2m})\right| \\ &\sim o(\rho^m). \end{aligned} \tag{2.3.7}$$

Thus, as $\rho \to 0$,

$$\lim_{m\to\infty} I_n^{P,m}(\rho) = I_n(\rho), \tag{2.3.8}$$

which means it is reasonable for us to use power series to estimate $I_n(\rho)$ for small ρ.

Substitute expression (2.3.53) into (2.2.50) and (2.2.56), we have the **power series** expansions of $h(t,x)$ and $g(t,x)$ as

$$\begin{aligned} h(t,x) &\sim \frac{\lambda_{12}\lambda_{21}\phi_2}{(\phi_2-\phi_1)(\lambda_{12}+\lambda_{21})}e^{-at}\cdot\left(\sum_{m=0}^{\infty}\frac{1}{\Gamma^2(m+1)}\left(\frac{\alpha(t^2+2bxt)^{\frac{1}{2}}}{2}\right)^{2m}\right. \\ &\left.-\frac{t}{t+2bx}\left(\frac{\alpha(t^2+2bxt)^{\frac{1}{2}}}{2}\right)^{2}\sum_{m=0}^{\infty}\frac{1}{\Gamma(m+1)\Gamma(m+3)}\left(\frac{\alpha(t^2+2bxt)^{\frac{1}{2}}}{2}\right)^{2m}\right) \\ &\sim \frac{\lambda_{12}\lambda_{21}\phi_2}{(\phi_2-\phi_1)(\lambda_{12}+\lambda_{21})}e^{-at}\cdot\left(\sum_{m=0}^{\infty}\left(\frac{\alpha}{2}\right)^{2m}\frac{(t^2+2bxt)^m}{\Gamma^2(m+1)}\left(1-\frac{t^2\left(\frac{\alpha}{2}\right)^2}{(m+1)(m+2)}\right)\right) \end{aligned} \tag{2.3.9}$$

and

$$\begin{aligned} g(t,x) &\sim \delta(t)+\alpha bx(t^2+2bxt)^{-\frac{1}{2}}e^{-at}\left(\frac{\alpha(t^2+2bxt)^{\frac{1}{2}}}{2}\times\right. \\ &\left.\sum_{m=0}^{\infty}\frac{1}{\Gamma(m+1)\Gamma(m+2)}\left(\frac{\alpha(t^2+2bxt)^{\frac{1}{2}}}{2}\right)^{2m}\right) \\ &\sim \delta(t)+\frac{\lambda_{12}\lambda_{21}x}{\phi_2-\phi_1}e^{-at}\cdot\left(\sum_{m=0}^{\infty}\left(\frac{\alpha}{2}\right)^{2m}\frac{(t^2+2bxt)^m}{\Gamma(m+1)\Gamma(m+2)}\right). \end{aligned} \tag{2.3.10}$$

Therefore,

$$\begin{aligned}
&\int_0^t h(v,x)dv \\
&\sim \frac{\lambda_{12}\lambda_{21}\phi_2}{(\phi_2-\phi_1)(\lambda_{12}+\lambda_{21})}\cdot\sum_{m=0}^{\infty}\frac{\alpha^{2m}}{\Gamma^2(m+1)2^{2m}}\times \\
&\qquad\int_0^t e^{-av}\cdot(v^2+2bxv)^m\left(1-\frac{v^2\left(\frac{\alpha}{2}\right)^2}{(m+1)(m+2)}\right)dv \\
&\sim \frac{\lambda_{12}\lambda_{21}\phi_2}{(\phi_2-\phi_1)(\lambda_{12}+\lambda_{21})}\cdot\sum_{m=0}^{\infty}\frac{\alpha^{2m}}{\Gamma^2(m+1)2^{2m}}\times \\
&\left(\int_0^t e^{-av}\cdot(v^2+2bxv)^m dv-\frac{\alpha^2}{4(m+1)(m+2)}\int_0^t e^{-av}\cdot(v+2bx)^m v^{m+2}dv\right)
\end{aligned} \tag{2.3.11}$$

and

$$\begin{aligned}
&\int_0^t e^{(\lambda_{12}+\lambda_{21})v}h(v,x)dv \\
&\sim \frac{\lambda_{12}\lambda_{21}\phi_2}{(\phi_2-\phi_1)(\lambda_{12}+\lambda_{21})}\cdot\sum_{m=0}^{\infty}\frac{\alpha^{2m}}{\Gamma^2(m+1)2^{2m}}\times \\
&\left(\int_0^t e^{-\tilde{a}v}\cdot(v^2+2bxv)^m dv\ -\frac{\alpha^2}{4(m+1)(m+2)}\int_0^t e^{-\tilde{a}v}\cdot(v+2bx)^m v^{m+2}dv\right).
\end{aligned} \tag{2.3.12}$$

Analogously,

$$\begin{aligned}
&\int_0^t g(v,x)dv \\
&\sim \int_0^t \delta(t)+\frac{\lambda_{12}\lambda_{21}x}{\phi_2-\phi_1}e^{-av}\cdot\left(\sum_{m=0}^{\infty}\left(\frac{\alpha}{2}\right)^{2m}\frac{(v^2+2bxv)^m}{\Gamma(m+1)\Gamma(m+2)}\right)dv \\
&\sim 1+\frac{\lambda_{12}\lambda_{21}x}{\phi_2-\phi_1}\int_0^t\sum_{m=0}^{\infty}\left(\frac{\alpha}{2}\right)^{2m}\frac{(v^2+2bxv)^m e^{-av}}{\Gamma(m+1)\Gamma(m+2)}dv \\
&\sim 1+\frac{\lambda_{12}\lambda_{21}x}{\phi_2-\phi_1}\sum_{m=0}^{\infty}\frac{\alpha^{2m}}{2^{2m}\Gamma(m+1)\Gamma(m+2)}\int_0^t(v^2+2bxv)^m e^{-av}dv
\end{aligned} \tag{2.3.13}$$

and

$$\int_0^t e^{(\lambda_{12}+\lambda_{21})v} g(v,x)dv \sim 1 + \frac{\lambda_{12}\lambda_{21}x}{\phi_2-\phi_1} \times \sum_{m=0}^{\infty} \frac{\alpha^{2m}}{2^{2m}\Gamma(m+1)\Gamma(m+2)} \int_0^t (v^2+2bxv)^m e^{-\tilde{a}v} dv \tag{2.3.14}$$

where a and $\tilde{a}$ are defined as

$$a = \frac{\lambda_{12}\phi_2 - \lambda_{21}\phi_1}{\phi_2-\phi_1}, \qquad \tilde{a} = \frac{\lambda_{12}\phi_1 - \lambda_{21}\phi_2}{\phi_2-\phi_1}, \tag{2.3.15}$$

α^2 and b are defined in (2.2.48) and (2.2.47) respectively.

For any positive integer m,

$$(v+2bx)^m = \sum_{k=0}^{m} \binom{m}{k} v^k (2bx)^{m-k}, \tag{2.3.16}$$

Thus,

$$\begin{aligned} \int_0^t (v+2bx)^m v^m e^{-av} dv &= \int_0^t \sum_{k=0}^{m} \binom{m}{k} (2bx)^{m-k} v^{m+k} e^{-av} dv \\ &= \sum_{k=0}^{m} \binom{m}{k} (2bx)^{m-k} \int_0^t v^{m+k} e^{-av} dv, \end{aligned} \tag{2.3.17}$$

where

$$\begin{aligned} \int_0^t v^{m+k} e^{-av} dv &= -\frac{1}{a^{m+k+1}} \left(\Gamma(m+k+1, at) - \Gamma(m+k+1, 0)\right) \\ &= -\frac{1}{a^{m+k+1}} (m+k)! \left(e^{-at} \sum_{l=0}^{m+k} \frac{(at)^l}{l!} - 1 \right). \end{aligned} \tag{2.3.18}$$

From that step we expand the integrals as

$$\int_0^t (v+2bx)^m v^m e^{-av} dv = \sum_{k=0}^{m} \binom{m}{k} \frac{(2bx)^{m-k}(m+k)!}{a^{m+k+1}} \left(1 - e^{-at} \sum_{l=0}^{m+k} \frac{(at)^l}{l!} \right), \tag{2.3.19}$$

and

$$\int_0^t (v+2bx)^m v^{m+2} e^{-av} dv = \sum_{k=0}^{m} \binom{m}{k} \frac{(2bx)^{m-k}(m+k+2)!}{a^{m+k+3}} \left(1 - e^{-at} \sum_{l=0}^{m+k+2} \frac{(at)^l}{l!}\right). \tag{2.3.20}$$

Consequently, we get the power series expansions of the integrals of h as:

$$\int_0^t h(v,x)dv = \frac{\lambda_{12}\lambda_{21}\phi_2}{(\phi_2-\phi_1)(\lambda_{12}+\lambda_{21})} \sum_{m=0}^{\infty} \frac{\alpha^{2m}\Omega_m(a,b,a;x,t)}{\Gamma^2(m+1)2^{2m}}, \tag{2.3.21}$$

$$\int_0^t e^{(\lambda_{12}+\lambda_{21})v} h(v,x)dv = \frac{\lambda_{12}\lambda_{21}\phi_2}{(\phi_2-\phi_1)(\lambda_{12}+\lambda_{21})} \sum_{m=0}^{\infty} \frac{\alpha^{2m}\Omega_m(a,b,\tilde{a};x,t)}{\Gamma^2(m+1)2^{2m}}, \tag{2.3.22}$$

where

$$\Omega_m(a,b,\gamma;x,t) = \sum_{k=0}^{m} \binom{m}{k} \frac{(2bx)^{m-k}(m+k)!}{a^{m+k+1}} \times \left\{1 - e^{-\gamma t} \sum_{l=0}^{m+k} \frac{(\gamma t)^l}{l!} \right.$$

$$\left. - \frac{\alpha^2}{4(m+1)(m+2)} \sum_{k=0}^{m} \binom{m}{k} \frac{(2bx)^{m-k}(m+k+2)!}{a^{m+k+3}} \left(1 - e^{-\gamma t} \sum_{l=0}^{m+k+2} \frac{(\gamma t)^l}{l!}\right)\right\}, \tag{2.3.23}$$

Similarly,

$$\int_0^t g(v,x)dv = 1 + \frac{\lambda_{12}\lambda_{21}x}{\phi_2-\phi_1} \sum_{m=0}^{\infty} \frac{\alpha^{2m}\chi_m(a,b,a;x,t)}{2^{2m}\Gamma(m+1)\Gamma(m+2)}, \tag{2.3.24}$$

$$\int_0^t e^{(\lambda_{12}+\lambda_{21})v} g(v,x)dv = 1 + \frac{\lambda_{12}\lambda_{21}x}{\phi_2-\phi_1} \times \sum_{m=0}^{\infty} \frac{\alpha^{2m}\chi_m(a,b,\tilde{a};x,t)}{2^{2m}\Gamma(m+1)\Gamma(m+2)}, \tag{2.3.25}$$

where

$$\chi_m(a,b,\gamma;x,t) = \sum_{k=0}^{m} \binom{m}{k} \frac{(2bx)^{m-k}(m+k)!}{a^{m+k+1}} \left(1 - e^{-\gamma t} \sum_{l=0}^{m+k} \frac{(\gamma t)^l}{l!}\right). \tag{2.3.26}$$

In conclusion, for short time, the solution $W^1(t,x)$ and $W^2(t,x)$ can be expressed as

$$W^1(t,x) = \begin{cases} \dfrac{\lambda_{21}}{\lambda_{12}+\lambda_{21}} + \dfrac{\lambda_{12}}{\lambda_{12}+\lambda_{21}} e^{-(\lambda_{12}+\lambda_{21})t}, \text{ for } 0 < t < \dfrac{x}{\phi_2} \\ \\ \dfrac{\lambda_{21}}{\lambda_{12}+\lambda_{21}} + \dfrac{\lambda_{12}}{\lambda_{12}+\lambda_{21}} e^{-(\lambda_{12}+\lambda_{21})t} \\ + \dfrac{\lambda_{12}\lambda_{21}\phi_2}{(\phi_2-\phi_1)(\lambda_{12}+\lambda_{21})} \displaystyle\sum_{m=0}^{\infty} \dfrac{\alpha^{2m}\Omega_m(a,b,a;x,t)}{\Gamma^2(m+1)2^{2m}} \\ - \dfrac{\lambda_{12}\lambda_{21}\phi_2}{(\phi_2-\phi_1)(\lambda_{12}+\lambda_{21})} \displaystyle\sum_{m=0}^{\infty} \dfrac{\alpha^{2m}\Omega_m(a,b,\tilde{a};x,t)}{\Gamma^2(m+1)2^{2m}}, \quad \text{for } t > \dfrac{x}{\phi_2} \end{cases} \tag{2.3.27}$$

and

$$W^2(t,x) = \begin{cases} \dfrac{\lambda_{12}}{\lambda_{12}+\lambda_{21}} \left(1 - e^{-(\lambda_{12}+\lambda_{21})t}\right), \text{ for } 0 < t < \dfrac{x}{\phi_2} \\ \\ \dfrac{\lambda_{12}}{\lambda_{12}+\lambda_{21}} \Bigg[1 - e^{-(\lambda_{12}+\lambda_{21})t} \\ + e^{\frac{-\lambda_{21}}{\phi_2}x} \left(1 + \dfrac{\lambda_{12}\lambda_{21}x}{\phi_2-\phi_1} \displaystyle\sum_{m=0}^{\infty} \dfrac{\alpha^{2m}\chi_m(a,b,a;x,t)}{2^{2m}\Gamma(m+1)\Gamma(m+2)}\right) \\ - e^{-(\lambda_{12}+\lambda_{21})t+\frac{\lambda_{12}}{\phi_2}x} \left(1 + \dfrac{\lambda_{12}\lambda_{21}x}{\phi_2-\phi_1} \displaystyle\sum_{m=0}^{\infty} \dfrac{\alpha^{2m}\chi_m(a,b,\tilde{a};x,t)}{2^{2m}\Gamma(m+1)\Gamma(m+2)}\right)\Bigg], \\ \qquad \text{for } t > \frac{x}{\phi_2} \end{cases} \tag{2.3.28}$$

2.3.2 Long-time Behavior Analysis — Asymptotic Series Expansion

Because $\rho = \rho(t, x) \to \infty$ as $t \to \infty$, in order to analyze the asymptotic long-time behavior of $t \to \infty$, it is equivalent to analyze the situation where $\rho \to \infty$. Thus in this subsection we will mainly discuss the behavior of modified Bessel functions of the first kind $I_n(\rho)$ as $\rho \to \infty$. Notice that $I_n(\rho)$ can be expressed in the following integral form for any $n \in \mathbb{Z}$:

$$I_n(\rho) = \frac{1}{\pi} \int_0^\pi e^{\rho \cos\theta} \cos(n\theta)\, d\theta. \tag{2.3.29}$$

Let

$$\varphi(\theta) = \rho \cos\theta, \tag{2.3.30}$$

notice that $\varphi(0)$ is the global maximum of $\varphi(\theta)$ for $\theta \in (0, \pi)$, and that

$$\varphi'(0) = 0, \varphi''(0) = -\rho\cos(0) = -\rho < 0. \tag{2.3.31}$$

We apply Laplace's Method by replacing the exponential term $\varphi(\theta)$ with its local series expansion around 0

$$\varphi(\theta) \sim \varphi(0) + \varphi'(0)\theta + \frac{\varphi''(0)\theta^2}{2} \sim \rho(1 - \frac{\theta^2}{2}), \tag{2.3.32}$$

and substitute $cos(n\theta)$ with its Taylor's series expansion, and get

$$\begin{aligned} I_n(\rho) &\sim \frac{1}{\pi}\int_0^{\pi} e^{\rho\left(1-\frac{\theta^2}{2}\right)} \sum_{k=0}^{\infty} \frac{(-1)^k (n\theta)^{2k}}{(2k)!} d\theta \\ &\sim \frac{e^{\rho}}{\pi}\int_0^{\pi} e^{-\frac{\theta^2}{2}\rho} \sum_{k=0}^{\infty} \frac{(-1)^k (n\theta)^{2k}}{(2k)!} d\theta \\ &\sim \frac{e^{\rho}}{\pi}\sum_{k=0}^{\infty}\int_0^{\pi} e^{-\frac{\theta^2}{2}\rho} \frac{(-1)^k (n\theta)^{2k}}{(2k)!} d\theta. \end{aligned} \tag{2.3.33}$$

If we focus on the first term of equation (2.3.33), namely,

$$I_n(\rho) \sim \frac{e^{\rho}}{\pi}\int_0^{\pi} e^{-\rho\frac{\theta^2}{2}} d\theta, \tag{2.3.34}$$

and let $u = \theta \cdot \left(\frac{\rho}{2}\right)^{\frac{1}{2}}$, we will get

$$I_n(\rho) \sim \frac{e^{\rho}}{\pi}\left(\frac{2}{\rho}\right)^{\frac{1}{2}} \int_0^{\pi\sqrt{\frac{\rho}{2}}} e^{-u^2} du. \tag{2.3.35}$$

As $\rho \to \infty$, $I_n(\rho)$ becomes

$$\begin{aligned} I_n(\rho) &\sim \frac{e^{\rho}}{\pi}\left(\frac{2}{\rho}\right)^{\frac{1}{2}} \int_0^{\infty} e^{-u^2} du \\ &\sim \frac{e^{\rho}}{\sqrt{2\pi\rho}}. \end{aligned} \tag{2.3.36}$$

For more terms included, as $\rho \to \infty$, equation (2.3.33) becomes

$$\begin{aligned} I_n(\rho) &\sim \frac{e^\rho}{\pi} \sum_{k=0}^{\infty} \frac{(-1)^k n^{2k}}{(2k)!} \int_0^{\pi} e^{-\frac{\rho}{2}\theta^2} \theta^{2k} d\theta \\ &\sim \frac{e^\rho}{\pi} \sum_{k=0}^{\infty} \frac{(-1)^k n^{2k}}{(2k)!} \int_0^{\pi\left(\frac{\rho}{2}\right)^{\frac{1}{2}}} u^{2k} \cdot e^{-u^2} \left(\frac{2}{\rho}\right)^{k+\frac{1}{2}} du \\ &\sim \frac{e^\rho}{\pi} \sum_{k=0}^{\infty} \frac{(-1)^k n^{2k}}{(2k)!} \left(\frac{2}{\rho}\right)^{k+\frac{1}{2}} \int_0^{\infty} u^{2k} \cdot e^{-u^2} du. \end{aligned} \tag{2.3.37}$$

Because we have

$$\int_0^{\infty} u^{2l} e^{-u^2} du = \frac{(2l-1)!!}{2^{l+1}} \sqrt{\pi}, \tag{2.3.38}$$

as $\rho \to \infty$, expression (2.3.37) can be written as

$$\begin{aligned} I_n(\rho) &\sim \frac{e^\rho}{\pi} \left\{ \sum_{k=0}^{\infty} \frac{(-1)^k n^{2k}}{(2k)!} \left(\frac{2}{\rho}\right)^{k+\frac{1}{2}} \frac{(2k-1)!!}{2^{k+1}} \sqrt{\pi} \right\} \\ &\sim \frac{e^\rho}{\sqrt{2\pi\rho}} \sum_{k=0}^{\infty} \frac{(-1)^k n^{2k}}{(2k)!! \rho^k}. \end{aligned} \tag{2.3.39}$$

So far we have given an asymptotic expression for $I_n(\rho)$ as $\rho \to \infty$, denoted by $I_n^A(\rho)$, hereinafter called the **asymptotic series** of $I_n(\rho)$:

$$I_n^A(\rho) \sim \frac{e^\rho}{\sqrt{2\pi\rho}} \sum_{k=0}^{\infty} \frac{(-1)^k n^{2k}}{(2k)!! \rho^k}. \tag{2.3.40}$$

Let $I_n^{A,m}(\rho)$ denotes the sum of preceding m terms of $I_n^A(\rho)$, namely,

$$I_n^{A,m}(\rho) = \frac{e^\rho}{\sqrt{2\pi\rho}} \sum_{k=0}^{m} \frac{(-1)^k n^{2k}}{(2k)!! \rho^k}, \tag{2.3.41}$$

then

$$\left| I_n(\rho) - I_n^{A,m}(\rho) \right| = \left| \frac{e^\rho}{\sqrt{2\pi\rho}} \sum_{k=m+1}^{\infty} \frac{(-1)^k n^{2k}}{(2k)!! \rho^k} \right|. \tag{2.3.42}$$

Thus, as for $\forall \rho > 1$,

$$\lim_{m\to\infty} \left| I_n(\rho) - I_n^{A,m}(\rho) \right| = \lim_{m\to\infty} \left| \frac{e^{\rho}}{\sqrt{2\pi\rho}} \sum_{k=m+1}^{\infty} \frac{(-1)^k n^{2k}}{(2k)!!\rho^k} \right| \to 0 \tag{2.3.43}$$

and

$$\lim_{m\to\infty} I_n^{A,m}(\rho) = I_n(\rho), \tag{2.3.44}$$

which means $\{I_n^{A,m}(\rho)\}$ is a series of functions that converges to $I_n(\rho)$.

Substitute expression (2.3.40) into (2.2.50) and (2.2.56), we have the **asymptotic series** of $h(t,x)$ and $g(t,x)$ as

$$\begin{aligned} h(t,x) \sim & \frac{\lambda_{12}\lambda_{21}\phi_2}{(\phi_2-\phi_1)(\lambda_{12}+\lambda_{21})} e^{-at} \times \\ & \left[\frac{e^{\alpha(t^2+2bxt)^{\frac{1}{2}}}}{\sqrt{2\pi\alpha(t^2+2bxt)^{\frac{1}{2}}}} \left(1 - \frac{t}{t+2bx} \sum_{m=0}^{\infty} \frac{(-1)^m 2^{2m}}{(2m)!! \left(\alpha(t^2+2bxt)^{\frac{1}{2}} \right)^m} \right) \right] \\ \sim & \frac{\lambda_{12}\lambda_{21}\phi_2 \cdot e^{-at+\alpha(t^2+2bxt)^{\frac{1}{2}}}}{\sqrt{2\pi\alpha}(\phi_2-\phi_1)(\lambda_{12}+\lambda_{21})(t^2+2bxt)^{\frac{1}{4}}} \left(1 - \frac{t}{t+2bx} \sum_{m=0}^{\infty} \frac{(-1)^m 2^{2m}}{(2m)!! \alpha^m (t^2+2bxt)^{\frac{m}{2}}} \right) \end{aligned} \tag{2.3.45}$$

and

$$\begin{aligned} g(t,x) \sim & \delta(t) + \alpha b x (t^2+2bxt)^{-\frac{1}{2}} e^{-at} \times \\ & \left(\frac{e^{\alpha(t^2+2bxt)^{\frac{1}{2}}}}{\sqrt{2\pi\alpha(t^2+2bxt)^{\frac{1}{2}}}} \sum_{m=0}^{\infty} \frac{(-1)^m}{(2m)!! \left(\alpha(t^2+2bxt)^{\frac{1}{2}} \right)^m} \right) \\ \sim & \delta(t) + \frac{bx\sqrt{\alpha}}{\sqrt{2\pi}} \frac{e^{-at+\alpha(t^2+2bxt)^{\frac{1}{2}}}}{(t^2+2bxt)^{\frac{3}{4}}} \sum_{m=0}^{\infty} \frac{(-1)^m}{(2m)!! \alpha^m (t^2+2bxt)^{\frac{m}{2}}}. \end{aligned} \tag{2.3.46}$$

Therefore,

$$\int_0^t h(v,x)dv \sim \frac{\lambda_{12}\lambda_{21}\phi_2}{\sqrt{2\pi\alpha}(\phi_2-\phi_1)(\lambda_{12}+\lambda_{21})}\cdot \left(\int_0^t \frac{e^{-av+\alpha(v^2+2bxv)^{\frac{1}{2}}}}{(v^2+2bxv)^{\frac{1}{4}}}dv - \sum_{m=0}^{\infty}\frac{(-1)^m 2^{2m}}{(2m)!!\alpha^m}\int_0^t \frac{e^{-av+\alpha(v^2+2bxv)^{\frac{1}{2}}}}{v^{\frac{m}{2}+\frac{5}{4}}(v+2bx)^{\frac{m}{2}-\frac{3}{4}}}dv\right) \tag{2.3.47}$$

and

$$\int_0^t e^{(\lambda_{12}+\lambda_{21})v}h(v,x)dv \sim \frac{\lambda_{12}\lambda_{21}\phi_2}{\sqrt{2\pi\alpha}(\phi_2-\phi_1)(\lambda_{12}+\lambda_{21})}\cdot \left(\int_0^t \frac{e^{-\tilde{a}v+\alpha(v^2+2bxv)^{\frac{1}{2}}}}{(v^2+2bxv)^{\frac{1}{4}}}dv - \sum_{m=0}^{\infty}\frac{(-1)^m 2^{2m}}{(2m)!!\alpha^m}\int_0^t \frac{e^{-\tilde{a}v+\alpha(v^2+2bxv)^{\frac{1}{2}}}}{v^{\frac{m}{2}+\frac{5}{4}}(v+2bx)^{\frac{m}{2}-\frac{3}{4}}}dv\right) \tag{2.3.48}$$

Analogously,

$$\begin{aligned}\int_0^t g(v,x)dv &\sim \int_0^t \delta(v) + \frac{bx\sqrt{\alpha}}{\sqrt{2\pi}}\frac{e^{-av+\alpha(v^2+2bxv)^{\frac{1}{2}}}}{(v^2+2bxv)^{\frac{3}{4}}}\sum_{m=0}^{\infty}\frac{(-1)^m}{(2m)!!\left(\alpha(v^2+2bxv)^{\frac{1}{2}}\right)^m}dv \\ &\sim 1+\frac{bx\sqrt{\alpha}}{\sqrt{2\pi}}\sum_{m=0}^{\infty}\frac{(-1)^m}{(2m)!!\alpha^m}\int_0^t\frac{e^{-av+\alpha(v^2+2bxv)^{\frac{1}{2}}}}{(v^2+2bxv)^{\frac{m}{2}+\frac{3}{4}}}dv,\end{aligned} \tag{2.3.49}$$

and

$$\int_0^t e^{(\lambda_{12}+\lambda_{21})v}g(v,x)dv \sim 1+\frac{bx\sqrt{\alpha}}{\sqrt{2\pi}}\sum_{m=0}^{\infty}\frac{(-1)^m}{(2m)!!\alpha^m}\int_0^t\frac{e^{-\tilde{a}v+\alpha(v^2+2bxv)^{\frac{1}{2}}}}{(v^2+2bxv)^{\frac{m}{2}+\frac{3}{4}}}dv, \tag{2.3.50}$$

where $a, \tilde{a}$ are defined in equation (2.3.15), α^2 and b are defined in (2.2.48) and (2.2.47) respectively.

In conclusion, for long time, the asymptotic form of solutions for $W^1(t,x)$ and $W^2(t,x)$ can be expressed as

$$
\boxed{
\begin{aligned}
&W^1(t,x) = \\
&\begin{cases}
\dfrac{\lambda_{21}}{\lambda_{12}+\lambda_{21}} + \dfrac{\lambda_{12}}{\lambda_{12}+\lambda_{21}} e^{-(\lambda_{12}+\lambda_{21})t}, \text{ for } 0 < t < \dfrac{x}{\phi_2} \\
\\
\dfrac{\lambda_{21}}{\lambda_{12}+\lambda_{21}} + \dfrac{\lambda_{12}}{\lambda_{12}+\lambda_{21}} e^{-(\lambda_{12}+\lambda_{21})t} + e^{\frac{-\lambda_{21}}{\phi_2}x} \times \dfrac{\lambda_{12}\lambda_{21}\phi_2}{\sqrt{2\pi\alpha}(\phi_2-\phi_1)(\lambda_{12}+\lambda_{21})} \cdot \\
\quad \left(\displaystyle\int_0^t \frac{e^{-av+\alpha(v^2+2bxv)^{\frac{1}{2}}}}{(v^2+2bxv)^{\frac{1}{4}}} dv - \sum_{m=0}^{\infty} \frac{(-1)^m 2^{2m}}{(2m)!!\alpha^m} \int_0^t \frac{e^{-av+\alpha(v^2+2bxv)^{\frac{1}{2}}}}{v^{\frac{m}{2}+\frac{5}{4}}(v+2bx)^{\frac{m}{2}-\frac{3}{4}}} dv \right) \\
- e^{\left\{-(\lambda_{12}+\lambda_{21})t+\frac{\lambda_{12}}{\phi_2}x\right\}} \dfrac{\lambda_{12}\lambda_{21}\phi_2}{\sqrt{2\pi\alpha}(\phi_2-\phi_1)(\lambda_{12}+\lambda_{21})} \cdot \\
\quad \left(\displaystyle\int_0^t \frac{e^{-\tilde{a}v+\alpha(v^2+2bxv)^{\frac{1}{2}}}}{(v^2+2bxv)^{\frac{1}{4}}} dv - \sum_{m=0}^{\infty} \frac{(-1)^m 2^{2m}}{(2m)!!\alpha^m} \int_0^t \frac{e^{-\tilde{a}v+\alpha(v^2+2bxv)^{\frac{1}{2}}}}{v^{\frac{m}{2}+\frac{5}{4}}(v+2bx)^{\frac{m}{2}-\frac{3}{4}}} dv \right) \\
\quad \text{, for } t > \frac{x}{\phi_2}
\end{cases}
\end{aligned}
} \tag{2.3.51}
$$

$$
\boxed{
\begin{aligned}
&W^2(t,x) = \\
&\begin{cases}
\dfrac{\lambda_{12}}{\lambda_{12}+\lambda_{21}} \left(1 - e^{-(\lambda_{12}+\lambda_{21})t}\right), \text{ for } 0 < t < \dfrac{x}{\phi_2} \\
\\
\dfrac{\lambda_{12}}{\lambda_{12}+\lambda_{21}} \Big[1 - e^{-(\lambda_{12}+\lambda_{21})t} \\
+ e^{\frac{-\lambda_{21}}{\phi_2}x} \left(1 + \dfrac{bx\sqrt{\alpha}}{\sqrt{2\pi}} \displaystyle\sum_{m=0}^{\infty} \frac{(-1)^m}{(2m)!!\alpha^m} \int_0^t \frac{e^{-av+\alpha(v^2+2bxv)^{\frac{1}{2}}}}{(v^2+2bxv)^{\frac{m}{2}+\frac{3}{4}}} dv \right) \\
- e^{\left\{-(\lambda_{12}+\lambda_{21})t+\frac{\lambda_{12}}{\phi_2}x\right\}} \left(1 + \dfrac{bx\sqrt{\alpha}}{\sqrt{2\pi}} \displaystyle\sum_{m=0}^{\infty} \frac{(-1)^m}{(2m)!!\alpha^m} \int_0^t \frac{e^{-\tilde{a}v+\alpha(v^2+2bxv)^{\frac{1}{2}}}}{(v^2+2bxv)^{\frac{m}{2}+\frac{3}{4}}} dv \right) \Big] \\
\quad \text{, for } t > \frac{x}{\phi_2}
\end{cases}
\end{aligned}
} \tag{2.3.52}
$$

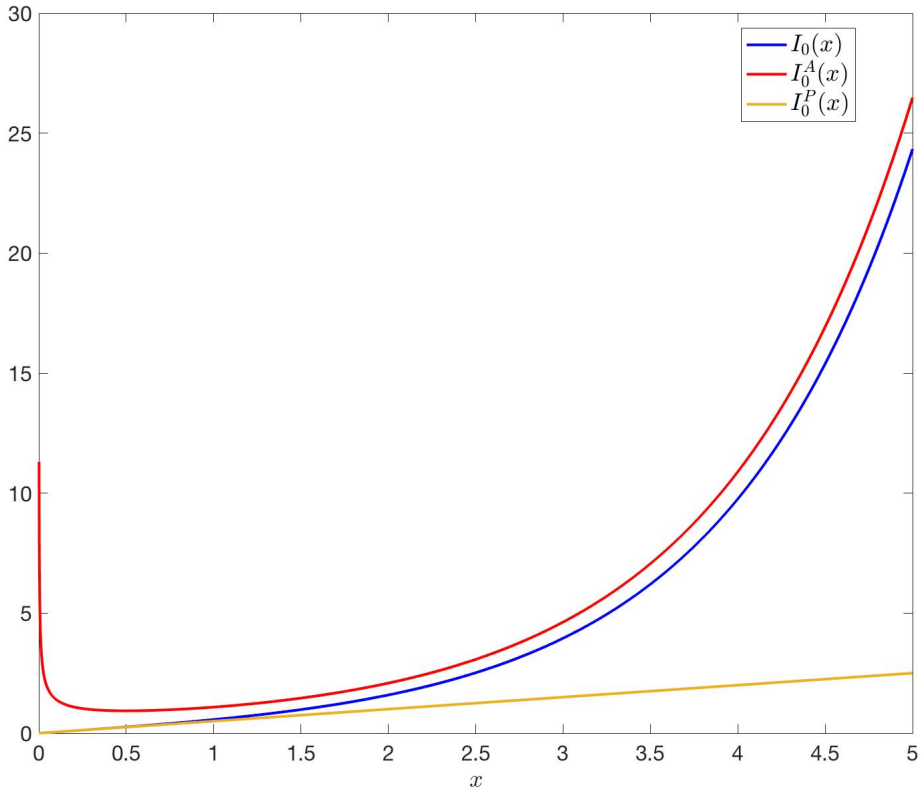

Figure 2.2: Leading Term of Asymptotic and Power Series for Bessel Functions $I_0(\rho)$

Figure 2.2 shows the relationship between the Bessel function $I_0(\rho)$, the first leading term of its asymptotic series and power series. We can conclude from the figure that the difference between Power Series and Bessel function is relatively small as ρ close to 0. Meanwhile, the difference of Asymptotic Series is small when ρ is sufficiently large. Another result can be drawn from the numerical experiment is that as we add more terms with higher orders into the series, the differences get smaller and smaller, which conforms to our expectation, except that when $\rho \to 0$ the Asymptotic Series goes to infinity.

2.3.3 Comprehensive Expansion

Consider that for short-time behavior $\rho = \rho(t, x) \to 0$ as $t \to 0$. Thus, $I_n(\rho)$ can be expressed in terms of the power series expansion

$$I_n^P(\rho) = \left(\frac{\rho}{2}\right)^n \sum_{k=0}^{\infty} \frac{1}{\Gamma(k+1)\,\Gamma(n+1+k)} \left(\frac{\rho}{2}\right)^{2k}. \tag{2.3.53}$$

If we use the terms up to order m of $I_n^P(\rho)$ as an approximation to $I_n(\rho)$, then the relative error of the remainder terms is

$$\begin{aligned} \varepsilon^P(\rho) &= \frac{\left\| I_n(\rho) - I_n^P(\rho) \right\|_2}{\left\| I_n(\rho) \right\|_2} \\ &\leq \frac{\left(\frac{\rho}{2}\right)^n \sum_{k=m+1}^{\infty} \frac{1}{\Gamma(k+1)\Gamma(n+1+k)} \left(\frac{\rho}{2}\right)^{2k}}{\left(\frac{\rho}{2}\right)^n \sum_{k=0}^{\infty} \frac{1}{\Gamma(k+1)\Gamma(n+1+k)} \left(\frac{\rho}{2}\right)^{2k}} \\ &\sim \mathcal{O}\left(\rho^{2m}\right), \end{aligned} \tag{2.3.54}$$

which decreases as ρ goes to 0.

Meanwhile, when we investigate the long-time behavior approximation, namely,

$$I_n^A(\rho) \sim \frac{e^{\rho}}{\sqrt{2\pi\rho}} \sum_{m=0}^{\infty} \frac{(-1)^m n^{2m}}{(2m)!!\rho^m}, \tag{2.3.55}$$

the relative error of the estimation with terms up to order m is

$$\begin{aligned}\varepsilon^A(\rho) &= \frac{\left\| I_n(\rho) - I_n^A(\rho) \right\|_2}{\left\| I_n(\rho) \right\|_2} \\ &\leq \frac{\frac{e^\rho}{\sqrt{2\pi\rho}} \sum_{k=m}^{\infty} \frac{(-1)^k n^{2k}}{(2k)!!\rho^k}}{\frac{e^\rho}{\sqrt{2\pi\rho}} \sum_{k=m}^{\infty} \frac{(-1)^k n^{2k}}{(2k)!!\rho^k}} \\ &\sim \mathcal{O}\left(\rho^{-m}\right).\end{aligned} \tag{2.3.56}$$

Thus, the $\varepsilon^A(\rho)$ will asymptotically decreases to zero as $\rho \to +\infty$.

A transparent observation is that $\varepsilon^A(\rho)$ and $\varepsilon^P(\rho)$ goes to opposite directions along with the variance of ρ. Consequently, starting from the critical point t_c, where

$$\left\| I_n\left(\rho\left(x, t_c\right)\right) - I_n^P\left(\rho\left(x, t_c\right)\right) \right\|_2 - \left\| I_n\left(\rho\left(x, t_c\right)\right) - I_n^A\left(\rho\left(x, t_c\right)\right) \right\|_2 < \varepsilon, \tag{2.3.57}$$

when t and $\rho(x,t)$ go to $+\infty$, the $\varepsilon^A(\rho)$ decreases, whereas when t and $\rho(x,t)$ go to 0, $\varepsilon^A(\rho)$ decreases. This property of error gives us a convenient way to control the error with the combination of the expansions. Let $\varepsilon^C(\rho)$ denote the combination approximation error. When $t < t_c$ and $\rho(x,t) < \rho(x,t_c)$, the power series are used for approximation, the error of which increasing with respect to ρ, so

$$\varepsilon^C(\rho) = \varepsilon^P(\rho) \leq \varepsilon^P(\rho(x,t_c)), \quad t < t_c. \tag{2.3.58}$$

On the other hand, When $t > t_c$ and $\rho(x,t) > \rho(x,t_c)$, the asymptotic series are used for approximation, the error of which decreasing with respect to ρ,

so

$$\varepsilon^C(\rho) = \varepsilon^A(\rho) \leq \varepsilon^A(\rho(x, t_c)), \quad t > t_c. \tag{2.3.59}$$

Such a behavior of error can be observed in **Figure** 2.3.

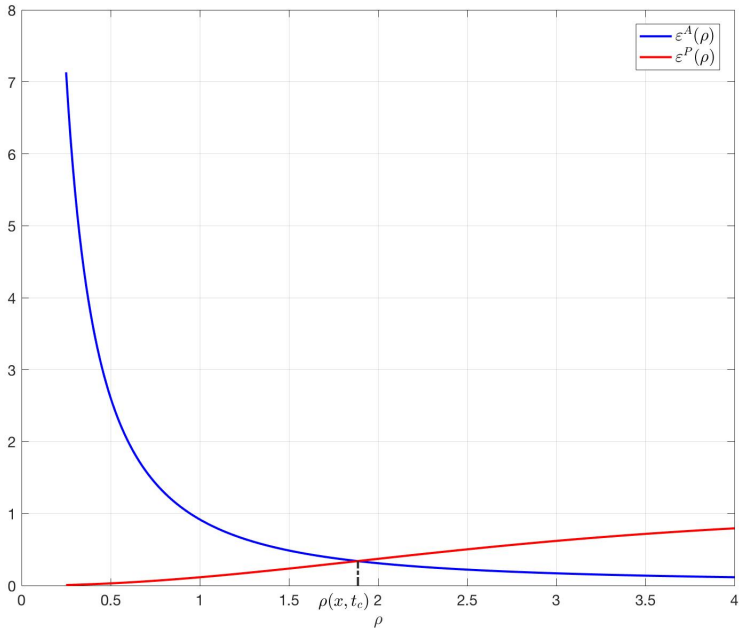

Figure 2.3: Relative Error Behavior of Power and Asymptotic Series

Now consider that t_c satisfies

$$\left|\varepsilon^P(\rho(x, t_c)) - \varepsilon^A(\rho(x, t_c))\right| < \frac{\varepsilon}{\|I_n\left(\rho(x, t_c)\right)\|_2}, \tag{2.3.60}$$

which means within error tolerance ε,

$$\varepsilon^C(\rho(x, t_c)) \approx \varepsilon^A(\rho(x, t_c)) \approx \varepsilon^P(\rho(x, t_c)) \tag{2.3.61}$$

Combining equation (2.3.58), (2.3.58) and (2.3.61), we can conclude that for $\forall t > 0$, $\varepsilon^C(\rho(x, t)) \leq \varepsilon^C(\rho(x, t_c))$. Thus, the error calculated at the critical

point t_c will give us a reliable upper bound for our approximation error. Furthermore, considering that I_n^P and I_n^C are continuous with respect to t, a proper estimation of the critical point t_c will also provide us a practical upper bound for the approximation error.

The critical value used for the approximation via combination can be calculated as

$$\left| I_n^P(x) - I_n(x) \right| = \left| I_n^A(x) - I_n(x) \right|, \tag{2.3.62}$$

or

$$\left| I_n^P(x) - I_n(x) \right| - \left| I_n^A(x) - I_n(x) \right| < \varepsilon, \tag{2.3.63}$$

where ε is the given error tolerance. Some practical critical values shown in **Table** 2.3 are used for approximation of lower orders with the error tolerance $\varepsilon = 10^{-6}$.

Critical Value (with 4 digits)		The Highest Order in Series	
		1	2
The Order of Bessel Function	$I_0(x)$	0.2579	2.7995
	$I_1(x)$	1.0320	3.7456
	$I_2(x)$	1.6399	6.1883

Table 2.3: Some Critical Values

Chapter 3

Numerical Results for HPC Resource Allocation

3.1 Data Simulation

In this section, we will present a numerical example of the Stochastic Fluid Queue (SFQ) model. Consider an ON-OFF fluid system, where state S_1 is the recovery state with buffer fluiding rate $r_1 - C = -1$ and S_2 is the attacking state with buffer fluiding rate $r_2 - C = 4$. Suppose the changing rate between two states are given as $\lambda_{12} = 1.3, \lambda_{21} = 0.4$. However, the state of system is hidden from our observation. The data we can observe from the network link is the real-time buffer content $Q(t)$. For the purpose of simulation, we generate the system evolving process by changing the system state with time intervals, the length of which follows exponential distributions with parameters $\lambda_{12}, \lambda_{21}$. Meanwhile, the variation of $Q(t)$ follows the equation

$$\frac{dQ(t)}{dt} = \begin{cases} r_i - C, & Q(t) \geq 0 \\ 0, & otherwise \end{cases} \tag{3.1.1}$$

for each $dt = 0.1s$. Consequently, we generate $Q(t)$ for t from 0 to 200. An example sample path of $Q(t)$ is shown in **Figure 3.1** .

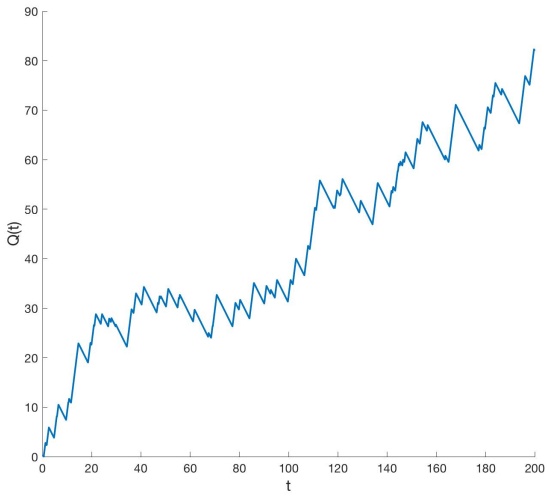

Figure 3.1: The Variation of $Q(t)$ with respect to t

Take difference of $Q(t)$ with the above stepwidth, we get the result shown in **Figure** 3.2.

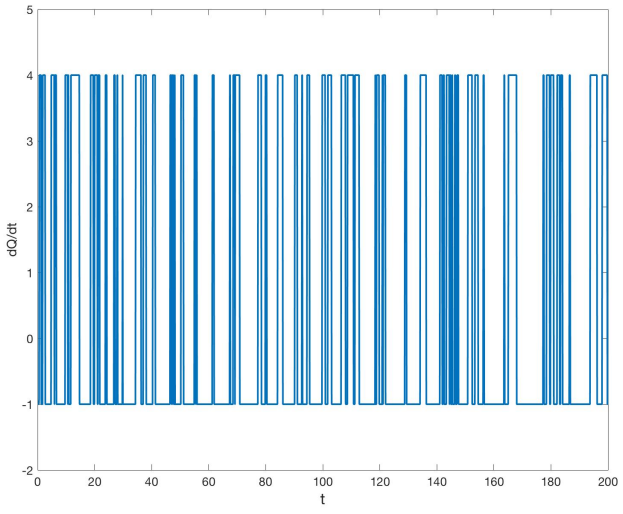

Figure 3.2: The Variation of $dQ(t)/dt$ with respect to t

3.2 Theoretical Solution

In this subsection, we will numerically compare the difference between the theoretical solution and the series expansion approximation. In the context of HPC resource allocation, we use the parameters $r_1 - C = -1$, $r_2 - C = 4$, $\lambda_{12} = 1.3$ and $\lambda_{21} = 0.4$ for the this comparison. In the context of insurance risk management, we use the parameter $r = 4$, $\lambda_{12} = 1.3$ and $\lambda_{21} = 0.4$. **Table 3.1** and **Table 3.2** describe the scenarios included in the numerical assessment. In each scenario, the difference of solutions getting from two different methods will be compared and analyzed. In each comparison, firstly, we will focus on comparing the probability function with respect to time t, namely, $F(t,x)$, $W^1(t,x)$ and $W^2(t,x)$, for fixed x ($x = 1$ in the experiment). The distances of solution functions and its comparative function in L_1, L_2 and L_∞ norm space are employed as criteria to evaluate the error, given t in a bounded close interval, say $t \in [0, 20]$. Meanwhile, we will show how the absolute error and relative error of each approximation vary with respect to time t.

Scenario	Description
I	Comparing the differences between the solution and its approximation of Power Series with the first leading term
II	Comparing the differences between the solution and its approximation from the combination of Power Series and Asymptotic Series with the first leading term
III	Comparing the differences between the solution and its approximation from the combination of Power Series and Asymptotic Series with the first and second leading terms
IV	Comparing the differences between the theoretical solution and simulation results
V	Comparing the differences between the simulation results and the approximation from the combination of Power Series and Asymptotic Series with the first leading term
VI	Comparing the differences between the simulation results and the approximation from the combination of Power Series and Asymptotic Series with the first and second leading terms

Table 3.1: Summary of Numerical Comparison Methodology

Scenario	Comparison Item (I)	Comparison Item (II)
I	Theoretical Solution	Approximation via Power Series with the First Leading Term
II	Theoretical Solution	Approximation via the Combination of Power Series and Asymptotic Series with the First Leading Term
III	Theoretical Solution	Approximation via the Combination of Power Series and Asymptotic Series with the First and Second Leading Term
IV	Monte Carlo Simulated Solution	Theoretical Solution
V	Monte Carlo Simulated Solution	Approximation via the Combination of Power Series and Asymptotic Series with the First Leading Term
VI	Monte Carlo Simulated Solution	Approximation via the Combination of Power Series and Asymptotic Series with the First and Second Leading Term

Table 3.2: Summary of Numerical Comparison Methodology(II)

Figure 3.3 shows the behavior of Prob$(Q(t) \leq x)$, namely, $F(t,x)$, and $W^1(t,x), W^2(t,x)$ with respect to t at $x = 1$.

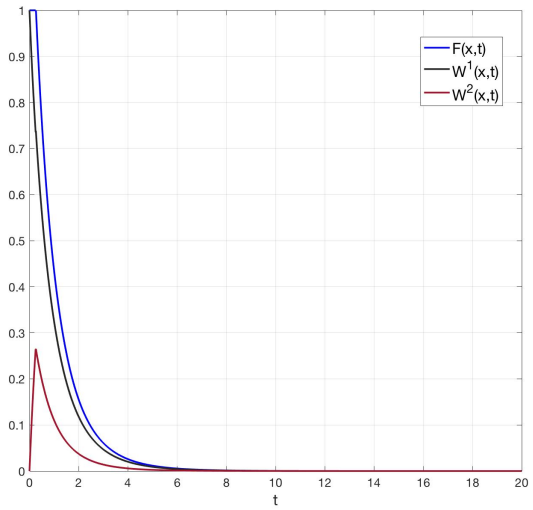

Figure 3.3: The Probability of $Q(t) \leq x$ with respect to t, Given $x = 1$

Figure 3.4 and **Figure** 3.5 show the variation of $F(t,x)$, $W^1(t,x)$ and $W^2(t,x)$ in Scenario III. **Figure** 3.6 shows the absolute error of approximations with respect to time t in Scenario III. These figures show the robustness of the proposed expansion from a graphical perspective, where **Figure** 3.4 highlights the closeness in behavior between the approximations of $F(t,x)$ and the its theoretical solution. This is further verified in **Figure** 3.6 , where the error behavior between the approximated and simulated responses of $F(t,x)$, where this trend continued when the authors investigated this behavior for all six cases.

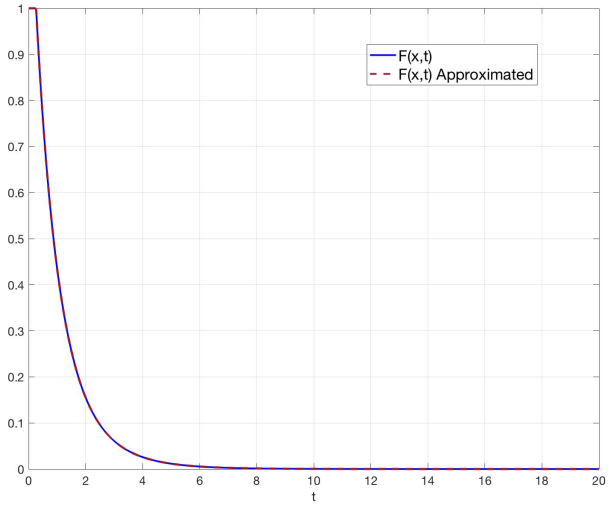

Figure 3.4: $F(t,x)$ and Approximation via the Combination of Power Series and Asymptotic Series with the First and Second Leading Terms with respect to t, Given $x = 1$

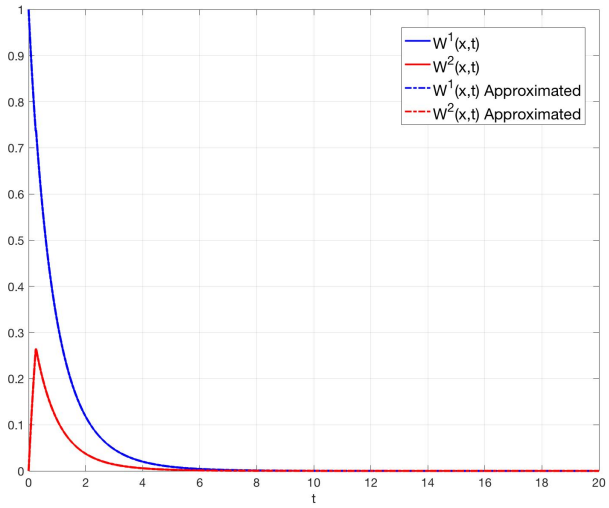

Figure 3.5: $W^1(t,x)$, $W^2(t,x)$ and Approximation via the Combination of Power Series and Asymptotic Series with the First and Second Leading Terms with respect to t, Given $x = 1$

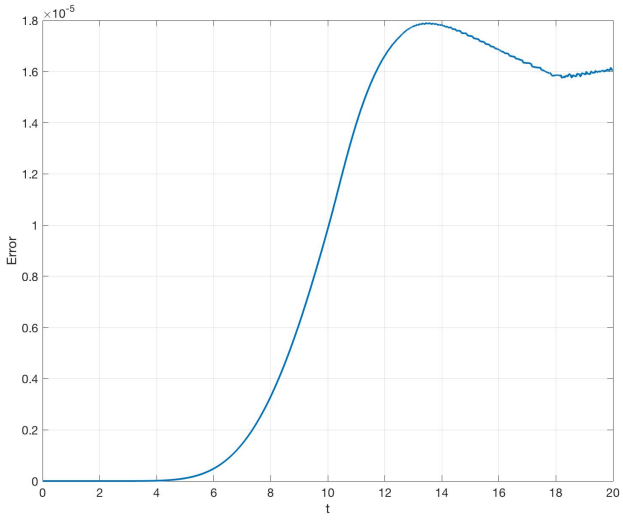

Figure 3.6: Error of $F(t,x)$ and the Approximation via the Combination of Power Series and Asymptotic Series with the First and Second Leading Term with respect to t, Given $x = 1$

3.3 Result

Scenario	Criteria		
	L_1 Distance	L_2 Distance	L_∞ Distance
I	0.1806	4.483×10^{-2}	1.210×10^{-4}
II	7.495×10^{-2}	1.798×10^{-2}	4.617×10^{-5}
III	8.898×10^{-6}	5.233×10^{-5}	1.790×10^{-7}
IV	2.922×10^{-2}	1.635×10^{-2}	2.314×10^{-4}
V	0.1039	2.551×10^{-2}	2.313×10^{-4}
VI	2.936×10^{-2}	1.635×10^{-2}	2.314×10^{-4}

Table 3.3: Numerical Results of Comparison

Table 3.3 shows the distances between theoretical solution and approximations in functional space for each scenario. The numerical result shows that the approximation using the combination of two series are reasonable small, and may be applied for a easier and intuitive estimation of $F(t, x)$. With the second order terms adding in, the distances decrease more by comparing Scenario II and III, which implies the combination series will universely convergence to the theoretical solution as terms goes to infinity. From the comparison of Scenario IV, V and VI, we can also conclude that the approximation are comparatively closer to the simulation with the theoretical solution, which implies it is reasonable to use the approximation result as an ideal frame of reference in the application of real data where stochastic error are included.

Chapter 4

Stochastic Fluid Queue Model for Ruin Theory

4.1 Overview

The surplus of an insurance company is the amount by which its asset exceeds its liability. If the surplus of an insurance company falls below the require level, the regulator can take over the company and announce its bankruptcy. Thus, it is important to focus on the surplus process of a company when predict the probability of its bankruptcy or evaluate the risk of the company. One of the classical model for the evaluation of insurance surplus process is known as the Cramer-Lundberg model. In their model, the insurance company collects premiums with a constant rate r and pays for the claims. Therefore the surplus process $\{R(t)\}$ in continuous time $t \geq 0$ is expressed as

$$R(t) = u + rt - \sum_{1 \leq k \leq N(t)} U_k, \tag{4.1.1}$$

where $u \geq 0$ is the initial surplus, $r \geq 0$ is the constant premium accumulating rate, $N(t)$ is the number of claims occurring in time interval $(0, t)$, and $\{U_k\}$ are sizes of claims for $k \geq 1$. Within the interval between two claims, the surplus increases at rate r. When the k'th claim occurs, the surplus drops down by U_k immediately. In the model's assumption, arrivals of claims are independent with each other and follow a Poisson process with parameter λ_{21}. Furthermore, sizes of claims are follow a given distribution $\mathcal{F}$ independently and identically. **Figure** 4.1 shows a sample path of the surplus process.

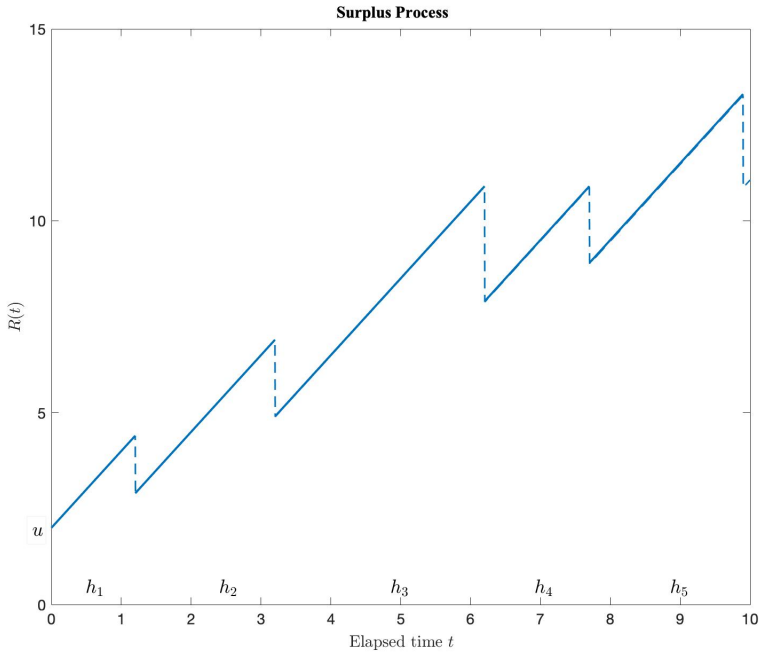

Figure 4.1: Surplus Process $R(t)$

Such definitions generate a discontinuous process, which will be hard for us to analyze. To avoid the discontinuity of the process, Badescu et al. introduced a fluid queue model which substitutes the jump process with a piecewise linear one [24]. The key of their method is transform the time t in the initial process $R(t)$ so that in the transformed process each claim of size U_k arrives continuously over a time interval of length U_k/r. We denote the buffer content of the transformed process by $Q(\tau)$. The relationship between the initial process and the transformed one is the following:

Every interval of time where $R(t)$ increases is retained, namely, $Q(\tau)$ increases at the same rate; whereas the k'th downward discontinuity point of

$R(t)$ is replaced by an interval on the time axis of length U_k/r, in which $Q(\tau)$ decreases linearly at rate $-r$, meanwhile the rest of the process is translated to the right of length U_k/r. Hence, the process $R(t)$ is transformed to a stochastic fluid queue process with buffer content $Q(\tau)$. Conversely, in time intervals where the fluid process $Q(\tau)$ increases, the surplus process $R(t)$ coincide with the fluid queue; meanwhile, time intervals are removed from $R(t)$ where the fluid process $Q(\tau)$ decreases. **Figure 4.2** is the sample path of $Q(\tau)$ related to the surplus process $R(t)$ in **Figure 4.1**.

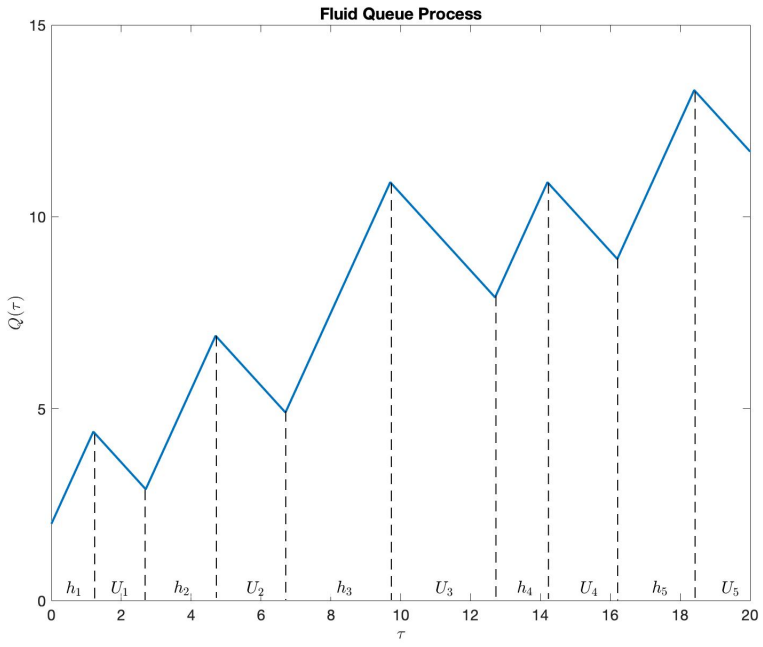

Figure 4.2: Fluid Queue Process $Q(\tau)$

We define the increasing and decreasing of the fluid queue as two states in a state space, $\mathcal{S} = \{S_1, S_2\}$, where state S_1 is the decreasing state, namely OFF state, and S_2 is increasing state, or ON state. Then the buffer content $Q(\tau)$ can

be expressed as a function with respect to τ,

$$Q(\tau) = \begin{cases} u + \int_0^{\tau} r_{S(v)} dv, \text{ if } Q(\nu) > 0 \text{ , for } \forall \nu \in (0, \tau) \\ 0, \qquad\qquad\qquad \text{otherwise} \end{cases} \tag{4.1.2}$$

where u is the initial surplus, which is also the fluid level at time zero. Noticing that the buffer content linearly increases at rate r at the state S_2 and decreases linearly at rate $-r$ at the state S_1, we have $r_2 = r$ and $r_1 = -r$. The behavior of buffer content $Q(\tau)$ is summarized in the following equation:

$$\frac{dQ}{d\tau} = \begin{cases} -r, & S(\tau) = S_1,\ Q(t) > 0 \\ r, & S(\tau) = S_2,\ Q(t) > 0 \\ 0, & \text{otherwise} \end{cases} . \tag{4.1.3}$$

Furthermore, the relationship between the company condition and the buffer content behavior is presented in **Table 4.1**.

	Condition	**Description of Buffer Content Behavior**
I	$r_i = r$, $Q(\tau) > 0$	The buffer content $Q(\tau)$ *increases* at rate r. The insurance company is of its normal business, and the surplus $R(t)$ is accumulated at rate r.
II	$r_i = -r$, $Q(\tau) > 0$	The buffer content $Q(\tau)$ *decreases* at rate $-r$. A claim is occurring and the surplus $R(t)$ decreases by U_k.
III	$Q(\tau) = 0$	The buffer content $Q(\tau) = 0$ has *no change*. The surplus $R(t)$ decrease to 0, which means the insurance company is under the bankruptcy protection.

Table 4.1: The Behavior of Buffer Content $Q(\tau)$ in the Context of Insurance Risk Management

With the assumption that the size of claims independently and identically follows an exponential distribution with parameter λ_{12}, namely, for any integer k, the cumulative distribution function of the claim size U_k is given by

$$\mathbf{P}\{U_k \leq x\} = \begin{cases} 1 - e^{-\lambda_{12} x}, \, x \geq 0 \\ 0, \, x < 0 \end{cases} . \tag{4.1.4}$$

Therefore,

$$\mathbf{P}\{U_k / r \leq x\} = \begin{cases} 1 - e^{-r\lambda_{12} x}, \, x \geq 0 \\ 0, \, x < 0 \end{cases} . \tag{4.1.5}$$

Under that condition, we know the remaining time for the state $S(\tau)$ at S_1 follows an exponential distribution and the remaining time at S_2 is governed by a Poisson arrival process, thus the state transformation of $S(\tau)$ can be regarded as a Continuous Time Markovian Chain. Therefore, the behavior of the buffer content $Q(\tau)$ follows a Markovian Fluid Queue, with the transition matrix

$$P = \begin{pmatrix} \lambda_{11} & r\lambda_{12} \\ \\ \lambda_{21} & \lambda_{22} \end{pmatrix}, \tag{4.1.6}$$

where λ_{21} is determined by the Poisson process of arrival, $\lambda_{11} = 1 - r\lambda_{12}$, and $\lambda_{22} = 1 - \lambda_{21}$. Demote $\lambda = r\lambda_{12}$ and $\mu = \lambda_{21}$, then the transition matrix can be written as

$$P = \begin{pmatrix} 1 - \lambda & \lambda \\ \\ \mu & 1 - \mu \end{pmatrix} . \tag{4.1.7}$$

Now consider the passage time for the surplus $R(t)$ from the level $u \geq 0$ to x, with t_0 denoting the real time and τ_0 being the length of time for the fluid queue $Q(\tau)$, during which the fluid queue increased for τ_2 and decrease for

time τ_1. We have the following relationship

$$\begin{cases} -r\tau_1 + r\tau_2 = x - u \\ \tau_1 + \tau_2 = \tau_0 \end{cases} . \tag{4.1.8}$$

Therefore, we have

$$\begin{cases} \tau_1 = \dfrac{\tau_0}{2} - \dfrac{x-u}{2r} \\ \tau_2 = \dfrac{\tau_0}{2} + \dfrac{x-u}{2r} \end{cases} . \tag{4.1.9}$$

Recall that the total length of increasing intervals τ_2 equals the elapsed time t_0 in the real world, namely

$$t_0 = \frac{\tau_0}{2} + \frac{x-u}{2r} \qquad \text{or} \qquad \tau_0 = 2t_0 - \frac{x-u}{r}. \tag{4.1.10}$$

Now define the Cumulative Distribution Function $F(\tau, x)$ of the buffer content $Q(\tau)$,

$$F(\tau, x) = \mathbf{P}\{Q(\tau) \leq x\}, \tag{4.1.11}$$

and the density function

$$p(\tau, x) = \frac{dF(\tau, x)}{dx} \tag{4.1.12}$$

Therefore, fix the initial surplus u, we have the probability distribution function of the surplus process at time t is

$$\psi(t, x) = \mathbf{P}\{R(t) \leq x\} = \int_{-\infty}^{x} p\left(2t - \frac{y-u}{r}, y\right) dy, \tag{4.1.13}$$

which means given the initial surplus, to compute the probability of bankruptcy, it is sufficient if we can determine the probability distribution function $F(\tau, x)$ of the buffer content $Q(\tau)$ in the fluid queue model.

We define two measures to analyze the probability behavior of the fluid queue, namely, the cumulative distribution function of buffer content $Q(\tau)$ at the state S_i

$$W^i(\tau, x) = \mathbf{P}\{Q(\tau) \leq x, S(\tau) = S_i\}. \tag{4.1.14}$$

Consequently, the unconditional CDF of the buffer content $Q(t)$ is

$$F(\tau, x) = \mathbf{P}\{Q(\tau) \leq x\} = W^1(\tau, x) + W^2(\tau, x). \tag{4.1.15}$$

The goal is to determine the expression of $W^1(\tau, x)$ and $W^2(\tau, x)$. The probabilistic transitions within a small time interval of length Δt can be represented as follows

$$\begin{aligned} W^1(\tau + \Delta t, x) &= (1 - \Delta t\lambda)\, W^1\left(\tau, x - (-r\Delta t)\right) \\ &\quad + \Delta t \cdot \mu W^2(\tau, x - r\Delta t) + \mathcal{O}\left((\Delta t)^2\right) \end{aligned} \tag{4.1.16}$$

$$\begin{aligned} W^2(\tau + \Delta t, x) &= (1 - \Delta t\mu)\, W^2\left(\tau, x - r\Delta t\right) \\ &\quad + \Delta t \cdot \lambda W^1(\tau, x - (-r\Delta t)) + \mathcal{O}\left((\Delta t)^2\right), \end{aligned} \tag{4.1.17}$$

where, on the right hand sides of (4.1.16) and (4.1.17), the first terms describe no transition between states, the second term models the transitions to the other state and the third terms are higher order terms of Δt.

It is observed that the right hand side of (4.1.16) and (4.1.17) can be written as

$$\begin{cases} \dfrac{W^1(\tau+\Delta t,x)-W^1(\tau,x)}{\Delta t}-r\dfrac{W^1(\tau,x+\Delta x)-W^1(\tau,x)}{\Delta x} \\ \qquad =-\lambda W^1(\tau,x+\Delta x)+\mu W^2(\tau,x-\Delta x)+\dfrac{\mathcal{O}\left((\Delta t)^2\right)}{\Delta t} \\ \dfrac{W^2(\tau+\Delta t,x)-W^2(\tau,x)}{\Delta t}+r\dfrac{W^2(\tau,x)-W^2(\tau,x-\Delta x)}{\Delta x} \\ \qquad =\lambda W^1(\tau,x+\Delta x)-\mu W^2(\tau,x-\Delta x)+\dfrac{\mathcal{O}\left((\Delta t)^2\right)}{\Delta t} \end{cases} \tag{4.1.18}$$

where $\Delta x = r\Delta t$. Therefore, as $\Delta t \to 0$ equation (4.1.18) becomes

$$\begin{cases} \dfrac{\partial W^1(\tau,x)}{\partial \tau}-r\dfrac{\partial W^1(\tau,x)}{\partial x}= & -\lambda W^1(\tau,x)+\mu W^2(\tau,x) \\ \dfrac{\partial W^2(\tau,x)}{\partial \tau}+r\dfrac{\partial W^2(\tau,x)}{\partial x}= & \lambda W^1(\tau,x)-\mu W^2(\tau,x) \end{cases}, \tag{4.1.19}$$

for any $\tau > 0$ and $x > 0$.

Now we should consider the Initial Conditions and Boundary Conditions of $W^1(\tau,x)$ and $W^2(\tau,x)$. We assume that the process of claim arrivals is a Markovian Arrival Process, so no claim arrives at time 0 with probability 1, the initial state at $\tau = 0$ is the "ON" state S_2 almost surely, namely

$$\mathbf{P}\{S(0)=S_1\}=0, \qquad \mathbf{P}\{S(0)=S_2\}=1. \tag{4.1.20}$$

Furthermore, considering the condition that $Q(0) = u$, we have the following

initial conditions:

$$W^1(0,x) = \mathbf{P}\{Q(0) \leq x, S(0) = S_1\} = 0. \tag{4.1.21}$$

and

$$W^2(0,x) = \mathbf{P}\{Q(0) \leq x, S(0) = S_2\} = \mathbf{P}\{Q(0) \leq x\} = \mathbf{P}\{u \leq x\} = \mathbf{1}_{\{x \geq u\}}$$

$$= \begin{cases} 1, x \geq u \\ 0, x < u \end{cases}, \tag{4.1.22}$$

where $\mathbf{1}_{\{\cdot\}}$ is the indicator function.

For the boundary conditions, notice that

$$W^i(\tau,0) = \mathbf{P}\{Q(\tau) \leq 0, S(\tau) = S_i\}, \qquad i = 1,2. \tag{4.1.23}$$

Considering that the buffer content $Q(\tau) \geq 0$ almost surely and that it strictly increases at state S_2, the probability of the buffer to be empty at state S_2 is 0, so we have the boundary condition

$$W^2(\tau,0) = 0. \tag{4.1.24}$$

With the boundary condition (4.1.24), the relationship (4.1.15) can now be expressed as

$$\mathbf{P}\{Q(\tau) \leq 0\} = F(\tau,0) = W^1(\tau,0), \tag{4.1.25}$$

which means the boundary condition for $W^1(\tau,0)$ is the probability of ruin for the insurance company with respect to the transformed time τ, which is the target function **to be determined**. Suppose the probability of ruin is $q(\tau)$,

namely the boundary condition for $W^1(\tau, x)$ is

$$W^1(\tau, 0) = q(\tau). \tag{4.1.26}$$

With the assumption of a distressed insurance company, we suppose that the company will bankrupt within finite time, which means

$$\lim_{\tau \to \infty} \mathbf{P}\{Q(\tau) \leq 0\} = 1. \tag{4.1.27}$$

Furthermore, for any $0 < \tau < \infty$, we have

$$\mathbf{P}\{Q(\tau) \leq \infty\} = 1, \tag{4.1.28}$$

which yields another boundary condition

$$\lim_{x \to +\infty} \mathbf{P}\{Q(\tau) \leq x\} = \lim_{x \to +\infty} \Big\{ W^1(\tau, x) + W^2(\tau, x) \Big\} = 1. \tag{4.1.29}$$

Boundary condition (4.1.29) also confirms that the probability functions $W^1(\tau, x)$ and $W^2(\tau, x)$ are almost surely bounded.

Therefore, in the context of ruin theory, we have constructed an Initial Boundary Value Problem for $W^1(\tau, x)$ and $W^2(\tau, x)$ as

$$\boxed{\begin{cases} \dfrac{\partial W^1(\tau,x)}{\partial \tau} - r\dfrac{\partial W^1(\tau,x)}{\partial x} = & -\lambda W^1(\tau,x) + \mu W^2(\tau,x) \\ \dfrac{\partial W^2(\tau,x)}{\partial \tau} + r\dfrac{\partial W^2(\tau,x)}{\partial x} = & \lambda W^1(\tau,x) - \mu W^2(\tau,x) \end{cases},} \tag{4.1.30}$$

with initial conditions

$$\boxed{\begin{cases} W^1(0,x) = 0 \\ W^2(0,x) = \mathbf{1}_{\{x \geq u\}} \end{cases},} \tag{4.1.31}$$

and boundary conditions

$$\boxed{\begin{cases} W^1(\tau,0) = q(\tau) \\ W^2(\tau,0) = 0 \end{cases}} \tag{4.1.32}$$

and

$$\boxed{\lim_{x \to +\infty} \left\{ W^1(\tau,x) + W^2(\tau,x) \right\} = 1,} \tag{4.1.33}$$

where $q(\tau)$ is the function to be determined.

4.2 Transient Analysis

In this section, we analyze the transient behavior of the system elaborated in the previous section. By taking Laplace transformation and inverse Laplace transformation, a theoretical solution to the SFQ is provided with given initial and boundary conditions.

Take Laplace transform for equations (4.1.19) with respect to τ yielding

$$\begin{cases} s\hat{W}^1(s,x) - W^1(0,x) - r\dfrac{d\hat{W}^1(s,x)}{dx} = -\lambda\hat{W}^1(s,x) + \mu\hat{W}^2(s,x) \\ s\hat{W}^2(s,x) - W^2(0,x) + r\dfrac{d\hat{W}^2(s,x)}{dx} = \lambda\hat{W}^1(s,x) - \mu\hat{W}^2(s,x). \end{cases} \tag{4.2.1}$$

Plugging in the initial condition, new equations after reconstruction are given as

$$\begin{cases} \dfrac{d\hat{W}^1(s,x)}{dx} = \dfrac{s+\lambda}{r}\hat{W}^1(s,x) - \dfrac{\mu}{r}\hat{W}^2(s,x) \\ \dfrac{d\hat{W}^2(s,x)}{dx} = \dfrac{\lambda}{r}\hat{W}^1(s,x) - \dfrac{\mu+s}{r}\hat{W}^2(s,x) + \dfrac{1}{r}\mathbf{1}_{\{x\geq u\}} \end{cases}, \tag{4.2.2}$$

with boundary conditions

$$\begin{aligned} \hat{W}^1(s,0) &= \mathcal{L}\{q_0(\tau)\} := \hat{q}_0(s) \\ \hat{W}^2(s,0) &= \mathcal{L}\{0\} = 0 \end{aligned}, \tag{4.2.3}$$

where $\hat{q}_0(s) = \mathcal{L}\{q_0(\tau)\}$. Let $\hat{\mathbf{W}} = \hat{\mathbf{W}}(s,x) = \begin{pmatrix} \hat{W}^1(s,x) \\ \hat{W}^2(s,x) \end{pmatrix}$ be the vector of function with respect to the variable x, then the equation (4.2.2) can be written

as

$$\frac{d\hat{\mathbf{W}}(x)}{dx} = \mathbf{A} \cdot \hat{\mathbf{W}} + \mathbf{H}, \tag{4.2.4}$$

where

$$\mathbf{A} = \begin{pmatrix} \frac{s+\lambda}{r} & -\frac{\mu}{r} \\ \frac{\lambda}{r} & -\frac{s+\mu}{r} \end{pmatrix} \quad \text{and} \quad \mathbf{H} = \begin{pmatrix} 0 \\ \\ \frac{1}{r}\mathbf{1}_{\{x \geq u\}} \end{pmatrix}, \tag{4.2.5}$$

subject to the boundary conditions

$$\hat{\mathbf{W}}(s,0) = \begin{pmatrix} \hat{q}_0(s) \\ \\ 0 \end{pmatrix}. \tag{4.2.6}$$

Notice that the eigenvalues of $\mathbf{A}$ are

$$\begin{aligned} \omega_0(s) &= \frac{1}{2r}\left(\lambda - \mu - \sqrt{T(s)}\right) \\ \omega_1(s) &= \frac{1}{2r}\left(\lambda - \mu + \sqrt{T(s)}\right) \end{aligned}, \tag{4.2.7}$$

where

$$T(s) = 4\left(s + \frac{\lambda+\mu}{2}\right)^2 - 4\lambda\mu, \tag{4.2.8}$$

with the fact that $T(s) \geq 0$ for $s > 0$. The eigenvectors of $\mathbf{A}$ associated with $\omega_0(s)$ and $\omega_1(s)$ are

$$\mathbf{V}_0 = \begin{pmatrix} \lambda + \mu + 2s - \sqrt{T(s)} \\ \\ 2\lambda \end{pmatrix}, \quad \mathbf{V}_1 = \begin{pmatrix} \lambda + \mu + 2s + \sqrt{T(s)} \\ \\ 2\lambda \end{pmatrix}. \tag{4.2.9}$$

Consequently, solutions to the homogeneous differential equation system

$$\frac{d\hat{\mathbf{W}}}{dx} = \mathbf{A} \cdot \hat{\mathbf{W}} \tag{4.2.10}$$

are of the form

$$\hat{\mathbf{W}} = K_0 \mathbf{V}_0 e^{\omega_0(s)x} + K_1 \mathbf{V}_1 e^{\omega_1(s)x}, \tag{4.2.11}$$

where K_0 and K_1 are constants to be determined by the boundary conditions. Let

$$\mathbf{\Phi}(s,x) = \begin{pmatrix} \left(\lambda+\mu+2s-\sqrt{T(s)}\right)\cdot e^{\omega_0(s)x} & \left(\lambda+\mu+2s+\sqrt{T(s)}\right)\cdot e^{\omega_1(s)x} \\ 2\lambda\cdot e^{\omega_0(s)x} & 2\lambda\cdot e^{\omega_1(s)x} \end{pmatrix}, \tag{4.2.12}$$

then the solution (2.2.23) can be written as

$$\hat{\mathbf{W}} = \mathbf{\Phi}\cdot\mathbf{K}, \tag{4.2.13}$$

where $\mathbf{K} = (K_0, K_1)^T$ is an arbitrary constant vector. Therefore, by applying the method of variation of constants, the solution to the non-homogeneous equation system (4.2.4) has the form of

$$\hat{\mathbf{W}} = \mathbf{\Phi}\cdot\left(\mathbf{K} + \int_0^x \mathbf{\Phi}^{-1}(s,y)\cdot\mathbf{H}dy\right), \tag{4.2.14}$$

where

$$\mathbf{\Phi}^{-1}(s,x) = \frac{1}{2\lambda\sqrt{T(s)}}\cdot\begin{pmatrix} -\lambda e^{-\omega_0(s)x} & \dfrac{\lambda+\mu+2s+\sqrt{T(s)}}{2}e^{-\omega_0(s)x} \\ \lambda e^{-\omega_1(s)x} & -\dfrac{\lambda+\mu+2s-\sqrt{T(s)}}{2}e^{-\omega_1(s)x} \end{pmatrix}, \tag{4.2.15}$$

With the boundary condition (4.2.6), we have

$$\hat{\mathbf{W}}(s,0) = \mathbf{\Phi}(s,0)\left(\mathbf{K} + \int_0^0 \mathbf{\Phi}^{-1}(s,y)\cdot\mathbf{H}dy\right), \tag{4.2.16}$$

which yields

$$\mathbf{K} = \mathbf{\Phi}^{-1}(s,0)\cdot\hat{\mathbf{W}}(s,0) = \begin{pmatrix} -\dfrac{\hat{q}_0(s)}{2\sqrt{T(s)}} \\ \dfrac{\hat{q}_0(s)}{2\sqrt{T(s)}} \end{pmatrix} \tag{4.2.17}$$

In addition, we have

$$\int_0^x \mathbf{\Phi}^{-1}(s,y)\cdot\mathbf{H}dy =$$

$$\begin{pmatrix} \dfrac{\left(\lambda+\mu+2s+\sqrt{T(s)}\right)\mathbf{1}_{\{x\geq u\}}}{4r\lambda\omega_0(s)\sqrt{T(s)}}\cdot\left(e^{-\omega_0(s)u}-e^{-\omega_0(s)x}\right) \\ -\dfrac{\left(\lambda+\mu+2s-\sqrt{T(s)}\right)\mathbf{1}_{\{x\geq u\}}}{4r\lambda\omega_1(s)\sqrt{T(s)}}\cdot\left(e^{-\omega_1(s)u}-e^{-\omega_1(s)x}\right) \end{pmatrix}. \tag{4.2.18}$$

Thus,

$$\begin{aligned} \hat{W}_1(s,x) = \frac{1}{2\sqrt{T(s)}}\cdot\Bigg\{ & \left(\frac{2\mu}{r\omega_1(s)}-\frac{2\mu}{r\omega_0(s)}\right)\mathbf{1}_{\{x\geq u\}} \\ & + e^{\omega_0(s)x}\left(\frac{2\mu}{r\omega_0(s)}e^{-\omega_0(s)u}\mathbf{1}_{\{x\geq u\}} - \left(\lambda+\mu+2s-\sqrt{T(s)}\right)\hat{q}_0(s)\right) \\ & + e^{\omega_1(s)x}\left(-\frac{2\mu}{r\omega_1(s)}e^{-\omega_1(s)u}\mathbf{1}_{\{x\geq u\}} + \left(\lambda+\mu+2s+\sqrt{T(s)}\right)\hat{q}_0(s)\right)\Bigg\} \end{aligned} \tag{4.2.19}$$

and

$$\hat{W}_2(s,x) = \frac{1}{2\sqrt{T(s)}} \cdot \left\{ \left(\frac{\lambda+\mu+2s-\sqrt{T(s)}}{r\omega_1(s)} - \frac{\lambda+\mu+2s+\sqrt{T(s)}}{r\omega_0(s)} \right) \mathbf{1}_{\{x\geq u\}} \right.$$
$$+e^{\omega_0(s)x}\left(\frac{\lambda+\mu+2s+\sqrt{T(s)}}{r\omega_0(s)} e^{-\omega_0(s)u}\mathbf{1}_{\{x\geq u\}} - 2\lambda\hat{q}_0(s) \right) \quad .$$
$$\left. +e^{\omega_1(s)x}\left(-\frac{\lambda+\mu+2s-\sqrt{T(s)}}{r\omega_1(s)} e^{-\omega_1(s)u}\mathbf{1}_{\{x\geq u\}} + 2\lambda\hat{q}_0(s) \right) \right\} \tag{4.2.20}$$

The boundary condition (4.1.33) implies that $\hat{\mathbf{W}}(s,x)$ is bounded as $x \to \infty$. Considering that $\omega_1(s) > 0$ for $s > 0$, $e^{\omega_1(s)x}$ diverges to infinity as $x \to \infty$, in order to satisfy the boundary condition (4.1.33), $\hat{q}_0(s)$ has to be properly chosen so that the exponential terms with respect to x can be vanished as $x \to \infty$. Therefore, as $x \to \infty$, $\hat{q}_0(s)$ needs to satisfy

$$\begin{cases} -\dfrac{2\mu}{r\omega_1(s)} e^{-\omega_1(s)u} + \left(\lambda+\mu+2s+\sqrt{T(s)} \right) \hat{q}_0(s) = 0 \\ -\dfrac{\lambda+\mu+2s-\sqrt{T(s)}}{r\omega_1(s)} e^{-\omega_1(s)u} + 2\lambda\hat{q}_0(s) = 0 \end{cases} , \tag{4.2.21}$$

which yields

$$\hat{q}_0(s) = \frac{2\mu e^{-\omega_1(s)u}}{r\omega_1(s)\left(\lambda+\mu+2s+\sqrt{T(s)}\right)}. \tag{4.2.22}$$

Next, we consider the case of the distressed insurance company where the current surplus is less than the initial surplus, namely, $x < u$. Under the

condition $x < u$ where $\mathbf{1}_{\{x \geq u\}} = 0$, we have

$$\hat{W}^1(s,x) = \frac{1}{2\sqrt{T(s)}} \left\{ \left(\lambda + \mu + 2s + \sqrt{T(s)} \right) \hat{q}_0(s) e^{\omega_1(s)} \right.$$
$$\left. - \left(\lambda + \mu + 2s - \sqrt{T(s)} \right) \hat{q}_0(s) e^{\omega_0(s)} \right\} \tag{4.2.23}$$

$$\hat{W}^2(s,x) = \frac{\lambda \hat{q}_0(s)}{\sqrt{T(s)}} \left(e^{\omega_1(s)x} - e^{\omega_0(s)x} \right). \tag{4.2.24}$$

Take inverse Laplace transform of solutions (4.2.23) and (4.2.24), we will get the solutions as a piecewise function after considerable simplification, where theoretical details of computing the inverse Laplace transform can be found in **Appendix D** (see **Section** 7.4):

1. when $0 < \tau \leq v_0$

$$\boxed{W^1(\tau, x) = 0} \tag{4.2.25}$$

$$\boxed{W^2(\tau, x) = 0}, \tag{4.2.26}$$

2. when $v_0 < \tau < \tilde{v}_0$

$$\begin{aligned}
&W^1(\tau,x) = \frac{\mu}{2(\lambda+\mu)} e^{-\frac{(\lambda-\mu)(u-x)}{2r}} \times \left\{ \left(1 - e^{-2a(\tau - v_0)}\right) \right. \\
&-(\lambda-\mu)\left(\int_{v_0}^{\tau} \frac{1}{2} e^{-av} I_0\left[\alpha y(v)\right] dv - e^{-2a\tau} \int_{v_0}^{\tau} \frac{1}{2} e^{av} I_0\left[\alpha y(v)\right] dv \right) \\
&\left. + \int_{v_0}^{\tau} \alpha v_0 e^{-av} y^{-1}(v) I_1\left[\alpha y(v)\right] dv - e^{-2a\tau} \int_{v_0}^{\tau} \alpha v_0 e^{av} y^{-1}(v) I_1\left[\alpha y(v)\right] dv \right\}
\end{aligned} \tag{4.2.27}$$

$$\begin{aligned}
&W^2(\tau,x) = e^{-\frac{(\lambda-\mu)(u-x)}{2r}} \times \left\{ \frac{\mu}{2(\lambda+\mu)} e^{-2a\tau} \left(\int_{v_0}^{\tau} \alpha v_0 e^{av} y^{-1}(v) I_1[\alpha y(v)] dv + e^{av_0} \right) \right. \\
&+ \frac{\lambda}{2(\lambda+\mu)} \left(\int_{v_0}^{\tau} \alpha v_0 e^{-av} y^{-1}(v) I_1[\alpha y(v)] dv + e^{-av_0} \right) - \frac{1}{2} e^{-a\tau} I_0(\alpha y(\tau)) \\
&\left. - \frac{\mu(\lambda-\mu)}{2(\lambda+\mu)} e^{-2a\tau} \int_{v_0}^{\tau} \frac{1}{2} e^{av} I_0[\alpha y(v)] dv - \frac{\lambda(\lambda-\mu)}{2(\lambda+\mu)} \int_{v_0}^{\tau} \frac{1}{2} e^{-av} I_0[\alpha y(v)] dv \right\},
\end{aligned} \tag{4.2.28}$$

3. when $\tau > \tilde{v}_0$

$$
\begin{aligned}
W^1(\tau,x) &= e^{-\frac{(\lambda-\mu)(u-x)}{2r}} \times \left\{ \frac{\mu}{2(\lambda+\mu)} \left(1 - e^{-2a(\tau-v_0)}\right) \right. \\
&- \frac{\mu(\lambda-\mu)}{2(\lambda+\mu)} \left(\int_{v_0}^{\tau} \frac{1}{2} e^{-av} I_0\left[\alpha y(v)\right] dv - e^{-2a\tau} \int_{v_0}^{\tau} \frac{1}{2} e^{av} I_0\left[\alpha y(v)\right] dv \right) \\
&+ \frac{\mu}{2(\lambda+\mu)} \left(\int_{v_0}^{\tau} \alpha v_0 e^{-av} y^{-1}(v) I_1\left[\alpha y(v)\right] dv - e^{-2a\tau} \int_{v_0}^{\tau} \alpha v_0 e^{av} y^{-1}(v) I_1\left[\alpha y(v)\right] dv \right) \\
&+ e^{-a\tau} \left(\frac{1}{\lambda} \alpha\tau \tilde{y}^{-1}(\tau) I_1[\alpha\tilde{y}(\tau)] + \frac{\lambda-\mu}{2\lambda} I_0[\alpha\tilde{y}(\tau)] - \frac{\alpha^2 \tilde{v}_0}{2\lambda} \right) \\
&+ \frac{\lambda(\lambda-\mu)}{2(\lambda+\mu)} \int_{\tilde{v}_0}^{\tau} \frac{1}{2} e^{-av} I_0[\alpha\tilde{y}(v)] dv - \frac{\mu^2(\lambda-\mu)}{2\lambda(\lambda+\mu)} e^{-2a\tau} \int_{\tilde{v}_0}^{\tau} \frac{1}{2} e^{av} I_0[\alpha\tilde{y}(v)] dv \\
&- \frac{\lambda}{2(\lambda+\mu)} \left(\int_{\tilde{v}_0}^{\tau} \alpha\tilde{v}_0 e^{-av} \tilde{y}^{-1}(v) I_1[\alpha\tilde{y}(v)] dv + e^{-a\tilde{v}_0} \right) \\
&+ \left. \frac{\mu^2}{2\lambda(\lambda+\mu)} e^{-2a\tau} \left(\int_{\tilde{v}_0}^{\tau} \alpha\tilde{v}_0 e^{av} \tilde{y}^{-1}(v) I_1[\alpha\tilde{y}(v)] dv + e^{a\tilde{v}_0} \right) \right\}
\end{aligned}
\tag{4.2.29}
$$

$$
\begin{aligned}
W^2(\tau,x) = e^{-\frac{(\lambda-\mu)(u-x)}{2r}} \times \Bigg\{ & \frac{\mu}{2(\lambda+\mu)} e^{-2a\tau} \left(\int_{v_0}^{\tau} \alpha v_0 e^{av} y^{-1}(v) I_1[\alpha y(v)] dv + e^{av_0} \right) \\
& + \frac{\lambda}{2(\lambda+\mu)} \left(\int_{v_0}^{\tau} \alpha v_0 e^{-av} y^{-1}(v) I_1[\alpha y(v)] dv + e^{-av_0} \right) - \frac{1}{2} e^{-a\tau} I_0[\alpha y(\tau)] \\
& - \frac{\mu(\lambda-\mu)}{2(\lambda+\mu)} e^{-2a\tau} \int_{v_0}^{\tau} \frac{1}{2} e^{av} I_0[\alpha y(v)] dv - \frac{\lambda(\lambda-\mu)}{2(\lambda+\mu)} \int_{v_0}^{\tau} \frac{1}{2} e^{-av} I_0[\alpha y(v)] dv \\
& - \frac{\mu}{2(\lambda+\mu)} e^{-2a\tau} \left(\int_{\tilde{v}_0}^{\tau} \alpha \tilde{v}_0 e^{av} \tilde{y}^{-1}(v) I_1[\alpha \tilde{y}(v)] dv + e^{a\tilde{v}_0} \right) \\
& - \frac{\lambda}{2(\lambda+\mu)} \left(\int_{\tilde{v}_0}^{\tau} \alpha \tilde{v}_0 e^{-av} \tilde{y}^{-1}(v) I_1[\alpha \tilde{y}(v)] dv + e^{-a\tilde{v}_0} \right) + \frac{1}{2} e^{-a\tau} I_0[\alpha \tilde{y}(\tau)] \\
& + \frac{\mu(\lambda-\mu)}{2(\lambda+\mu)} e^{-2a\tau} \int_{\tilde{v}_0}^{\tau} \frac{1}{2} e^{av} I_0[\alpha \tilde{y}(v)] dv + \frac{\lambda(\lambda-\mu)}{2(\lambda+\mu)} \int_{\tilde{v}_0}^{\tau} \frac{1}{2} e^{-av} I_0[\alpha \tilde{y}(v)] dv \Bigg\},
\end{aligned}
\tag{4.2.30}
$$

where

$$
a = \frac{\lambda+\mu}{2}, \qquad \alpha = \sqrt{\lambda\mu}, \tag{4.2.31}
$$

$$
v_0 = \frac{1}{r}(u-x), \qquad \tilde{v}_0 = \frac{1}{r}(u+x), \tag{4.2.32}
$$

$$
y(\tau) = \sqrt{\tau^2 - v_0^2}, \qquad \tilde{y}(\tau) = \sqrt{\tau^2 - \tilde{v}_0^2} \tag{4.2.33}
$$

and $I_n(y)$, $n = 0, 1$ are the modified Bessel functions of the first kind. Notice that $\tau = \tilde{v}_0$ being a removable discontinuity of $W^1(\tau, x)$ and $W^2(\tau, x)$, so we

define

$$W^1(\tilde{v}_0, x) = \lim_{\tau \to \tilde{v}_0} W^1(\tau, x) \tag{4.2.34}$$

$$W^2(\tilde{v}_0, x) = \lim_{\tau \to \tilde{v}_0} W^2(\tau, x), \tag{4.2.35}$$

then $W^1(\tau, x)$ and $W^2(\tau, x)$ are continuous functions for any $\tau > 0$ and $x > 0$.

4.3 Asymptotic Expansions of Solutions

4.3.1 Short-time Behavior Analysis

For short-time behavior, from equation (4.2.33) we can see that for any $X \geq 0$, $y = y(\tau, x) \to 0$ and the modified Bessel function $I_n(y)$ can be expressed using power series expanding approach around $y = 0$ as

$$I_n(y) = \left(\frac{y}{2}\right)^n \sum_{k=0}^{\infty} \frac{1}{\Gamma(k+1)\Gamma(n+k+1)} \left(\frac{y}{2}\right)^{2k}. \tag{4.3.1}$$

Notice that

$$\begin{aligned} &\int_{v_0}^{\tau} \alpha v_0 e^{av} y^{-1}(v) I_1[\alpha y(v)] dv \\ &= \frac{\alpha^2 v_0}{2} \sum_{k=0}^{\infty} \frac{1}{\Gamma(k+1)\Gamma(k+2)} \left(\frac{\alpha}{2}\right)^{2k} \int_{v_0}^{\tau} e^{av} (v^2 - v_0^2)^k dv, \end{aligned} \tag{4.3.2}$$

$$\begin{aligned} &\int_{v_0}^{\tau} \alpha v_0 e^{-av} y^{-1}(v) I_1[\alpha y(v)] dv \\ &= \frac{\alpha^2 v_0}{2} \sum_{k=0}^{\infty} \frac{1}{\Gamma(k+1)\Gamma(k+2)} \left(\frac{\alpha}{2}\right)^{2k} \int_{v_0}^{\tau - v_1} e^{-av} (v^2 - v_0^2)^k dv. \end{aligned} \tag{4.3.3}$$

Let

$$\Omega_k(\tau; v_0, a) = \int_{v_0}^{\tau} e^{av} (v^2 - v_0^2)^k dv, \tag{4.3.4}$$

$$\Omega_k(\tau; v_0, -a) = \int_{v_0}^{\tau} e^{-av} (v^2 - v_0^2)^k dv, \tag{4.3.5}$$

we have

$$\begin{aligned}\Omega_k(\tau; v_0, a) &= \int_{v_0}^{\tau} e^{av} \sum_{i=0}^{k} (-1)^{k-i} \binom{k}{i} v_0^{2(k-i)} v^{2i} dv \\ &= \sum_{i=0}^{k} (-1)^{k-i} \binom{k}{i} v_0^{2(k-i)} \frac{(2i+1)!}{a^{2i+1}} \left(\sum_{m=0}^{2i} \frac{(-1)^m a^m}{m!} \left(\tau^m e^{a\tau} - v_0^m e^{av_0}\right) \right)\end{aligned}, \tag{4.3.6}$$

$$\Omega_k(\tau; v_0, -a) = \sum_{i=0}^{k} (-1)^{k-i} \binom{k}{i} v_0^{2(k-i)} \frac{(2i+1)!}{(-a)^{2i+1}} \left(\sum_{m=0}^{2i} \frac{a^m}{m!} \left(\tau^m e^{-a\tau} - v_0^m e^{-av_0}\right) \right). \tag{4.3.7}$$

Therefore,

$$\int_{v_0}^{\tau} \alpha v_0 e^{av} y^{-1}(v) I_1[\alpha y(v)] dv = \frac{\alpha^2 v_0}{2} \sum_{k=0}^{\infty} \frac{1}{\Gamma(k+1)\Gamma(k+2)} \left(\frac{\alpha}{2}\right)^{2k} \Omega_k(\tau; v_0, a), \tag{4.3.8}$$

$$\int_{v_0}^{\tau} \alpha v_0 e^{-av} y^{-1}(v) I_1[\alpha y(v)] dv = \frac{\alpha^2 v_0}{2} \sum_{k=0}^{\infty} \frac{1}{\Gamma(k+1)\Gamma(k+2)} \left(\frac{\alpha}{2}\right)^{2k} \Omega_k(\tau; v_0, -a). \tag{4.3.9}$$

In addition,

$$\int_{v_0}^{\tau} I_0[\alpha y(v)] e^{av} dv = \sum_{k=0}^{\infty} \frac{1}{\Gamma(k+1)^2} \left(\frac{\alpha}{2}\right)^{2k} \Omega_k(\tau; v_0, a), \tag{4.3.10}$$

$$\int_{v_0}^{\tau} I_0[\alpha y(v)] e^{-av} dv = \sum_{k=0}^{\infty} \frac{1}{\Gamma(k+1)^2} \left(\frac{\alpha}{2}\right)^{2k} \Omega_k(\tau; v_0, -a). \tag{4.3.11}$$

Hence, for $v_0 < \tau < \tilde{v}_0$, the short-time expansion for $W^1(\tau, x)$ is

$$\begin{aligned}W^1(\tau, x) = \frac{\mu}{2(\lambda+\mu)} e^{-\frac{(\lambda-\mu)(u-x)}{2r}} \times \Bigg\{ &\left(1 - e^{-2a(\tau - v_0)}\right) \\ &- \frac{\lambda-\mu}{2} \sum_{k=0}^{\infty} \frac{1}{\Gamma(k+1)^2} \left(\frac{\alpha}{2}\right)^{2k} \left(\Omega_k(\tau; v_0, -a) - e^{-2a\tau} \Omega_k(\tau; v_0, a)\right) \\ &+ \frac{\alpha^2 v_0}{2} \sum_{k=0}^{\infty} \frac{1}{\Gamma(k+1)\Gamma(k+2)} \left(\frac{\alpha}{2}\right)^{2k} \left(\Omega_k(\tau; v_0, -a) - e^{-2a\tau} \Omega_k(\tau; v_0, a)\right) \Bigg\}.\end{aligned} \tag{4.3.12}$$

The short-time expansion for $W^2(\tau, x)$ is

$$
\begin{aligned}
W^2(\tau,x) = e^{-\frac{(\lambda-\mu)(u-x)}{2r}} \times \Bigg\{ & \frac{\mu e^{-2a\tau+av_0} + \lambda e^{-av_0}}{2(\lambda+\mu)} - \frac{1}{2}e^{-a\tau}\sum_{k=0}^{\infty}\frac{1}{\Gamma(k+1)^2}\left(\frac{\alpha y(\tau)}{2}\right)^{2k} \\
& + \frac{\alpha^2 v_0}{2(\lambda+\mu)}\sum_{k=0}^{\infty}\frac{1}{\Gamma(k+1)\Gamma(k+2)}\left(\frac{\alpha}{2}\right)^{2k}\left(\frac{\mu}{2}e^{-2a\tau}\Omega_k(\tau;v_0,a) + \frac{\lambda}{2}\Omega_k(\tau;v_0,-a)\right) \\
& - \frac{(\lambda-\mu)}{2(\lambda+\mu)}\sum_{k=0}^{\infty}\frac{1}{\Gamma(k+1)^2}\left(\frac{\alpha}{2}\right)^{2k}\left(\frac{\mu}{2}e^{-2a\tau}\Omega_k(\tau;v_0,a) + \frac{\lambda}{2}\Omega_k(\tau;v_0,-a)\right)\Bigg\}
\end{aligned}
\tag{4.3.13}
$$

For $\tau > \tilde{v}_0$, we have

$$
\begin{aligned}
W^1(\tau,x) = e^{-\frac{(\lambda-\mu)(u-x)}{2r}} \Bigg\{ & \frac{\mu}{2(\lambda+\mu)}\left(1 - e^{-2a(\tau-v_0)}\right) - \frac{\lambda}{2(\lambda+\mu)}e^{-a\tilde{v}_0} \\
& + \frac{\mu^2}{2\lambda(\lambda+\mu)}e^{-2a\tau}e^{a\tilde{v}_0} + e^{-a\tau}\left(\frac{\alpha^2\tau}{2\lambda}\sum_{k=0}^{\infty}\frac{1}{\Gamma(k+1)\Gamma(k+2)}\left(\frac{\alpha\tilde{y}(\tau)}{2}\right)^{2k}\right. \\
& \left. + \frac{\lambda-\mu}{2\lambda}\sum_{k=0}^{\infty}\frac{1}{\Gamma(k+1)^2}\left(\frac{\alpha\tilde{y}(\tau)}{2}\right)^{2k} - \frac{\alpha^2\tilde{v}_0}{2\lambda}\right) \\
& - \frac{\mu(\lambda-\mu)}{4(\lambda+\mu)}\sum_{k=0}^{\infty}\frac{1}{\Gamma(k+1)^2}\left(\frac{\alpha}{2}\right)^{2k}\left(\Omega_k(\tau;v_0,-a) - e^{-2a\tau}\Omega_k(\tau;v_0,a)\right) \\
& + \frac{\mu\alpha^2 v_0}{4(\lambda+\mu)}\sum_{k=0}^{\infty}\frac{1}{\Gamma(k+1)\Gamma(k+2)}\left(\frac{\alpha}{2}\right)^{2k}\left(\Omega_k(\tau;v_0,-a) - e^{-2a\tau}\Omega_k(\tau;v_0,a)\right) \\
& + \frac{\lambda-\mu}{2(\lambda+\mu)}\sum_{k=0}^{\infty}\frac{1}{\Gamma(k+1)^2}\left(\frac{\alpha}{2}\right)^{2k}\left(\frac{\lambda}{2}\Omega_k(\tau;\tilde{v}_0,-a) - \frac{\mu^2}{2\lambda}e^{-2a\tau}\Omega_k(\tau;\tilde{v}_0,a)\right) \\
& - \frac{\alpha^2 v_0}{2(\lambda+\mu)}\sum_{k=0}^{\infty}\frac{1}{\Gamma(k+1)\Gamma(k+2)}\left(\frac{\alpha}{2}\right)^{2k}\left(\frac{\lambda}{2}\Omega_k(\tau;\tilde{v}_0,-a) - \frac{\mu^2}{2\lambda}e^{-2a\tau}\Omega_k(\tau;\tilde{v}_0,a)\right)\Bigg\},
\end{aligned}
\tag{4.3.14}
$$

$$
\begin{aligned}
W^2(\tau,x) &= e^{-\frac{(\lambda-\mu)(u-x)}{2r}} \times \left\{ \frac{\mu e^{-2a\tau+av_0}+\lambda e^{-av_0}}{2(\lambda+\mu)} - \frac{\mu e^{-2a\tau+a\tilde{v}_0}+\lambda e^{-a\tilde{v}_0}}{2(\lambda+\mu)} \right. \\
&-\frac{1}{2}e^{-a\tau}\sum_{k=0}^{\infty}\frac{1}{\Gamma(k+1)^2}\left(\frac{\alpha y(\tau)}{2}\right)^{2k} + \frac{1}{2}e^{-a\tau}\sum_{k=0}^{\infty}\frac{1}{\Gamma(k+1)^2}\left(\frac{\alpha \tilde{y}(\tau)}{2}\right)^{2k} \\
&+\frac{\alpha^2 v_0}{2(\lambda+\mu)}\sum_{k=0}^{\infty}\frac{1}{\Gamma(k+1)\Gamma(k+2)}\left(\frac{\alpha}{2}\right)^{2k}\left(\frac{\lambda}{2}\Omega_k(\tau;\tilde{v}_0,-a)+\frac{\mu}{2}e^{-2a\tau}\Omega_k(\tau;\tilde{v}_0,a)\right) \\
&-\frac{(\lambda-\mu)}{2(\lambda+\mu)}\sum_{k=0}^{\infty}\frac{1}{\Gamma(k+1)^2}\left(\frac{\alpha}{2}\right)^{2k}\left(\frac{\lambda}{2}\Omega_k(\tau;\tilde{v}_0,-a)+\frac{\mu}{2}e^{-2a\tau}\Omega_k(\tau;\tilde{v}_0,a)\right) \\
&-\frac{\alpha^2 v_0}{2(\lambda+\mu)}\sum_{k=0}^{\infty}\frac{1}{\Gamma(k+1)\Gamma(k+2)}\left(\frac{\alpha}{2}\right)^{2k}\left(\frac{\lambda}{2}\Omega_k(\tau;\tilde{v}_0,-a)+\frac{\mu}{2}e^{-2a\tau}\Omega_k(\tau;\tilde{v}_0,a)\right) \\
&\left. +\frac{(\lambda-\mu)}{2(\lambda+\mu)}\sum_{k=0}^{\infty}\frac{1}{\Gamma(k+1)^2}\left(\frac{\alpha}{2}\right)^{2k}\left(\frac{\lambda}{2}\Omega_k(\tau;\tilde{v}_0,-a)+\frac{\mu}{2}e^{-2a\tau}\Omega_k(\tau;\tilde{v}_0,a)\right)\right\}.
\end{aligned}
\tag{4.3.15}
$$

4.3.2 Long-time Behavior Analysis

The asymptotic expression for $I_n(y)$ as $y \to \infty$ can be expressed as:

$$I_n^A(y) \sim \frac{e^y}{\sqrt{2\pi y}} \sum_{k=0}^{\infty} \frac{(-1)^k n^{2k}}{(2k)!! y^k}, \text{for } n \geq 1 \tag{4.3.16}$$

and

$$I_0^A(y) \sim \frac{e^y}{\sqrt{2\pi y}}. \tag{4.3.17}$$

Notice that as $\tau \to \infty$, $y(\tau) \to \infty$ and

$$\int_{v_0}^{\tau} \alpha v_0 e^{av} y^{-1}(v) I_1[\alpha y(v)] dv \sim \sum_{k=0}^{\infty} \frac{(-1)^k}{(2k)!! \alpha^k} \sqrt{\frac{\alpha v_0^2}{2\pi}} \int_{v_0}^{\tau} \frac{e^{av+\alpha y(v)}}{y(v)^{k+\frac{3}{2}}} dv \tag{4.3.18}$$

$$\int_{v_0}^{\tau} \alpha v_0 e^{-av} y^{-1}(v) I_1[\alpha y(v)] dv \sim \sum_{k=0}^{\infty} \frac{(-1)^k}{(2k)!! \alpha^k} \sqrt{\frac{\alpha v_0^2}{2\pi}} \int_{v_0}^{\tau} \frac{e^{-av+\alpha y(v)}}{y(v)^{k+\frac{3}{2}}} dv. \tag{4.3.19}$$

Let

$$\chi_k(\tau; v_0, a) = \sqrt{\frac{1}{2\pi\alpha}} \int_{v_0}^{\tau} \frac{e^{av+\alpha y(v)}}{y(v)^{k+\frac{3}{2}}} dv \tag{4.3.20}$$

$$\chi_k(\tau; v_0, -a) = \sqrt{\frac{1}{2\pi\alpha}} \int_{v_0}^{\tau} \frac{e^{-av+\alpha y(v)}}{y(v)^{k+\frac{3}{2}}} dv, \tag{4.3.21}$$

we have

$$\int_{v_0}^{\tau} I_0[\alpha y(v)] e^{av} dv \sim \sqrt{\frac{1}{2\pi\alpha}} \int_{v_0}^{\tau} \frac{e^{av+\alpha y(v)}}{y(v)^{\frac{1}{2}}} dv = \chi_{-1}(\tau; v_0, a), \tag{4.3.22}$$

$$\int_{v_0}^{\tau} I_0[\alpha y(v)] e^{-av} dv \sim \sqrt{\frac{1}{2\pi\alpha}} \int_{v_0}^{\tau} \frac{e^{-av+\alpha y(v)}}{y(v)^{\frac{1}{2}}} dv = \chi_{-1}(\tau; v_0, -a), \tag{4.3.23}$$

and

$$\int_{v_0}^{\tau} \alpha v_0 e^{av} y^{-1}(v) I_1[\alpha y(v)] dv \sim \sum_{k=0}^{\infty} \frac{(-1)^k \alpha v_0}{(2k)!! \alpha^k} \chi_k(\tau; v_0, a), \tag{4.3.24}$$

$$\int_{v_0}^{\tau} \alpha v_0 e^{-av} y^{-1}(v) I_1[\alpha y(v)] dv \sim \sum_{k=0}^{\infty} \frac{(-1)^k \alpha v_0}{(2k)!! \alpha^k} \chi_k(\tau; v_0, a). \tag{4.3.25}$$

Therefore, as $\tau \to \infty$, we have the asymptotic expansion for $W^1(\tau, x)$ and $W^2(\tau, x)$ as the followings.

$$\begin{aligned}
W^1(\tau, x) = e^{-\frac{(\lambda-\mu)(u-x)}{2r}} \times \Bigg\{ & \frac{\mu}{2(\lambda+\mu)} \left(1 - e^{-2a(\tau - v_0)}\right) - \frac{\lambda}{2(\lambda+\mu)} e^{-a\tilde{v}_0} \\
& + \frac{\mu^2}{2\lambda(\lambda+\mu)} e^{-2a\tau} e^{a\tilde{v}_0} + e^{-a\tau} \left(\frac{\alpha\tau}{\lambda} \frac{1}{\sqrt{2\pi\alpha}} \frac{e^{\alpha y(\tau)}}{y(\tau)^{\frac{3}{2}}} + \frac{\lambda - \mu}{2\lambda} \frac{1}{\sqrt{2\pi\alpha}} \frac{e^{\alpha y(\tau)}}{y(\tau)^{\frac{1}{2}}} - \frac{\alpha^2 \tilde{v}_0}{2\lambda} \right) \\
& - \frac{\mu(\lambda - \mu)}{2(\lambda+\mu)} \left(\frac{1}{2} \chi_{-1}(\tau; v_0, -a) - \frac{1}{2} e^{-2a\tau} \chi_{-1}(\tau; v_0, a) \right) \\
& + \frac{\mu}{2(\lambda+\mu)} \sum_{k=0}^{\infty} \frac{(-1)^k \alpha v_0}{(2k)!! \alpha^k} \left(\chi_k(\tau; v_0, -a) - e^{-2a\tau} \chi_k(\tau; v_0, a) \right) \\
& + \frac{(\lambda - \mu)}{2(\lambda+\mu)} \left(\frac{\lambda}{2} \chi_{-1}(\tau; \tilde{v}_0, -a) - \frac{\mu^2}{2\lambda} e^{-2a\tau} \chi_{-1}(\tau; \tilde{v}_0, a) \right) \\
& - \frac{\lambda}{2(\lambda+\mu)} \sum_{k=0}^{\infty} \frac{(-1)^k \alpha \tilde{v}_0}{(2k)!! \alpha^k} \left(\frac{\lambda}{2} \chi_k(\tau; \tilde{v}_0, -a) - \frac{\mu^2}{2\lambda} e^{-2a\tau} \chi_k(\tau; \tilde{v}_0, a) \right) \Bigg\}
\end{aligned} \tag{4.3.26}$$

$$
\begin{aligned}
W^2(\tau,x) &= e^{-\frac{(\lambda-\mu)(u-x)}{2r}} \times \left\{ \frac{\mu e^{-2a\tau+av_0}+\lambda e^{-av_0}}{2(\lambda+\mu)} - \frac{\mu e^{-2a\tau+a\tilde{v}_0}+\lambda e^{-a\tilde{v}_0}}{2(\lambda+\mu)} \right. \\
&-\frac{1}{2}e^{-a\tau}\left(\frac{1}{\sqrt{2\pi\alpha}}\frac{e^{\alpha y(\tau)}}{y(\tau)^{\frac{1}{2}}}+\frac{1}{\sqrt{2\pi\alpha}}\frac{e^{\alpha \tilde{y}(\tau)}}{\tilde{y}(\tau)^{\frac{1}{2}}}\right) \\
&+\frac{1}{2(\lambda+\mu)}\sum_{k=0}^{\infty}\frac{(-1)^k\alpha v_0}{(2k)!!\alpha^k}\left(\frac{\lambda}{2}\chi_k(\tau;v_0,-a)+\frac{\mu}{2}e^{-2a\tau}\chi_k(\tau;v_0,a)\right) \\
&-\frac{\lambda-\mu}{2(\lambda+\mu)}\left(\frac{\lambda}{2}\chi_{-1}(\tau;v_0,-a)+\frac{\mu}{2}e^{-2a\tau}\chi_{-1}(\tau;v_0,a)\right) \\
&-\frac{1}{2(\lambda+\mu)}\sum_{k=0}^{\infty}\frac{(-1)^k\alpha \tilde{v}_0}{(2k)!!\alpha^k}\left(\frac{\lambda}{2}\chi_k(\tau;\tilde{v}_0,-a)+\frac{\mu}{2}e^{-2a\tau}\chi_k(\tau;\tilde{v}_0,a)\right) \\
&\left.+\frac{\lambda-\mu}{2(\lambda+\mu)}\left(\frac{\lambda}{2}\chi_{-1}(\tau;\tilde{v}_0,-a)+\frac{\mu}{2}e^{-2a\tau}\chi_{-1}(\tau;\tilde{v}_0,a)\right)\right\}
\end{aligned}
\quad . \tag{4.3.27}
$$

4.3.3 Proposed Comprehensive Expansion

Next, the series representations, described in **Sections** 4.3.1 and 4.3.2, are incorporated to approximate the transient behavior of $W^1(\tau, x)$ and $W^2(\tau, x)$. We want to construct an approximation with the least error for all τ. It is noteworthy to mention that there exist critical points τ_c and $\tilde{\tau}_c$ that serve as the transition points between short and long-time behavior, which is estimated numerically via examining the error differences between the modified Bessel function I_n and the respective power series and asymptotic approximations, I_n^P and I_n^A, given by equations (4.3.1), (4.3.17) and (4.3.16). Our proposed combination is that for $\tau < \tau_c$, the power series are used as our approximation, for $\tau > \tilde{\tau}_c$, the asymptotic series are used as our approximation, while for $\tau_c < \tau < \tilde{\tau}_c$, the asymptotic series are employed for terms of $I_n(y(v))$, whereas the power series are employed for terms of $I_n(\tilde{y}(v))$. With such a combination, the approximation with less error are used for each interval of τ. So we estimate τ_c and $\tilde{\tau}_c$ given the following relationship

$$\begin{aligned}
&\left\| I_n\left(y\left(\tau_c\right)\right) - I_n^P\left(y\left(\tau_c\right)\right)\right\|_2 - \left\| I_n\left(y\left(\tau_c\right)\right) - I_n^A\left(y\left(\tau_c\right)\right)\right\|_2 < \varepsilon, \\
&\left\| I_n\left(\tilde{y}\left(\tilde{\tau}_c\right)\right) - I_n^P\left(\tilde{y}\left(\tilde{\tau}_c\right)\right)\right\|_2 - \left\| I_n\left(\tilde{y}\left(\tilde{\tau}_c\right)\right) - I_n^A\left(\tilde{y}\left(\tilde{\tau}_c\right)\right)\right\|_2 < \varepsilon,
\end{aligned} \tag{4.3.28}$$

for $n = 0, 1$, where ε is the error tolerance. Notice that although τ_c and $\tilde{\tau}_c$ may change for different parameter chosen, $y(\tau_c)$ and $\tilde{y}(\tilde{\tau}_c)$ will be the same constant value. The critical values shown in **Table** 2.3 are also practical values of $y(\tau_c)$ and $\tilde{y}(\tilde{\tau}_c)$ used for approximation of lower orders with the error tolerance $\varepsilon = 10^{-6}$.

Chapter 5

Numerical Results for Ruin Theory

In this chapter, numerical experiments are conducted to illustrate the fidelity of the series expansion approximation in the context of insurance risk management, where the surplus premium rate, the transition rates and the initial surplus are $r = 1$, $\lambda = 2$, $\mu = 5$ and $u = 2$. Additionally, to check the correctness of our solutions, we perform Monte Carlo methods to produce a simulation of the surplus process with totally 1,000 trials. Similar to our discussion in **Chapter** 3, we will use **Table** 3.1 and **Table** 3.2 to describe the scenarios included in the numerical assessment. In each scenario, the difference of solutions getting from two different methods will be compared and analyzed. In each comparison, we will firstly focus on comparing the probability function $F(\tau, x)$, $W^1(\tau, x)$ and $W^2(\tau, x)$ for fixed x ($x = 1$ in the experiment) with respect to τ. The distances of solution functions and its comparative function in L_1, L_2 and L_∞ norm space are employed as criteria to evaluate the error, given t in a bounded close interval, say $\tau \in [0, 20]$. Meanwhile, we will show how the absolute error and relative error of each approximation vary with respect to time τ.

Table 5.1 shows the distances between theoretical solution and approximations in functional space for each scenario. The numerical result shows that the approximation using the combination of two series are reasonable small, and may be applied for a easier and intuitive estimation of $F(\tau, x)$. With the second order terms adding in, the distances decrease more by comparing Scenario II and III, which implies the combination series will universally convergence to the theoretical solution as terms goes to infinity. From the comparison

of Scenario IV, V and VI, we can also conclude that the approximation are comparatively closer to the simulation with the theoretical solution, which implies it is reasonable to use the approximation result as an ideal frame of reference in the application of real data where stochastic error are included.

Scenario	Criteria		
	L_1 Distance	L_2 Distance	L_∞ Distance
I	0.6144	0.6944	0.8715
II	0.0095	0.0102	0.0114
III	0.0077	0.0084	0.0094
IV	0.0060	0.0083	0.0283
V	0.0086	0.0106	0.0294
VI	0.0075	0.0094	0.0273

Table 5.1: Numerical Result of Comparison

Figure 5.1 presents the relative error of our proposed expansion with respect to τ, which shows the robustness of the proposed expansion from a graphical perspective. From the figure we can find that the relative error of our proposed expansion is of order $\mathcal{O}(10^{-2})$ and the error decreases as τ tends to infinity.

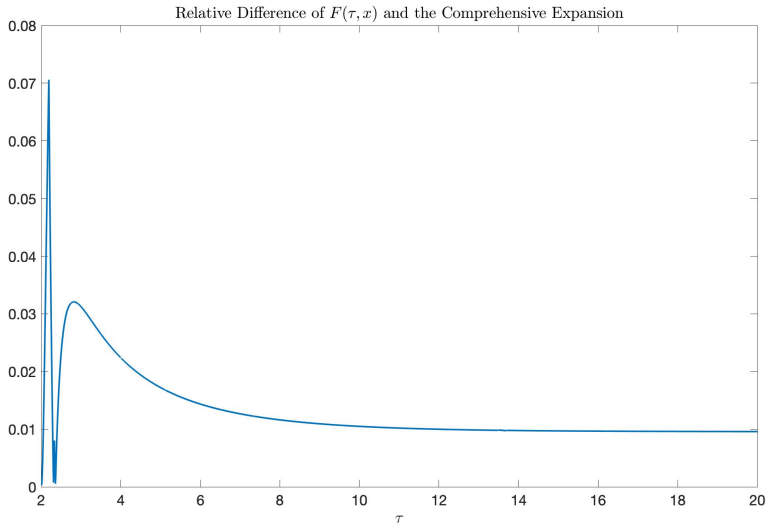

Figure 5.1: Relative error of $F(\tau, x)$ between the four-term approximated solutions and the theoretical solution where x = 1.

Figure 5.2 and 5.3 compare the expansion with the Monte Carlo simulated results. The closeness in 5.2 shows that the behavior of our approximation are consistent with the simulation of real cases. This is further verified in **Figure** 5.3, where the error behavior between the approximated and simulated responses of $F(\tau, x)$ consistently decreases and tend to 0 as $\tau \to \infty$ or as the number of trails added.

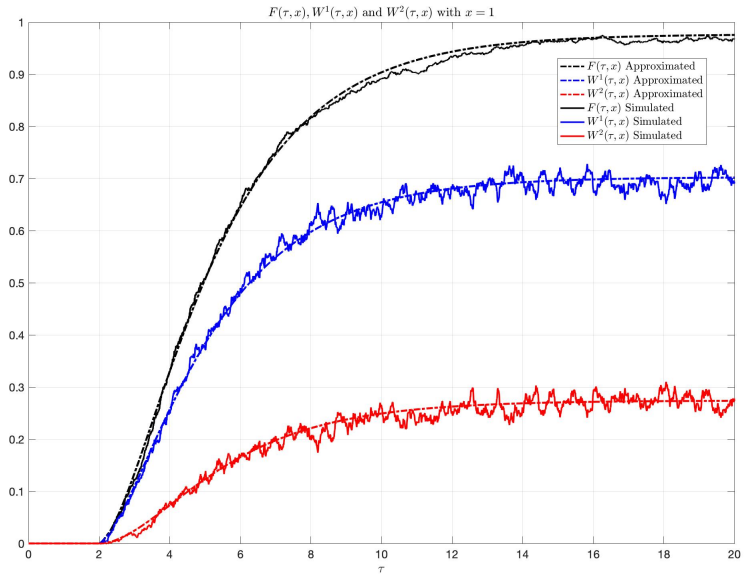

Figure 5.2: Comparison of transient responses between $F(\tau,x), W^1(\tau,x)$ and $W^2(\tau,x)$, where x = 1, between the four-term approximated solutions and those generated by Monte Carlo simulation.

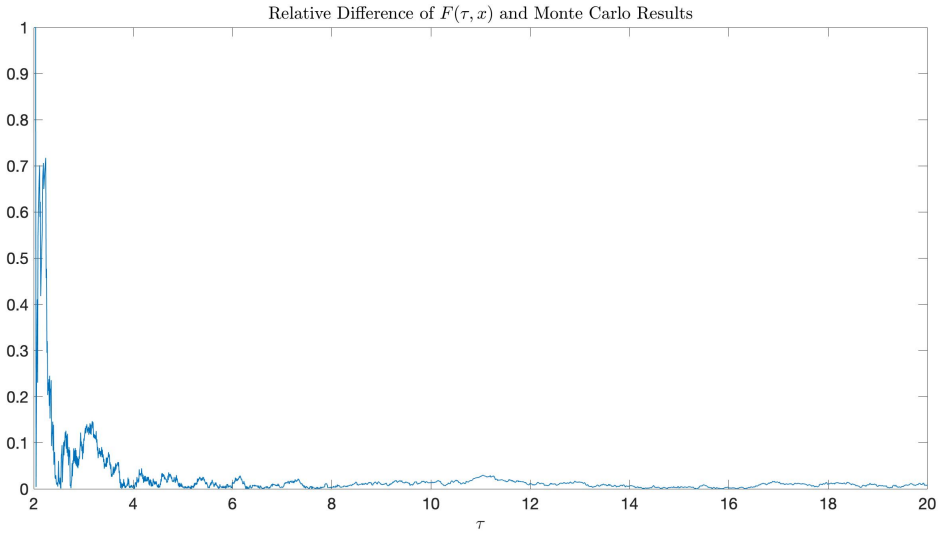

Figure 5.3: Relative error of $F(\tau,x)$ between the four-term approximated solutions and those generated by Monte Carlo simulation where x = 1.

Chapter 6

Conclusion and Future Work

This thesis models the job burst behavior in HPC environments and the surplus process of insurance companies in the context of ruin theory as stochastic fluid queues. We focus on analyzing the transient behavior of stochastic fluid queue fed by a single ON-OFF source and analyzes the transient behavior. We provide the analytical expressions of the cumulative distribution functions of the buffer content considering different cases with the initial state to be either ON or OFF. The asymptotic analysis is employed to provide robust approximations for both short and long-time behavior. Furthermore, comprehensive approximations are proposed towards two cases that show direct correlations between the transient behavior and the parameters like the job burst rate in the HPC case or the premium rate in the premium case. Moreover, using only a few terms can achieve an approximation of these behaviors with high accuracy.

The results of this work have several applications that can benefit researchers not only studying these models, but also their applications. For example, this work can be applied to understand the behavior of fast-packet switching, from theoretical and practical viewpoints, within various distributed networks such as wireless and high-performance computing environments. This work can also be used to understand other types of fluid queues such as multi-dimensional fluid queues, those driven by M/M/1 queues, and tandem fluid queues [28]. On the other hand, the results of this work have several applications provide a explicit expression of the cumulative distribution function of the insurer's surplus in the context of ruin theory, which can be used to calculate the expectation value of the company in the future. Furthermore,

with the distribution function of surplus, we can not only determine the probability of ruin, but also get the Value of Risk easily and consequently help the understanding of the risk management regarding the insurance companies.

Future explorations of this work include extending and generalizing this approach to provide robust transient solutions of fluid queues fed by multiple ON-OFF sources, where the applications include analyzing the effects of traffic congestion. Other explorations of this work include applying these results to quantify the reliability in heterogeneous ultra-dense distributed networks. In addition, from the perspective of insurance risk management, the future exploration directions also include establishing a comprehensive risk analysis strategy for distressed insurers and generalizing the arrival process and the size distribution of claims. Moreover, future researchers can extend this approach to provide robust transient solutions of fluid queues fed by multiple ON-OFF sources. Other explorations of this work include applying these results to solving other stochastic processes like geometric Brownian Motion [29].

Bibliography

[1] Jack Dongarra et al. “High-performance computing: clusters, constellations, MPPs, and future directions”. In: *Computing in Science & Engineering* 7.2 (2005), pp. 51–59.

[2] P Gonzalo et al. “HPC scheduling in a brave new world”. PhD thesis. Umeå universitet, 2017.

[3] Wilfried Haensch et al. “Silicon CMOS devices beyond scaling”. In: *IBM Journal of Research and Development* 50.4.5 (2006), pp. 339–361.

[4] Ning Liu et al. “On the role of burst buffers in leadership-class storage systems”. In: *012 ieee 28th symposium on mass storage systems and technologies (msst)*. IEEE. 2012, pp. 1–11.

[5] Martin F Grace, Robert W Klein, and Richard D Phillips. “Insurance Company Failures: Why Do They Cost So Much?” In: *Georgia State University Center for Risk Management and Insurance Research Working Paper* 03-1 (2003).

[6] Viral V Acharya and Matthew Richardson. “Is the insurance industry systemically risky?” In: *Modernizing insurance regulation* (2014), pp. 151–80.

[7] Karl Henrik Borch. *The mathematical theory of insurance: an annotated selection of papers on insurance published 1960-1972*. Lexington Books, 1974.

[8] Matthias Hovestadt et al. “Scheduling in HPC resource management systems: Queuing vs. planning”. In: *Workshop on Job Scheduling Strategies for Parallel Processing*. Springer. 2003, pp. 1–20.

[9] Nenad Milidrag, George Kesidis, and Mihail Devetsikiotis. "Overview of fluid-based quick simulation techniques for large packet-switched communication networks". In: *Scalability and Traffic Control in IP Networks*. Vol. 4526. International Society for Optics and Photonics. 2001, pp. 271–278.

[10] D. Anick, D. Mitra, and M. M. Sondhi. "Stochastic Theory of a Data-Handling System with Multiple Sources". In: *Bell Labs Technical Journal* 61.8 (1982), pp. 1871–1894.

[11] Lingjia Liu et al. "Resource allocation and quality of service evaluation for wireless communication systems using fluid models". In: *IEEE Transactions on Information Theory* 53.5 (2007), pp. 1767–1777.

[12] Ning Liu. "Modeling the Impact of Intentional Behavior in Supercomputing Environments via 1-D and 2-D Stochastic Fluid Queues Fed by an ON-OFF Source". PhD thesis. Johns Hopkins University, 2018.

[13] Nigel G Bean and Małgorzata M O'Reilly. "A stochastic two-dimensional fluid model". In: *Stochastic Models* 29.1 (2013), pp. 31–63.

[14] Aviva Samuelson, MM O'Reilly, and NG Bean. "Generalised reward generator for stochastic fluid models". In: *Submitted to the 9th International Conference on Matrix-Analytic Methods in Stochastic Models*. 2016.

[15] Takeshi Tanaka, On Hashida, and Yukio Takahashi. "Transient analysis of fluid model for ATM statistical multiplexer". In: *Performance evaluation* 23.2 (1995), pp. 145–162.

[16] P.R. Parthasarathy and K. V. Vijayashree. "A Fluid Queue Fed by an On-Off Source". In: *IEEE Annual INDICON*. IEEE. 2005, pp. 396–398.

[17] S. Aalto and W. R. W. Scheinhardt. "Tandem Fluid Queues Fed by Homogeneous On–Off Sources". In: *Operations Research Letters* 27.2 (2000), pp. 73–82.

[18] Christopher D Daykin et al. "Assessing the solvency and financial strength of a general insurance company". In: *Journal of the Institute of Actuaries* 114.2 (1987), pp. 227–325.

[19] Tomasz Rolski et al. *Stochastic processes for insurance and finance*. Vol. 505. John Wiley & Sons, 2009.

[20] Freddy Delbaen and Jean Haezendonck. "Classical risk theory in an economic environment". In: *Insurance: Mathematics and Economics* 6.2 (1987), pp. 85–116.

[21] Hans U Gerber, Marc J Goovaerts, and Rob Kaas. "On the probability and severity of ruin". In: *ASTIN Bulletin: The Journal of the IAA* 17.2 (1987), pp. 151–163.

[22] Hans U Gerber and Elias SW Shiu. "On the time value of ruin". In: *North American Actuarial Journal* 2.1 (1998), pp. 48–72.

[23] François Dufresne and Hans U Gerber. "The probability and severity of ruin for combinations of exponential claim amount distributions and their translations". In: *Insurance: Mathematics and Economics* 7.2 (1988), pp. 75–80.

[24] Andrei Badescu et al. "Risk processes analyzed as fluid queues". In: *Scandinavian Actuarial Journal* 2005.2 (2005), pp. 127–141.

[25] Vaidyanathan Ramaswami. "Passage times in fluid models with application to risk processes". In: *Methodology and Computing in Applied Probability* 8.4 (2006), pp. 497–515.

[26] Tao Zhou et al. "Numerical solution for ruin probability of continuous time model based on neural network algorithm". In: *Neurocomputing* 331 (2019), pp. 67–76.

[27] Martin Eling and Ines Holzmüller. "An Overview and Comparison of Risk-Based Capital Standards." In: *Journal of Insurance Regulation* 26.4 (2008).

[28] K.V. Vijayashree and A. Anjuka. "Fluid Queue Driven by an M/M/1 Queue Subject to Bernoulli-Schedule-Controlled Vacation and Vacation Interruption". In: *Advanced in Operations Research* (2016).

[29] Søren Asmussen. "Stationary distributions for fluid flow models with or without Brownian noise". In: *Communications in statistics. Stochastic models* 11.1 (1995), pp. 21–49.

[30] Murray R Spiegel. *Laplace transforms*. McGraw-Hill New York, 1965.

Chapter 7

Appendix

7.1 Appendix A: Codes of Numerical Results for HPC Resource Allocation

Listing 7.1: Codes of Numerical Results for HPC Resource Allocation

```
close all
clear
warning off
tic
Lambda_est=[1.3,0.4];
R=[-1,4];
x_fix=1;
dt=0.01;
t_n=20;
t=0:dt:t_n;
close
[F,W_1,W_2]=FQ(Lambda_est(1),Lambda_est(2),R(1),R(2),
   x_fix,'O',1,t_n,dt);
[F_PS,W_1PS,W_2PS]=FQ(Lambda_est(1),Lambda_est(2),R(1),
   R(2),x_fix,'P',1,t_n,dt);
[F_AS,W_1AS,W_2AS]=FQ(Lambda_est(1),Lambda_est(2),R(1),
   R(2),x_fix,'A',1,t_n,dt);
[F_C,W_1C,W_2C]=FQ(Lambda_est(1),Lambda_est(2),R(1),R
   (2),x_fix,'C',1,t_n,dt);
```

```
[F_C2,W_1C2,W_2C2]=FQ(Lambda_est(1),Lambda_est(2),R(1),
   R(2),x_fix,'C',5,t_n,dt);
[F_M,W_1M,W_2M]=MonteCarloSimulationFQ(Lambda_est(1),
   Lambda_est(2),R(1),R(2),x_fix,t_n,dt);

%% Senario I
% F vs PS
figure
title('Comparison of Senario I')
subplot(2,2,1)
figure
plot(t,F(round(t/dt)+1))
hold on
plot(t,F_PS(round(t/dt)+1))
%title('(a) Prob(Q(t) \leq x)','fontsize',16)
legend('F(t,x)','F(t,x) Approximated')
% axis([0,20,0,1])

subplot(2,2,2)
plot(t,W_1(round(t/dt)+1),'b')
hold on
plot(t,W_2(round(t/dt)+1),'r')
plot(t,W_1PS(round(t/dt)+1),'b-.')
plot(t,W_2PS(round(t/dt)+1),'r-.')
title('(b) W^1(t,x) and W^2(t,x)','fontsize',16)
legend('W^1(t,x)','W^2(t,x)','W^1(t,x) Approximated','W
   ^2(t,x) Approximated')
% axis([0,20,0,1])

subplot(2,2,3)
plot(t,abs(F(round(t/dt)+1)-F_PS(round(t/dt)+1)))
hold on
title('(c) Absolute Difference of F(t,x)','fontsize'
   ,16)
%axis([0,20])

subplot(2,2,4)
```

```
plot(t,(abs(F_PS(round(t/dt)+1)-F(round(t/dt)+1))./F(round(t/dt)+1)))
hold on
title('(d) Relative Difference of F(t,x)','fontsize',16)

% Distance
L1_I=sum(abs(F(round(t/dt)+1)-F_PS(round(t/dt)+1))*dt);
L2_I=sqrt(sum(((F(round(t/dt)+1)-F_PS(round(t/dt)+1)).^2)*dt));
Linf_I=max(abs(F(round(t/dt)+1)-F_PS(round(t/dt)+1))*dt);
Lmean_I=mean(abs(F(round(t/dt)+1)-F_PS(round(t/dt)+1))*dt);
L_I=[L1_I L2_I Linf_I Lmean_I];


%% Senario II
% F vs AS
figure
title('Comparison of Senario II')
subplot(2,2,1)
plot(t,F(round(t/dt)+1))
hold on
plot(t,F_AS(round(t/dt)+1))
title('(a) Prob(Q(t) \leq x)','fontsize',16)
legend('F(t,x)','F(t,x) Approximated')
%axis([0,20,0,1])

subplot(2,2,2)
plot(t,W_1(round(t/dt)+1),'b')
hold on
plot(t,W_2(round(t/dt)+1),'r')
plot(t,W_1AS(round(t/dt)+1),'b-.')
plot(t,W_2AS(round(t/dt)+1),'r-.')
title('(b) W^1(t,x) and W^2(t,x)','fontsize',16)
legend('W^1(t,x)','W^2(t,x)','W^1(t,x) Approximated','W^2(t,x) Approximated')
```

```
%axis([0,20,0,1])

subplot(2,2,3)
plot(t,abs(F(round(t/dt)+1)-F_AS(round(t/dt)+1)))
hold on
title('(c) Absolute Difference of F(t,x)','fontsize'
   ,16)
%axis([0,20])

subplot(2,2,4)
plot(t,(abs(F_AS(round(t/dt)+1)-F(round(t/dt)+1))./F(
   round(t/dt)+1)))
hold on
title('(d) Relative Difference of F(t,x)','fontsize'
   ,16)
% Distance
L1_II=sum(abs(F(round(t/dt)+1)-F_AS(round(t/dt)+1))*dt)
   ;
L2_II=sqrt(sum(((F(round(t/dt)+1)-F_AS(round(t/dt)+1))
   .^2)*dt));
Linf_II=max(abs(F(round(t/dt)+1)-F_AS(round(t/dt)+1))*
   dt);
Lmean_II=mean(abs(F(round(t/dt)+1)-F_AS(round(t/dt)+1))
   *dt);
L_II=[L1_II L2_II Linf_II Lmean_II];

%% Senario III
% F vs Combination
figure
title('Comparison of Senario III')
subplot(2,2,1)
plot(t,F(round(t/dt)+1))
hold on
plot(t,F_C(round(t/dt)+1))
title('(a) Prob(Q(t) \leq x)','fontsize',16)
legend('F(t,x)','F(t,x) Approximated')
%axis([0,20,0,1])

```

```
subplot(2,2,2)
plot(t,W_1(round(t/dt)+1),'b')
hold on
plot(t,W_2(round(t/dt)+1),'r')
plot(t,W_1C(round(t/dt)+1),'b-.')
plot(t,W_2C(round(t/dt)+1),'r-.')
title('(b) W^1(t,x) and W^2(t,x)','fontsize',16)
legend('W^1(t,x)','W^2(t,x)','W^1(t,x) Approximated','W^2(t,x) Approximated')
%axis([0,20,0,1])

subplot(2,2,3)
plot(t,abs(F(round(t/dt)+1)-F_C(round(t/dt)+1)))
hold on
title('(c) Absolute Difference of F(t,x)','fontsize',16)
%axis([0,20])

subplot(2,2,4)
plot(t,(abs(F_C(round(t/dt)+1)-F(round(t/dt)+1))./F(round(t/dt)+1)))
hold on
title('(d) Relative Difference of F(t,x)','fontsize',16)

% Distance
L1_III=sum(abs(F(round(t/dt)+1)-F_C(round(t/dt)+1))*dt);
L2_III=sqrt(sum(((F(round(t/dt)+1)-F_C(round(t/dt)+1)).^2)*dt));
Linf_III=max(abs(F(round(t/dt)+1)-F_C(round(t/dt)+1))*dt);
Lmean_III=mean(abs(F(round(t/dt)+1)-F_C(round(t/dt)+1))*dt);

L_III=[L1_III L2_III Linf_III Lmean_III];

%% Senario IV
```

```
% F vs Combination 2
figure
title('Comparison of Senario IV')
subplot(2,2,1)
plot(t,F(round(t/dt)+1))
hold on
plot(t,F_C2(round(t/dt)+1))
title('(a) Prob(Q(t) \leq x)','fontsize',16)
legend('F(t,x)','F(t,x) Approximated')
%axis([0,20,0,1])

subplot(2,2,2)
plot(t,W_1(round(t/dt)+1),'b')
hold on
plot(t,W_2(round(t/dt)+1),'r')
plot(t,W_1C2(round(t/dt)+1),'b-.')
plot(t,W_2C2(round(t/dt)+1),'r-.')
title('(b) W^1(t,x) and W^2(t,x)','fontsize',16)
legend('W^1(t,x)','W^2(t,x)','W^1(t,x) Approximated','W
   ^2(t,x) Approximated')
%axis([0,20,0,1])

subplot(2,2,3)
plot(t,abs(F(round(t/dt)+1)-F_C2(round(t/dt)+1)))
hold on
title('(c) Absolute Difference of F(t,x)','fontsize'
   ,16)
%axis([0,20])

subplot(2,2,4)
plot(t,(abs(F_C2(round(t/dt)+1)-F(round(t/dt)+1))./F(
   round(t/dt)+1)))
hold on
title('(d) Relative Difference of F(t,x)','fontsize'
   ,16)

% Distance
```

```
L1_IV=sum(abs(F(round(t/dt)+1)-F_C2(round(t/dt)+1))*dt)/t_n;
L2_IV=sqrt(sum(((F(round(t/dt)+1)-F_C2(round(t/dt)+1)).^2)*dt));
Linf_IV=max(abs(F(round(t/dt)+1)-F_C2(round(t/dt)+1))*dt);
Lmean_IV=mean(abs(F(round(t/dt)+1)-F_C2(round(t/dt)+1))*dt);
L_IV=[L1_IV L2_IV Linf_IV Lmean_IV];

%% Senario V
% F vs MC
figure
title('Comparison of Senario V')
subplot(2,2,1)
plot(t,F(round(t/dt)+1))
hold on
plot(t,F_M(round(t/dt)+1))
title('(a) Prob(Q(t) \leq x)','fontsize',16)
legend('F(t,x)','F(t,x) Simulated')
% axis([0,20,0,1])

subplot(2,2,2)
plot(t,W_1(round(t/dt)+1),'b')
hold on
plot(t,W_2(round(t/dt)+1),'r')
plot(t,W_1M(round(t/dt)+1),'b-.')
plot(t,W_2M(round(t/dt)+1),'r-.')
title('(b) W^1(t,x) and W^2(t,x)','fontsize',16)
legend('W^1(t,x)','W^2(t,x)','W^1(t,x) Simulated','W^2(t,x) Simulated')
% axis([0,20,0,1])

subplot(2,2,3)
plot(t,abs(F(round(t/dt)+1)-F_M(round(t/dt)+1)))
hold on
title('(c) Absolute Difference of F(t,x)','fontsize',16)
```

```
%axis([0,20])

subplot(2,2,4)
plot(t,(abs(F_M(round(t/dt)+1)-F(round(t/dt)+1))./F(
   round(t/dt)+1)))
hold on
title('(d) Relative Difference of F(t,x)','fontsize'
   ,16)

% Distance
L1_V=sum(abs(F(round(t/dt)+1)-F_M(round(t/dt)+1))*dt);
L2_V=sqrt(sum(((F(round(t/dt)+1)-F_M(round(t/dt)+1))
   .^2)*dt));
Linf_V=max(abs(F(round(t/dt)+1)-F_M(round(t/dt)+1))*dt)
   ;
Lmean_V=mean(abs(F(round(t/dt)+1)-F_M(round(t/dt)+1))*
   dt);

L_V=[L1_V L2_V Linf_V Lmean_V];


%% Senario VI
% Combination 2 vs MC
figure
title('Comparison of Senario VI')
subplot(2,2,1)
plot(t,F_C2(round(t/dt)+1))
hold on
plot(t,F_M(round(t/dt)+1))
title('(a) Prob(Q(t) \leq x)','fontsize',16)
legend('F(t,x) Approximated','F(t,x) Simulated')
% axis([0,20,0,1])

subplot(2,2,2)
plot(t,W_1C2(round(t/dt)+1),'b')
hold on
plot(t,W_2C2(round(t/dt)+1),'r')
plot(t,W_1M(round(t/dt)+1),'b-.')
```

```
plot(t,W_2M(round(t/dt)+1),'r-.')
title('(b) W^1(t,x) and W^2(t,x)','fontsize',16)
legend('W^1(t,x) Approximated','W^2(t,x) Approximated',
    'W^1(t,x) Simulated','W^2(t,x) Simulated')
% axis([0,20,0,1])

subplot(2,2,3)
plot(t,abs(F_C2(round(t/dt)+1)-F_M(round(t/dt)+1)))
hold on
title('(c) Absolute Difference of F(t,x)','fontsize'
    ,16)
%axis([0,20])

subplot(2,2,4)
plot(t,(abs(F_M(round(t/dt)+1)-F_C2(round(t/dt)+1))./
    F_C2(round(t/dt)+1)))
hold on
title('(d) Relative Difference of F(t,x)','fontsize'
    ,16)

% Distance
L1_VI=sum(abs(F_C2(round(t/dt)+1)-F_M(round(t/dt)+1))*
    dt);
L2_VI=sqrt(sum(((F_C2(round(t/dt)+1)-F_M(round(t/dt)+1)
    ).^2)*dt));
Linf_VI=max(abs(F_C2(round(t/dt)+1)-F_M(round(t/dt)+1))
    *dt);
Lmean_VI=mean(abs(F_C2(round(t/dt)+1)-F_M(round(t/dt)
    +1))*dt);

L_VI=[L1_VI L2_VI Linf_VI Lmean_VI];

%%
L1_VII=sum(abs(F_C(round(t/dt)+1)-F_M(round(t/dt)+1))*
    dt);
L2_VII=sqrt(sum(((F_C(round(t/dt)+1)-F_M(round(t/dt)+1)
    ).^2)*dt));
```

```
Linf_VII=max(abs(F_C(round(t/dt)+1)-F_M(round(t/dt)+1))
   *dt);
Lmean_VII=mean(abs(F_C(round(t/dt)+1)-F_M(round(t/dt)
   +1))*dt);

L_VII=[L1_VII L2_VII Linf_VII Lmean_VII];
%%

L=[L_I;L_III;L_IV;L_V;L_VII;L_VI];
toc
```

Listing 7.2: FQ.m

```
function [W,F_0,F_1]=FQ(lambda,mu,r_0,r_1,x,Senario,
   Order,t_n,dt)

    if nargin < 9, dt=0.5; end
    if nargin < 8, t_n=20; end
    if nargin < 7, Order = 1; end
    if nargin < 6, Senario = 'o'; end
    %% Constants
    a=(lambda*r_1-mu*r_0)/(r_1-r_0);
    b=(-1/2)*(1/r_0-1/r_1);
    alpha=sqrt(-4*lambda*mu*r_0*r_1/((r_1-r_0)^2));

    %% Functions
    K=@(t) ((t+2*b*x)./t).^(1/2);

    %
    %{ BesselI Functions
    I_0=BI(0,Senario,Order);
    I_1=BI(1,Senario,Order);
    I_2=BI(2,Senario,Order);
    %}


    % Testing Version
        Convol_left=@(t) exp((lambda+mu).*t);
        %% g
```

```
26
27          g= @(t) (1/2)*alpha*exp(-a*t).*(K(t)-1./K(t)).*
                I_1(alpha*K(t).*t);
28      Convol_g=@(t) Convol_left(t).*g(t);
29      Integral_g_1=@(t) integral(g,0,t);
30      Integral_g_2=@(t) -exp(-(lambda+mu).*(t-x/r_1)).*
           integral(Convol_g,0,t);
31      Integral_g=@(t) 1-exp(-(lambda+mu).*(t-x/r_1))+
           Integral_g_1(t)+Integral_g_2(t);
32      F_1_first= @(t) (lambda/(lambda+mu))*(1-exp(-(
           lambda+mu)*t));
33      F_1_second=@(t) -(lambda/(lambda+mu))*exp(-mu*x/r_1
           )*Integral_g(t);
34
35      F_1=zeros(1,t_n+1);
36      for t=0:dt:t_n
37          F_1(round(t/dt)+1)=F_1_first(t);
38          if t>x/r_1
39              F_1(round(t/dt)+1)=F_1_first(t)+F_1_second(
                   t);
40          end
41      end
42      %W=F_1;
43      %{
44      figure
45      hold on
46      plot([0:1:t_n],F_1);
47      %}
48      %%
49     % h
50      h=@(t) ((lambda*mu*r_1)/(r_1-r_0))*exp(-a*t).*( I_0
           (alpha*K(t).*t)-(K(t).^(-2)) .*I_2(alpha*K(t).*t
           )) ;
51      Convol_h=@(t) Convol_left(t).*h(t);
52      Integral_h_1=@(t) integral(h,0,t);
53      Integral_h_2=@(t) -exp(-(lambda+mu).*(t-x/r_1)).*
           integral(Convol_h,0,t);
54
```

```
55      F_0_first= @(t) (mu/(lambda+mu)+lambda/(lambda+mu)*
           exp(-(lambda+mu)*t));
56      F_0_second=@(t) -(1/(lambda+mu))*exp(-mu*x/r_1)*(
           Integral_h_1(t)+Integral_h_2(t));
57
58
59      F_0=zeros(1,t_n+1);
60      for t=0:dt:t_n
61          F_0(round(t/dt)+1)=F_0_first(t);
62          if t>x/r_1
63              F_0(round(t/dt)+1)=F_0_first(t)+F_0_second(
                   t);
64          end
65      end
66      F_0(1)=1;
67      F_1(1)=0;
68
69      W= F_0+F_1;
70  end
```

Listing 7.3: MonteCarloSimulationFQ.m

```
1  % Monte Carlo simulating Stochastic Fluid Queue
2  function [W,F1,F2]=MonteCarloSimulationFQ(lambda,mu,r_0
      ,r_1,x,t_end,dt,u,s0,iter)
3      if nargin < 10, iter=1000; end
4      if nargin < 9, s0=0; end
5      if nargin < 8, u=0; end
6      if nargin < 7, dt=0.5; end
7      if nargin < 6, t_end=20; end
8
9  % 2 states
10 % Number of Agents
11 % N=1;
12 % Rates Transforming between states
13 r=[r_0,r_1];
14 lambda=[lambda,mu];
15
16 % Distribution function
```

```
17
18 W=zeros(t_end/dt+1,1);
19 F1=zeros(t_end/dt+1,1);
20 F2=zeros(t_end/dt+1,1);
21  for k=1:iter
22      rng(k);
23     S=zeros(t_end/dt+1,1);    %State
24     S(1)=s0;
25     % X=zeros(t_end/dt,1);
26
27     % Buffer Content
28     Q=zeros(t_end/dt+1,1);
29     Q(1)=u;
30
31 %% Simulation of Q(t)
32
33     for ti=2:t_end/dt+1
34         p=exprnd(1/lambda(S(ti-1)+1));
35         Q(ti)=max(Q(ti-1)+(r(S(ti-1)+1))*dt,0);
36         % if Q(ti)==0
37            % break
38         % end
39         if p<=dt     % Change State
40             S(ti)=mod(S(ti-1)+1,2);
41         else
42             S(ti)=mod(S(ti-1),2);
43         end
44     end
45     W=W+(Q<=x); % ECDF
46     F1=F1+((Q<=x).*(S==0));
47     F2=F2+((Q<=x).*(S==1));
48     % figure; plot(Q);
49  end
50
51     W=W/k;
52     F1=F1/k;
53     F2=F2/k;
54     W=W';
```

```
    F1=F1';
    F2=F2';
end
```

Listing 7.4: BI.m

```
function Bessel=BI(n,senario,m)
%   n - Bessel Function type
%   senario - 'o' for original, 'p' for power series, 'm' for asymptotic
%   series
%   m - orders used for approximation

    %   Combination of 1st order P.S and A.S
    if nargin < 3, m = 1; end
    if nargin < 2, senario = 'o'; end
    if(senario=='o' | senario=='O' )
        Bessel=@(t) besseli(n,t);
        return;
    end
    if(senario=='p' | senario=='P' )
        B=@(t) 0;
        for k=0:m
            I_PS=@(t) ((t/2).^n).*(1/(gamma(k+1).*gamma(k+n+1))).*(t/2).^(2*k));
            B= @(t) B(t)+I_PS(t);
        end
        Bessel=@(t) B(t);
        return;
    end
    if(senario=='a' | senario=='A' )
        B=@(t) 0;
        for k=0:m
            I_AS=@(t) (1./(2*pi*t)).^(1/2).*exp(t).*(((-1)^k)*(n^(2*k))./(double_factorial(2*k).*(t.^(2*k)))));
            B= @(t) B(t)+I_AS(t);
        end
        Bessel=@(t) B(t);
```

```
30          return;
31      end
32      if(senario=='c' | senario=='C' )
33          B=@(t) besseli(n,t);
34          B_AS=@(t) 0;
35          B_PS=@(t) 0;
36          for k=0:m
37              I_AS=@(t) (1./(2*pi*t)).^(1/2).*exp(t)
                    .*(((-1)^k)*(n^(2*k))./((
                    double_factorial(2*k).*(t.^(2*k)))));
38              B_AS= @(t) B_AS(t)+I_AS(t);
39              I_PS=@(t) ((t/2).^n).*(1/(gamma(k+1).*gamma
                    (k+n+1)).*(t/2).^(2*k));
40              B_PS= @(t) B_PS(t)+I_PS(t);
41          end
42              Bessel=@(t) (abs(B_AS(t)-B(t))<abs(B_PS(t)-
                    B(t))).*B_AS(t)+(abs(B_AS(t)-B(t))>=abs(
                    B_PS(t)-B(t))).*B_PS(t);
43          return;
44      end
45
46      Bessel=0;
47
48      function result = double_factorial(n)
49          if (n == 1 || n==0)
50              result = 1;
51              elseif (mod(n,2) == 0) % the number is even
52                  result = prod(2:2:n);
53              else % the number is odd
54                  result = prod(1:2:n);
55          end
56      end
57
58  end
```

7.2 Appendix B: MATLAB Codes of Numerical Results for Ruin Theory

Listing 7.5: MATLAB Codes of Numerical Results for Ruin Theory

```
close all
clear
warning off
tic

r=1; lambda=2; mu=5; u=3; x=2;

Lambda_est=[lambda,mu];
R=[-r,r];
x_fix=1;
dt=1/128;
t_n=20;
t=0:dt:t_n;
close


[F,W_1,W_2]=RuinProb(Lambda_est(1),Lambda_est(2),R(1),R(2),x_fix,'O',1,t_n,dt,u);   % Theoretical
rmmissing([F,W_1,W_2]); F=[0;F]; W_1=[0;W_1]; W_2=[0;W_2];
[F_PS,W_1PS,W_2PS]=RuinProb(Lambda_est(1),Lambda_est(2),R(1),R(2),x_fix,'P',1,t_n,dt,u);    % Power Series 1
rmmissing([F_PS,W_1PS,W_2PS]); F_PS=[0;F_PS]; W_1PS=[0;W_1PS]; W_2PS=[0;W_2PS];
[F_C,W_1C,W_2C]=RuinProb(Lambda_est(1),Lambda_est(2),R(1),R(2),x_fix,'C',1,t_n,dt,u);   % Combination 1
rmmissing([F_C,W_1C,W_2C]); F_C=[0;F_C]; W_1C=[0;W_1C]; W_2C=[0;W_2C];
[F_C2,W_1C2,W_2C2]=RuinProb(Lambda_est(1),Lambda_est(2),R(1),R(2),x_fix,'C',2,t_n,dt,u);    % Combination 2
rmmissing([F_C2,W_1C2,W_2C2]); F_C2=[0;F_C2]; W_1C2=[0;W_1C2]; W_2C2=[0;W_2C2];
```

```
25 [F_M,W_1M,W_2M]=MonteCarloSimulationFQ(Lambda_est(1),
      Lambda_est(2),R(1),R(2),x_fix,t_n,dt,u,1); % Monte
      Carlo Result
26 F_M=F_M'; W_1M=W_1M'; W_2M=W_2M';
27 %% Senario I
28 % F vs PS
29 figure
30 title('Comparison of Senario I')
31 subplot(2,2,1)
32 plot(t,F((t/dt)+1))
33 hold on
34 plot(t,F_PS((t/dt)+1))
35 legend('F(t,x)','F(t,x) Approximated')
36 subplot(2,2,2)
37 plot(t,W_1((t/dt)+1),'b')
38 hold on
39 plot(t,W_2((t/dt)+1),'r')
40 plot(t,W_1PS((t/dt)+1),'b-.')
41 plot(t,W_2PS((t/dt)+1),'r-.')
42 title('(b) W^1(t,x) and W^2(t,x)','fontsize',16)
43 legend('W^1(t,x)','W^2(t,x)','W^1(t,x) Approximated','W
      ^2(t,x) Approximated')
44 % axis([0,20,0,1])
45
46 subplot(2,2,3)
47 plot(t,abs(F((t/dt)+1)-F_PS((t/dt)+1)))
48 hold on
49 title('(c) Absolute Difference of F(t,x)','fontsize'
      ,16)
50 %axis([0,20])
51
52 subplot(2,2,4)
53 plot(t,(F((t/dt)+1)>0).*(abs(F_PS((t/dt)+1)-F((t/dt)+1)
      )./F((t/dt)+1)))
54 hold on
55 title('(d) Relative Difference of F(t,x)','fontsize'
      ,16)
56
```

```
% Distance
L1_I=sum(rmmissing(abs(F((t/dt)+1)-F_PS((t/dt)+1))*dt))
   /t_n;
L2_I=sqrt(sum(rmmissing(((F((t/dt)+1)-F_PS((t/dt)+1))
   .^2)*dt))/t_n);
Linf_I=max(rmmissing(abs(F((t/dt)+1)-F_PS((t/dt)+1))));
Lmean_I=mean(rmmissing(abs(F((t/dt)+1)-F_PS((t/dt)+1)))
   );
L_I=[L1_I L2_I Linf_I Lmean_I];

%% Senario II
% F vs Combination
figure
title('Comparison of Senario II')
subplot(2,2,1)
plot(t,F((t/dt)+1))
hold on
plot(t,F_C((t/dt)+1))
title('(a) Prob(Q(t) \leq x)','fontsize',16)
legend('F(t,x)','F(t,x) Approximated')
%axis([0,20,0,1])

subplot(2,2,2)
plot(t,W_1((t/dt)+1),'b')
hold on
plot(t,W_2((t/dt)+1),'r')
plot(t,W_1C((t/dt)+1),'b-.')
plot(t,W_2C((t/dt)+1),'r-.')
title('(b) W^1(t,x) and W^2(t,x)','fontsize',16)
legend('W^1(t,x)','W^2(t,x)','W^1(t,x) Approximated','W
   ^2(t,x) Approximated')
%axis([0,20,0,1])

subplot(2,2,3)
plot(t,abs(F((t/dt)+1)-F_C((t/dt)+1)))
hold on
title('(c) Absolute Difference of F(t,x)','fontsize'
   ,16)
```

```
%axis([0,20])

subplot(2,2,4)
plot(t,(F((t/dt)+1)>0).*(abs(F_C((t/dt)+1)-F((t/dt)+1))
   ./F((t/dt)+1)))
hold on
title('(d) Relative Difference of F(t,x)','fontsize'
   ,16)

% Distance
L1_II=sum(rmmissing(abs(F((t/dt)+1)-F_C((t/dt)+1))*dt))
   /t_n;
L2_II=sqrt(sum(rmmissing(((F((t/dt)+1)-F_C((t/dt)+1))
   .^2)*dt))/t_n);
Linf_II=max(rmmissing(abs(F((t/dt)+1)-F_C((t/dt)+1))));
Lmean_II=mean(rmmissing(abs(F((t/dt)+1)-F_C((t/dt)+1)))
   );

L_II=[L1_II L2_II Linf_II Lmean_II];

%% Senario III
% F vs Combination 2
figure
title('Comparison of Senario III')
subplot(2,2,1)
plot(t,F((t/dt)+1))
hold on
plot(t,F_C2((t/dt)+1))
title('(a) Prob(Q(t) \leq x)','fontsize',16)
legend('F(t,x)','F(t,x) Approximated')
%axis([0,20,0,1])

subplot(2,2,2)
plot(t,W_1((t/dt)+1),'b')
hold on
plot(t,W_2((t/dt)+1),'r')
plot(t,W_1C2((t/dt)+1),'b-.')
plot(t,W_2C2((t/dt)+1),'r-.')
```

```
title('(b) W^1(t,x) and W^2(t,x)','fontsize',16)
legend('W^1(t,x)','W^2(t,x)','W^1(t,x) Approximated','W^2(t,x) Approximated')
%axis([0,20,0,1])

subplot(2,2,3)
plot(t,abs(F((t/dt)+1)-F_C2((t/dt)+1)))
hold on
title('(c) Absolute Difference of F(t,x)','fontsize',16)
%axis([0,20])

subplot(2,2,4)
plot(t,(F((t/dt)+1)>0).*(abs(F_C2((t/dt)+1)-F((t/dt)+1))./F((t/dt)+1)))
hold on
title('(d) Relative Difference of F(t,x)','fontsize',16)

% Distance
L1_III=sum(rmmissing(abs(F((t/dt)+1)-F_C2((t/dt)+1))*dt)/t_n);
L2_III=sqrt(sum(rmmissing(((F((t/dt)+1)-F_C2((t/dt)+1)).^2)*dt))/t_n);
Linf_III=max(rmmissing(abs(F((t/dt)+1)-F_C2((t/dt)+1))));
Lmean_III=mean(rmmissing(abs(F((t/dt)+1)-F_C2((t/dt)+1))));
L_III=[L1_III L2_III Linf_III Lmean_III];

%% Senario IV
% F vs MC
figure
title('Comparison of Senario IV')
subplot(2,2,1)
plot(t,F((t/dt)+1))
hold on
plot(t,F_M((t/dt)+1))
```

```
153 title('(a) Prob(Q(t) \leq x)','fontsize',16)
154 legend('F(t,x)','F(t,x) Simulated')
155 % axis([0,20,0,1])
156
157 subplot(2,2,2)
158 plot(t,W_1((t/dt)+1),'b')
159 hold on
160 plot(t,W_2((t/dt)+1),'r')
161 plot(t,W_1M((t/dt)+1),'b-.')
162 plot(t,W_2M((t/dt)+1),'r-.')
163 title('(b) W^1(t,x) and W^2(t,x)','fontsize',16)
164 legend('W^1(t,x)','W^2(t,x)','W^1(t,x) Simulated','W^2(
      t,x) Simulated')
165 % axis([0,20,0,1])
166
167 subplot(2,2,3)
168 plot(t,abs(F((t/dt)+1)-F_M((t/dt)+1)))
169 hold on
170 title('(c) Absolute Difference of F(t,x)','fontsize'
      ,16)
171 %axis([0,20])
172
173 subplot(2,2,4)
174 plot(t,(F((t/dt)+1)>0).*(abs(F_M((t/dt)+1)-F((t/dt)+1))
      ./F((t/dt)+1)))
175 hold on
176 title('(d) Relative Difference of F(t,x)','fontsize'
      ,16)
177
178 % Distance
179 L1_IV=sum(rmmissing(abs(F((t/dt)+1)-F_M((t/dt)+1))*dt)/
      t_n);
180 L2_IV=sqrt(sum(rmmissing(((F((t/dt)+1)-F_M((t/dt)+1))
      .^2)*dt))/t_n);
181 Linf_IV=max(rmmissing(abs(F((t/dt)+1)-F_M((t/dt)+1))));
182 Lmean_IV=mean(rmmissing(abs(F((t/dt)+1)-F_M((t/dt)+1))*
      dt));
183
```

```
L_IV=[L1_IV L2_IV Linf_IV Lmean_IV];

%% Senario V
% Combination vs MC

figure
title('Comparison of Senario V')
subplot(2,2,1)
plot(t,F_C((t/dt)+1))
hold on
plot(t,F_M((t/dt)+1))
title('(a) Prob(Q(t) \leq x)','fontsize',16)
legend('F(t,x) Approximated','F(t,x) Simulated')
% axis([0,20,0,1])

subplot(2,2,2)
plot(t,W_1C((t/dt)+1),'b')
hold on
plot(t,W_2C((t/dt)+1),'r')
plot(t,W_1M((t/dt)+1),'b-.')
plot(t,W_2M((t/dt)+1),'r-.')
title('(b) W^1(t,x) and W^2(t,x)','fontsize',16)
legend('W^1(t,x) Approximated','W^2(t,x) Approximated',
   'W^1(t,x) Simulated','W^2(t,x) Simulated')
% axis([0,20,0,1])

subplot(2,2,3)
plot(t,abs(F_C((t/dt)+1)-F_M((t/dt)+1)))
hold on
title('(c) Absolute Difference of F(t,x)','fontsize'
   ,16)
%axis([0,20])

subplot(2,2,4)
plot(t,(F_C((t/dt)+1)>0).*(abs(F_M((t/dt)+1)-F_C((t/dt)
   +1))./F_C((t/dt)+1)))
hold on
```

```
title('(d) Relative Difference of F(t,x)','fontsize',16)

% Distance
L1_V=sum(rmmissing(abs(F_C((t/dt)+1)-F_M((t/dt)+1))*dt)/t_n);
L2_V=sqrt(sum(rmmissing(((F_C((t/dt)+1)-F_M((t/dt)+1)).^2)*dt))/t_n);
Linf_V=max(rmmissing(abs(F_C((t/dt)+1)-F_M((t/dt)+1))));
Lmean_V=mean(rmmissing(abs(F_C((t/dt)+1)-F_M((t/dt)+1))));

L_V=[L1_V L2_V Linf_V Lmean_V];



%% Senario VI
% Combination 2 vs MC
figure
title('Comparison of Senario VI')
subplot(2,2,1)
plot(t,F_C2((t/dt)+1))
hold on
plot(t,F_M((t/dt)+1))
title('(a) Prob(Q(t) \leq x)','fontsize',16)
legend('F(t,x) Approximated','F(t,x) Simulated')
% axis([0,20,0,1])

subplot(2,2,2)
plot(t,W_1C2((t/dt)+1),'b')
hold on
plot(t,W_2C2((t/dt)+1),'r')
plot(t,W_1M((t/dt)+1),'b-.')
plot(t,W_2M((t/dt)+1),'r-.')
title('(b) W^1(t,x) and W^2(t,x)','fontsize',16)
legend('W^1(t,x) Approximated','W^2(t,x) Approximated','W^1(t,x) Simulated','W^2(t,x) Simulated')
```

```
% axis([0,20,0,1])

subplot(2,2,3)
plot(t,abs(F_C2((t/dt)+1)-F_M((t/dt)+1)))
hold on
title('(c) Absolute Difference of F(t,x)','fontsize'
   ,16)
%axis([0,20])

subplot(2,2,4)
plot(t,(F_C2((t/dt)+1)>0).*(abs(F_M((t/dt)+1)-F_C2((t/
   dt)+1))./F_C2((t/dt)+1)))
hold on
title('(d) Relative Difference of F(t,x)','fontsize'
   ,16)

% Distance
L1_VI=sum(rmmissing(abs(F_C2((t/dt)+1)-F_M((t/dt)+1))*
   dt)/t_n);
L2_VI=sqrt(sum(rmmissing(((F_C2((t/dt)+1)-F_M((t/dt)+1)
   ).^2)*dt))/t_n);
Linf_VI=max(rmmissing(abs(F_C2((t/dt)+1)-F_M((t/dt)+1))
   ));
Lmean_VI=mean(rmmissing(abs(F_C2((t/dt)+1)-F_M((t/dt)
   +1))));

L_VI=[L1_VI L2_VI Linf_VI Lmean_VI];

%%

L=real([L_I;L_II;L_III;L_IV;L_V;L_VI]);
toc
```

Listing 7.6: RuinProb.m

```
function [W,W_0,W_1]=RuinProb(lambda,mu,r_0,r_1,x,
   Senario,Order,t_end,dt,u,s0,iter)

    if nargin < 9, dt=0.5; end
```

```
4       if nargin < 8, t_end=20; end
5       if nargin < 7, Order = 1; end
6       if nargin < 6, Senario = 'o'; end
7       %% Constants
8           r=r_1;
9           a = (lambda+mu)/2;
10          alpha = sqrt(lambda*mu);
11          v0 = (u-x) / r ;
12          y = @(t) (t.^2-v0^2).^(1/2);
13          v0tilde = (u+x) / r ;
14          ytilde = @(t) (t.^2-v0tilde^2).^(1/2);
15
16      %{ BesselI Functions
17      I_0=BI(0,Senario,Order);
18      I_1=BI(1,Senario,Order);
19      I_2=BI(2,Senario,Order);
20      %}
21
22      CE=exp(-(lambda-mu)*(u-x)/(2*r));
23
24
25  %% W1
26      % t > v0
27      g31in = @(t,v) (1/2)*exp(-a*v).*I_0(alpha*y(v));
28      g32in = @(t,v) (1/2)*exp(a*v).*I_0(alpha*y(v));
29      g3 = @(t) (-mu*(lambda-mu)/(2*(lambda+mu)))*(
           integral(@(v) g31in(t,v), v0, t) - exp(-2*a*t)
           .*( integral(@(v) g32in(t,v), v0, t)));
30
31      g41in = @(t,v) alpha*v0*exp(-a*v).*(1./y(v)).*I_1(
           alpha*y(v));
32      g42in = @(t,v) alpha*v0*exp(a*v).*(1./y(v)).*I_1(
           alpha*y(v));
33      g4 = @(t) (mu/(2*(lambda+mu)))*(  integral(@(v)
           g41in(t,v), v0, t) + exp(-a*v0) - exp(-2*a*t).*(
            integral(@(v) g42in(t,v), v0, t) + exp(a*v0) )
           );
34
```

```
35      % t > v0tilde
36      g91in = @(t,v) (1/2)*exp(-a*v).*I_0( alpha*ytilde(v
           ));
37      g92in = @(t,v) (1/2)*exp(-(lambda+mu)*(t-v)).*exp(-
           a*v).*I_0(alpha*ytilde(v));
38      g9 = @(t) ( (1/lambda)*alpha*t.*(1/ytilde(t)).*I_1(
           alpha*ytilde(t))+((lambda-mu)/(2*lambda))*I_0(
           alpha*ytilde(t)) ).*exp(-a*t)+ (lambda*(lambda-
           mu)/(2*lambda+mu)) .* integral(@(v) g91in(t,v),
           v0tilde, t) - (mu^2)*(lambda-mu)/(2*lambda*(
           lambda+mu)) .* integral(@(v) g92in(t,v), v0tilde
           , t);
39
40      g101in = @(t,v) (alpha*v0tilde)*exp(-a*v).*(1./
           ytilde(v)).*I_1(alpha*ytilde(v));
41      g102in = @(t,v) exp(-(lambda+mu)*(t-v)).*exp(-a*v)*
           alpha*v0tilde.*(1./ytilde(v)).*I_1(alpha*ytilde(
           v));
42      g10 = @(t)  (1/lambda)*exp(-a*t)*alpha*v0tilde
           .*(1./ytilde(t)).*I_1(alpha*ytilde(t)) + lambda
           /(2*(lambda+mu)).*(  integral(@(v) g101in(t,v),
           v0tilde, t) +exp(-a*v0tilde)  ) - (mu^2)/(2*
           lambda*(lambda+mu)) .*( integral(@(v) g102in(t,v
           ), v0tilde, t) + exp( -(lambda+mu)*(t-v0tilde)-a
           *v0tilde ) );
43
44      F1 = @(t) CE.* (t>v0).*( g3(t)+g4(t) ) + CE.*(t>
           v0tilde).*( g9(t)-g10(t) );
45
46      %% W2
47      f11in = @(t,v) exp(a*v)*alpha*v0.*(1./y(v)).*I_1(
           alpha*y(v));
48      f11 = @(t) ( mu / (2*( lambda + mu )) )*exp(-2*a*t)
           .*( integral(@(v) f11in(t,v), v0, t) + exp(a*v0)
            );
49
50      f12in = @(t,v) exp(a*v)*alpha*v0tilde.*(1./ytilde(v
           )).*I_1(alpha*ytilde(v));
```

```
51      f12 = @(t) -( mu / (2*( lambda + mu )) )*exp(-2*a*t
          ).*( integral(@(v) f12in(t,v), v0tilde, t) + exp
          (a*v0tilde) );
52
53      f21in = @(t,v) exp(-a*v)*alpha*v0.*(1./y(v)).*I_1(
          alpha*y(v));
54      f21 = @(t) ( lambda / (2*(lambda+mu)) )*( integral
          (@(v) f21in(t,v), v0, t) + exp(-a*v0) );
55
56      f22in = @(t,v) exp(-a*v)*alpha*v0tilde.*(1./ytilde(
          v)).*I_1(alpha*ytilde(v));
57      f22 = @(t) -( lambda / (2*(lambda+mu)) )*( integral
          (@(v) f22in(t,v), v0tilde, t) + exp(-a*v0tilde)
          );
58
59      f31in = @(t,v) exp(a*v).*I_0(alpha*y(v));
60      f31 = @(t) - (mu*(lambda-mu)/(2*(lambda+mu)))
          *((1/2)*exp(-2*a*t).*integral(@(v) f31in(t,v),
          v0, t));
61
62      f32in = @(t,v) exp(a*v).*I_0(alpha*ytilde(v));
63      f32 = @(t) (mu*(lambda-mu)/(2*(lambda+mu))) * (
          (1/2)*exp(-2*a*t) .*integral(@(v) f32in(t,v), v0
          , t)  );
64
65      f41 = @(t) -(1/2)*exp(-a*t).*I_0(alpha*y(t));
66      f42 = @(t) (1/2)*exp(-a*t).*I_0(alpha*ytilde(t));
67
68      f51in = @(t,v) (1/2)*exp(-a*v).*I_0(alpha*y(v));
69      f51 = @(t) -(lambda*(lambda-mu)/(2*(lambda+mu)))*
          integral(@(v) f51in(t,v), v0, t);
70
71      f52in = @(t,v) (1/2)*exp(-a*v).*I_0(alpha*ytilde(v)
          );
72      f52 = @(t) (lambda*(lambda-mu)/(2*(lambda+mu)))*
          integral(@(v) f52in(t,v), v0tilde, t);
73
```

```
74      F2= @(t) CE.*( (t>v0).*( f11(t)+f21(t)+f31(t)+f41(t
            )+f51(t)) + (t>v0tilde).*(f12(t)+f22(t)+f32(t)+
            f42(t)+f52(t)) );
75
76      t_start=0;
77      W_0 = zeros((t_end-t_start)/dt+1,1) ;
78      W_1 = zeros((t_end-t_start)/dt+1,1) ;
79      for tt=t_start:dt:t_end
80          W_0((tt-t_start)/dt+1)=F1(tt);
81          W_1((tt-t_start)/dt+1)=F2(tt);
82      end
83      W=W_0+W_1;
84  end
```

7.3 Appendix C: Technical Details for the Inverse Laplace Transform in Chapter 2

From (2.2.39) we know that

$$\begin{aligned} W^1(t,x) &= \mathcal{L}^{-1}\left\{\hat{W}^1(s,x)\right\} \\ &= \frac{\lambda_{21}}{\lambda_{12}+\lambda_{21}}\mathcal{L}^{-1}\left\{\frac{1}{s}\right\} + \frac{\lambda_{12}}{\lambda_{12}+\lambda_{21}}\mathcal{L}^{-1}\left\{\frac{1}{s+\lambda_{12}+\lambda_{21}}\right\} \\ &- \mathcal{L}^{-1}\left\{\frac{s+\lambda_{21}+\phi_2\omega_0(s)}{s(s+\lambda_{12}+\lambda_{21})}e^{\omega_0(s)x}\right\}. \end{aligned} \tag{7.3.1}$$

According to the inverse Laplace Transform table [30],

$$\mathcal{L}^{-1}\left\{\frac{1}{s}\right\} = 1, \tag{7.3.2}$$

and

$$\mathcal{L}^{-1}\left\{\frac{1}{s+\lambda_{12}+\lambda_{21}}\right\} = e^{-(\lambda_{12}+\lambda_{21})t}. \tag{7.3.3}$$

Thus,

$$\begin{aligned} &\mathcal{L}^{-1}\left\{\frac{s+\lambda_{21}+\phi_2\omega_0(s)}{s(s+\lambda_{12}+\lambda_{21})}e^{\omega_0(s)x}\right\} \\ &= \mathcal{L}^{-1}\left\{\left(\frac{1}{s}-\frac{1}{s+\lambda_{12}+\lambda_{21}}\right)\cdot\frac{s+\lambda_{21}+\phi_2(\beta(s)+\eta(s))}{\lambda_{12}+\lambda_{21}}e^{\beta(s)x+\eta(s)x}\right\} \\ &= \mathcal{L}^{-1}\left\{\left(\frac{1}{s}-\frac{1}{s+\lambda_{12}+\lambda_{21}}\right)e^{\beta(s)x}\cdot\frac{\phi_2\eta(s)}{\lambda_{12}+\lambda_{21}}e^{\eta(s)x}\right\} \\ &= \mathcal{L}^{-1}\left\{\left(\frac{1}{s}-\frac{1}{s+\lambda_{12}+\lambda_{21}}\right)e^{\beta(s)x}\right\} * \mathcal{L}^{-1}\left\{\frac{\phi_2\eta(s)}{\lambda_{12}+\lambda_{21}}e^{\eta(s)x}\right\}, \end{aligned} \tag{7.3.4}$$

where $*$ is the convolution operator. The inverse Laplace Transform of the first term of equation (7.3.4) can be represented as

$$\begin{aligned}
&\mathcal{L}^{-1}\left\{\left(\frac{1}{s}-\frac{1}{s+\lambda_{12}+\lambda_{21}}\right)e^{\beta(s)x}\right\}\\
&=\mathcal{L}^{-1}\left\{\frac{1}{s}e^{-\left(\frac{1}{\phi_2}s+\frac{\lambda_{21}}{\phi_2}\right)x}\right\}-\mathcal{L}^{-1}\left\{\frac{1}{s+\lambda_{12}+\lambda_{21}}e^{-\left(\frac{1}{\phi_2}s+\frac{\lambda_{21}}{\phi_2}\right)x}\right\}\\
&=e^{-\frac{\lambda_{21}}{\phi_2}x}\left(\mathcal{L}^{-1}\left\{\frac{1}{s}e^{-\frac{x}{\phi_2}s}\right\}-\mathcal{L}^{-1}\left\{\frac{1}{s+\lambda_{12}+\lambda_{21}}e^{-\frac{x}{\phi_2}s}\right\}\right) \qquad (7.3.5)\\
&=\begin{cases}0, & 0<t<\dfrac{x}{\phi_2}\\ e^{-\frac{\lambda_{21}}{\phi_2}x}\left(1-e^{-(\lambda_{12}+\lambda_{21})\left(t-\frac{x}{\phi_2}\right)}\right), & t>\dfrac{x}{\phi_2}\end{cases}.
\end{aligned}$$

We define the second term of equation (7.3.4) as

$$h(t,x)=\mathcal{L}^{-1}\left\{\frac{\phi_2\eta(s)}{\lambda_{12}+\lambda_{21}}e^{\eta(s)x}\right\}, \qquad (7.3.6)$$

which can be represented as

$$\begin{aligned}
h(t,x)=&\frac{\phi_2}{\lambda_{12}+\lambda_{21}}\mathcal{L}^{-1}\left\{b\left((s+a)-\left((s+a)^2-\alpha^2\right)^{\frac{1}{2}}\right)e^{\left(b(s+a)-b\left[(s+a)^2-\alpha^2\right]^{\frac{1}{2}}\right)x}\right\}\\
=&\frac{\phi_2}{\lambda_{12}+\lambda_{21}}e^{-at}\mathcal{L}^{-1}\left\{b\left(s-\left(s^2-\alpha^2\right)^{\frac{1}{2}}\right)e^{bx\left(s-\left(s^2-\alpha^2\right)^{\frac{1}{2}}\right)}\right\}.
\end{aligned} \qquad (7.3.7)$$

Let

$$p=\left(s^2-\alpha^2\right)^{\frac{1}{2}} \qquad (7.3.8)$$

so that

$$s^2-p^2=\alpha^2 \qquad (7.3.9)$$

and equation (7.3.7) can be arranged as

$$\begin{aligned} h(t,x) =& \frac{\phi_2}{\lambda_{12}+\lambda_{21}} e^{-at} \mathcal{L}^{-1} \left\{ b\left(s-p\right) e^{bx(s-p)} \right\} \\ =& \frac{b\phi_2}{\lambda_{12}+\lambda_{21}} e^{-at} \mathcal{L}^{-1} \left\{ \frac{2p\left(s+p\right)\left(\left(s-p\right)\left(s+p\right)\right)}{2p\left(s+p\right)^2} e^{bx(s-p)} \right\} \\ =& \frac{b\alpha^2\phi_2}{2\left(\lambda_{12}+\lambda_{21}\right)} e^{-at} \mathcal{L}^{-1} \left\{ \frac{\left(s+p\right)^2-\alpha^2}{p\left(s+p\right)^2} e^{bx(s-p)} \right\} \\ =& \frac{b\alpha^2\phi_2}{2\left(\lambda_{12}+\lambda_{21}\right)} e^{-at} \mathcal{L}^{-1} \left\{ p^{-1}\left(1-\alpha^2\left(s+p\right)^{-2}\right) e^{bx(s-p)} \right\}. \end{aligned} \tag{7.3.10}$$

Define P as

$$P = s+p, \tag{7.3.11}$$

and we have

$$h(t,x) = \frac{b\alpha^2\phi_2}{2\left(\lambda_{12}+\lambda_{21}\right)} e^{-at} \left(\mathcal{L}^{-1}\left\{ p^{-1} e^{bx(s-p)} \right\} - \alpha^2 \mathcal{L}^{-1}\left\{ p^{-1}P^{-2} e^{bx(s-p)} \right\} \right). \tag{7.3.12}$$

According to the inverse Laplace Transform table [30],

$$\mathcal{L}^{-1}\left\{ p^{-1} e^{bx(s-p)} \right\} = I_0\left[\alpha\left(t^2+2bxt\right)^{\frac{1}{2}} \right] \tag{7.3.13}$$

and

$$\mathcal{L}^{-1}\left\{ \alpha^2 p^{-1}P^{-2} e^{bx(s-p)} \right\} = t\left(t+2bx\right)^{-1} I_2\left[\alpha\left(t^2+2bxt\right)^{\frac{1}{2}} \right], \tag{7.3.14}$$

where $I_\nu\left(x\right)$ is the modified Bessel Function of the first kind with order ν, given by the results of differential equation (7.3.15),

$$x^2y'' + xy' - \left(x^2+\nu^2\right) y = 0. \tag{7.3.15}$$

Let

$$\kappa\left(t,x\right)=\left(\frac{t+2bx}{t}\right)^{\frac{1}{2}}=\left(1-\left(\frac{1}{\phi_1}-\frac{1}{\phi_2}\right)\frac{x}{t}\right)^{\frac{1}{2}}, \tag{7.3.16}$$

and

$$\rho(t,x)=\alpha\kappa(t,x)t, \tag{7.3.17}$$

then

$$\left(t^2+2bxt\right)^{\frac{1}{2}}=t\kappa\left(t,x\right)=\frac{\rho(t,x)}{\alpha} \tag{7.3.18}$$

Thus, we summarize equations (7.3.13) to (7.3.18) and substitute back into (7.3.12), which yields

$$h\left(t,x\right)=\frac{b\alpha^2\phi_2}{2\left(\lambda_{12}+\lambda_{21}\right)}e^{-at}\left(I_0\left[\rho(t,x)\right]-\frac{1}{\kappa^2\left(t,x\right)}I_2\left[\rho(t,x)\right]\right) \tag{7.3.19}$$

Combine the equations above together and plug into equation (7.3.1), we have

$$W^1\left(t,x\right)=\begin{cases}\dfrac{\lambda_{21}}{\lambda_{12}+\lambda_{21}}+\dfrac{\lambda_{12}}{\lambda_{12}+\lambda_{21}}e^{-(\lambda_{12}+\lambda_{21})t}, & 0<t<\dfrac{x}{\phi_2}\\ \dfrac{\lambda_{21}}{\lambda_{12}+\lambda_{21}}+\dfrac{\lambda_{12}}{\lambda_{12}+\lambda_{21}}e^{-(\lambda_{12}+\lambda_{21})t} & \\ \qquad -e^{-\frac{\lambda_{21}}{\phi_2}x}\displaystyle\int_0^t f_1(t-v,x)\cdot h\left(v,x\right)dv, & t>\dfrac{x}{\phi_2}.\end{cases} \tag{7.3.20}$$

which is (2.2.49), where

$$h\left(t,x\right)=\frac{b\alpha^2\phi_2}{2\left(\lambda_{12}+\lambda_{21}\right)}e^{-at}\left(I_0\left[\rho(t,x)\right]-\frac{1}{\kappa^2\left(t,x\right)}I_2\left[\rho(t,x)\right]\right)\quad, \tag{7.3.21}$$

$$f_1(t,x)=1-e^{-(\lambda_{12}+\lambda_{21})\left(t-\frac{x}{\phi_2}\right)}, \tag{7.3.22}$$

$$\kappa(t,x) = \left(\frac{t+2bx}{t}\right)^{\frac{1}{2}} = \left(1 - \left(\frac{1}{\phi_1} - \frac{1}{\phi_2}\right)\frac{x}{t}\right)^{\frac{1}{2}}, \tag{7.3.23}$$

$$\rho(t,x) = \alpha\kappa(t,x)t, \tag{7.3.24}$$

and $I_n(x), n = 0,1,2$ are the modified Bessel functions of the first kind.

Similarly, we have

$$\begin{aligned} W^2(t,x) &= \mathcal{L}^{-1}\left\{\hat{W}^2(s,x)\right\} \\ &= \mathcal{L}^{-1}\left\{\left(\frac{\lambda_{12}}{\lambda_{12}+\lambda_{21}}\right)\left(\frac{1}{s} - \frac{1}{s+\lambda_{12}+\lambda_{21}}\right)\left(1 - e^{\omega_0(s)x}\right)\right\} \\ &= \frac{\lambda_{12}}{\lambda_{12}+\lambda_{21}} \cdot \left(\mathcal{L}^{-1}\left\{\frac{1}{s}\right\} - \mathcal{L}^{-1}\left\{\frac{1}{s+\lambda_{12}+\lambda_{21}}\right\}\right. \\ &\qquad \left. -\mathcal{L}^{-1}\left\{\left(\frac{1}{s} - \frac{1}{s+\lambda_{12}+\lambda_{21}}\right)e^{\omega_0(s)x}\right\}\right), \end{aligned} \tag{7.3.25}$$

where

$$\begin{aligned} &\mathcal{L}^{-1}\left\{\left(\frac{1}{s} - \frac{1}{s+\lambda_{12}+\lambda_{21}}\right)e^{\omega_0(s)x}\right\} \\ &= \mathcal{L}^{-1}\left\{\left(\frac{1}{s} - \frac{1}{s+\lambda_{12}+\lambda_{21}}\right)e^{\beta(s)x}e^{\eta(s)x}\right\} \\ &= \mathcal{L}^{-1}\left\{\left(\frac{1}{s} - \frac{1}{s+\lambda_{12}+\lambda_{21}}\right)e^{\beta(s)x}\right\} * \mathcal{L}^{-1}\left\{e^{\eta(s)x}\right\}. \end{aligned} \tag{7.3.26}$$

The inverse Laplace Transform of the first term of equation (7.3.26) can be

represented as

$$\begin{aligned}
&\mathcal{L}^{-1}\left\{\left(\frac{1}{s}-\frac{1}{s+\lambda_{12}+\lambda_{21}}\right)e^{\beta(s)x}\right\}\\
&=\mathcal{L}^{-1}\left\{\frac{1}{s}e^{\beta(s)x}\right\}-\mathcal{L}^{-1}\left\{\frac{1}{s+\lambda_{12}+\lambda_{21}}e^{\beta(s)x}\right\}\\
&=e^{-\frac{\lambda_{21}x}{\phi_2}}\left(\mathcal{L}^{-1}\left\{\frac{1}{s}e^{\frac{-x}{\phi_2}s}\right\}-\mathcal{L}^{-1}\left\{\frac{1}{s+\lambda_{12}+\lambda_{21}}e^{\frac{-x}{\phi_2}s}\right\}\right)\\
&=\begin{cases}0, & 0<t<\dfrac{x}{\phi_2}\\ e^{-\frac{\lambda_{21}x}{\phi_2}}\left(1-e^{-(\lambda_{12}+\lambda_{21})\left(t-\frac{x}{\phi_2}\right)}\right), & t>\dfrac{x}{\phi_2}.\end{cases}
\end{aligned} \tag{7.3.27}$$

Define $g(t,x)$ to be the second term of equation (7.3.26), namely,

$$g(t,x)=\mathcal{L}^{-1}\left\{e^{\eta(s)x}\right\}, \tag{7.3.28}$$

then we have

$$\begin{aligned}
g(t,x)&=\mathcal{L}^{-1}\left\{e^{bx\left((s+a)-\left((s+a)^2-\alpha^2\right)^{\frac{1}{2}}\right)}\right\}\\
&=e^{-at}\mathcal{L}^{-1}\left\{e^{bx(s-p)}\right\}\\
&=e^{-at}\left(\mathcal{L}^{-1}\left\{e^{bx(s-p)}-1\right\}+\mathcal{L}^{-1}\{1\}\right)
\end{aligned} \tag{7.3.29}$$

According to the inverse Laplace Transform table ([30]),

$$\mathcal{L}^{-1}\left\{e^{bx(s-p)}-1\right\}=\alpha bx\left(t^2+2bxt\right)^{-\frac{1}{2}}I_1\left[\alpha\left(t^2+2bxt\right)^{\frac{1}{2}}\right], \tag{7.3.30}$$

and

$$\mathcal{L}^{-1}\{1\}=\delta(t). \tag{7.3.31}$$

Plug equation (7.3.30) and (7.3.31) into (7.3.29), we can represent $g(t,x)$ as

$$\begin{aligned} g(t,x) &= e^{-at}\left(\alpha bx\left(t^2+2bxt\right)^{-\frac{1}{2}} I_1\left[\alpha\left(t^2+2bxt\right)^{\frac{1}{2}}\right]+\delta(t)\right) \\ &= e^{-at}\left(\alpha\frac{bx}{t\kappa(t,x)} I_1\left[\alpha\kappa(t,x)\,t\right]+\delta(t)\right) \\ &= e^{-at}\left(\frac{\alpha}{2\kappa(t,x)}\left(\kappa(t,x)^2-1\right) I_1\left[\rho(t,x)\right]+\delta(t)\right) \end{aligned} \tag{7.3.32}$$

Plug equations (7.3.27) and (7.3.32) into (2.2.54), we have

$$W^2(t,x) = \begin{cases} \dfrac{\lambda_{12}}{\lambda_{12}+\lambda_{21}}\left(1-e^{-(\lambda_{12}+\lambda_{21})t}\right), 0<t<\dfrac{x}{\phi_2} \\ \dfrac{\lambda_{12}}{\lambda_{12}+\lambda_{21}}\Big(1-e^{-(\lambda_{12}+\lambda_{21})t} \\ \qquad -e^{-\frac{\lambda_{21}}{\phi_2}x}\displaystyle\int_0^t f_1(t-v,x)\cdot g(v,x)\,dv\Big), t>\dfrac{x}{\phi_2}, \end{cases} \tag{7.3.33}$$

which is (2.2.55), where $f_1(t,x)$ is defined in (7.3.22) and $g(t,x)$ is defined as

$$g(t,x) = e^{-at}\left(\frac{\alpha}{2\kappa(t,x)}\left(\kappa(t,x)^2-1\right) I_1\left[\rho(t,x)\right]+\delta(t)\right) \tag{7.3.34}$$

where $\delta(t)$ is the Dirac delta function.

7.4 Appendix D: Technical Details for the Inverse Laplace Transform in Chapter 4

From the solutions (4.2.23), we will get that for $x < u$,

$$\begin{aligned}\hat{W}^1(s,x) &= -\frac{\mu(\lambda-\mu-\sqrt{T(s)})}{2s(\lambda+\mu+s)\sqrt{T(s)}}e^{-\omega_1(s)u}\left(e^{\omega_1(s)x} - \frac{(\lambda+\mu+2s-\sqrt{T(s)})^2}{4\lambda\mu}e^{\omega_0(s)x}\right) \\ &= \hat{g}_1(s,x) + \hat{g}_2(s,x)\end{aligned} \tag{7.4.1}$$

where

$$\hat{g}_1(s,x) = -\frac{\mu(\lambda-\mu-\sqrt{T(s)})}{2s(\lambda+\mu+s)\sqrt{T(s)}}e^{-\omega_1(s)(u-x)} \tag{7.4.2}$$

and

$$\hat{g}_2(s,x) = \frac{\mu(\lambda-\mu-\sqrt{T(s)})}{2s(\lambda+\mu+s)\sqrt{T(s)}}\frac{(\lambda+\mu+2s-\sqrt{T(s)})^2}{4\lambda\mu}e^{-\omega_1(u-x)}. \tag{7.4.3}$$

Notice that

$$\begin{aligned}\hat{g}_1(s,x) = &-\frac{\mu(\lambda-\mu)}{2s(\lambda+\mu+s)}e^{-\frac{(\lambda-\mu)(u-x)}{2r}}\cdot\frac{1}{\sqrt{T(s)}}e^{-\frac{(u-x)\sqrt{T(s)}}{2r}} \\ &+\frac{\mu}{2s(\lambda+\mu+s)}e^{-\frac{(\lambda-\mu)(u-x)}{2r}}\cdot e^{-\frac{(u-x)\sqrt{T(s)}}{2r}}\end{aligned} \tag{7.4.4}$$

Let

$$a = \frac{\lambda+\mu}{2}, \qquad \alpha = \sqrt{\lambda\mu} \tag{7.4.5}$$

and

$$v_0 = \frac{u-x}{r} \tag{7.4.6}$$

we have

$$\mathcal{L}^{-1}\left\{-\frac{1}{2s(\lambda+\mu+s)}e^{-\frac{(\lambda-\mu)(u-x)}{2r}}\right\} = -\frac{1}{2(\lambda+\mu)}e^{-\frac{(\lambda-\mu)(u-x)}{2r}}\left(1-e^{-(\lambda+\mu)\tau}\right), \tag{7.4.7}$$

$$\mathcal{L}^{-1}\left\{\frac{1}{\sqrt{T(s)}}e^{-\frac{(u-x)\sqrt{T(s)}}{2r}}\right\}=\frac{1}{2}e^{-a\tau}I_0\left[\alpha y(\tau)\right]\mathbf{1}_{\{\tau>v_0\}}, \tag{7.4.8}$$

and

$$\mathcal{L}^{-1}\left\{e^{-\frac{(u-x)\sqrt{T(s)}}{2r}}\right\}=e^{-a\tau}\left(\alpha v_0 y^{-1}(v)I_1\left[\alpha y(\tau)\right]\mathbf{1}_{\{\tau>v_0\}}+\delta(\tau-v_0)\right), \tag{7.4.9}$$

which yields

$$\begin{aligned}
&g_1(\tau,x)=\mathcal{L}^{-1}\left\{\hat{g}_1(s,x)\right\}\\
&=-\frac{\mu(\lambda-\mu)}{2(\lambda+\mu)}e^{-\frac{(\lambda-\mu)(u-x)}{2r}}\mathbf{1}_{\{\tau>v_0\}}\int_{v_0}^{\tau}\frac{1}{2}e^{-av}I_0[\alpha y(v)]\left(1-e^{-(\lambda+\mu)(\tau-v)}\right)dv\\
&+\frac{\mu}{2(\lambda+\mu)}e^{-\frac{(\lambda-\mu)(u-x)}{2r}}\mathbf{1}_{\{\tau>v_0\}}\int_{v_0}^{\tau}e^{-av}\alpha v_0 y^{-1}(v)I_1[\alpha y(v)]\left(1-e^{-(\lambda+\mu)(\tau-v)}\right)dv'\\
&+\frac{\mu}{2(\lambda+\mu)}e^{-\frac{(\lambda-\mu)(u-x)}{2r}}\mathbf{1}_{\{\tau>v_0\}}\left(1-e^{-(\lambda+\mu)(\tau-v_0)}\right)
\end{aligned} \tag{7.4.10}$$

where I_0 and I_1 are the modified Bessel functions of the first kind, $\mathbf{1}_{\{\cdot\}}$ is the indicator function and

$$y(\tau)=(\tau^2-v_0^2)^{\frac{1}{2}}. \tag{7.4.11}$$

On the other hand, we can write $\hat{g}_2(s,x)$ as

$$\begin{aligned}
&\hat{g}_2(s,x)=e^{-\frac{(u+x)\sqrt{T(s)}}{2r}-\frac{(\lambda-\mu)(u-x)}{2r}}\\
&\times\left[\left(\frac{2}{\sqrt{T(s)}}+\frac{2s}{\lambda\sqrt{T(s)}}+\frac{\lambda(\lambda-\mu)}{s\sqrt{T(s)}}-\frac{\mu^2(\lambda-\mu)}{2\lambda(\lambda+\mu)}\frac{1}{(s+\lambda+\mu)\sqrt{T(s)}}\right).\right.\\
&\left.-\left(\frac{1}{\lambda}+\frac{\lambda}{2(\lambda+\mu)}\cdot\frac{1}{s}-\frac{\mu^2}{2\lambda(\lambda+\mu)}\cdot\frac{1}{s+\lambda+\mu}\right)\right]
\end{aligned} \tag{7.4.12}$$

Let

$$\tilde{v}_0=\frac{u+x}{r} \tag{7.4.13}$$

and

$$\tilde{y}(\tau) = \left(\tau^2 - \tilde{v}_0^2\right)^{\frac{1}{2}}, \tag{7.4.14}$$

Notice that

$$\mathcal{L}^{-1}\left\{\frac{1}{s}e^{-\frac{(u-x)\sqrt{T(s)}}{2r}}\right\} = \int_{v_0}^{\tau} e^{-av}\alpha v_0 y^{-1}(v) I_1[\alpha y(v)]dv + e^{-av_0}, \text{ for } \tau > v_0 \tag{7.4.15}$$

and

$$\mathcal{L}^{-1}\left\{\frac{1}{s\sqrt{T(s)}}e^{-\frac{(u-x)\sqrt{T(s)}}{2r}}\right\} = \int_{v_0}^{\tau} \frac{1}{2}e^{-av} I_0[\alpha y(v)]dv, \text{ for } \tau > v_0, \tag{7.4.16}$$

so the inverse Laplace Transform of (7.4.12) yields

$$\begin{aligned}
&g_2(\tau, x) = \mathcal{L}^{-1}\left\{\hat{g}_2(s, x)\right\} \\
&= e^{-\frac{(\lambda-\mu)(u-x)}{2r}}\mathbf{1}_{\{\tau > \tilde{v}_0\}} \\
&\times \left\{e^{-a\tau}\left(\frac{1}{\lambda}\alpha\tau\tilde{y}^{-1}(\tau) I_1[\alpha\tilde{y}(\tau)] + \frac{\lambda-\mu}{2\lambda} I_0[\alpha\tilde{y}(\tau)] - \frac{\alpha^2\tilde{v}_0}{2\lambda}\right)\right. \\
&+\frac{\lambda(\lambda-\mu)}{2(\lambda+\mu)}\int_{\tilde{v}_0}^{\tau}\frac{1}{2}e^{-av} I_0[\alpha\tilde{y}(v)]dv - \frac{\mu^2(\lambda-\mu)}{2\lambda(\lambda+\mu)}e^{-2a\tau}\int_{\tilde{v}_0}^{\tau}\frac{1}{2}e^{av} I_0[\alpha\tilde{y}(v)]dv \\
&-\frac{\lambda}{2(\lambda+\mu)}\left(\int_{\tilde{v}_0}^{\tau}\alpha\tilde{v}_0 e^{-av}\tilde{y}^{-1}(v) I_1[\alpha\tilde{y}(v)]dv + e^{-a\tilde{v}_0}\right) \\
&\left.+\frac{\mu^2}{2\lambda(\lambda+\mu)}e^{-2a\tau}\left(\int_{\tilde{v}_0}^{\tau}\alpha\tilde{v}_0 e^{av}\tilde{y}^{-1}(v) I_1[\alpha\tilde{y}(v)]dv + e^{a\tilde{v}_0}\right)\right\}
\end{aligned} \tag{7.4.17}$$

Combine equation (7.4.10) and (7.4.17), we will get the solution for $W^1(\tau, x)$ shown as (4.2.25), (4.2.27) and (4.2.29).

Similarly, we can write $\hat{W}^2(s,x)$ as

$$\hat{W}^2(s,x) = e^{-\frac{(\lambda-\mu)(u-x)}{2r}}\left(e^{-\frac{(u-x)\sqrt{T(s)}}{2r}} - e^{-\frac{(u+x)\sqrt{T(s)}}{2r}}\right)$$

$$\times\left(\frac{\mu}{2(\lambda+\mu)}\cdot\frac{1}{s+\lambda+\mu} + \frac{\lambda}{2(\lambda+\mu)}\cdot\frac{1}{s}\right. \qquad , \quad (7.4.18)$$

$$\left.-\frac{\mu(\lambda-\mu)}{2(\lambda+\mu)}\cdot\frac{1}{(s+\lambda+\mu)\sqrt{T(s)}} - \frac{1}{\sqrt{T(s)}} - \frac{\lambda(\lambda-\mu)}{2(\lambda+\mu)}\cdot\frac{1}{s\sqrt{T(s)}}\right)$$

the inverse of which will result in solutions (4.2.26), (4.2.28) and (4.2.30).

Vita

Yu Shao was born on November 29, 1995 in Anyang, Henan, China. He got his Bachelor's Degree of Science and Engineering in 2017 at School of Information, Renmin University of China, specializing in Mathematics and Applied Mathematics. He furthered his graduate studies in mathematics and earned a Master of Science in Engineering specializing in Financial Mathematics at Johns Hopkins University in 2019. He also worked as a Graduate Research Assistant at Johns Hopkins University and has published a research paper at the 2018 IEEE Ubiquitous Computing, Electronics and Mobile Communication Conference (UEMCON). His research interests include stochastic processes, market prediction and financial mathematics. He plans to pursue his Ph.D. in Statistics at Boston University to expand his knowledge horizon.